

Task 4.1

Task Title

Risk, Safety and Societal Acceptance

Research Partners

Swiss Seismological Service (SED), Institute for Geophysics (IfG) at ETH Zurich, Department of Civil, Environmental and Geomatic Engineering (D-BAUG) at ETH Zurich, Department of Environmental Systems Science (D-USYS) at ETH Zurich, Laboratory of Cryospheric Sciences (CRYOS) at EPF Lausanne, Paul Scherrer Institute (PSI)

Current Projects (presented on the following pages)

Accounting for uncertainty in the propagation of dam break flood waves in the Rhone River: from hazards to risks

A. Darcourt, J.P. Matos, A.J. Schleiss

Risk GOVeRnance of electricity pOrtfolioS (RIGOROUSt): Cross-technology and spatial tradeoffs of multiple risks

E. Trutnevyte, P. Berntsen, T. Knoblauch, S. Volken

Impact of combined wind and solar energy on the Swiss electricity system

J. Dujardin, A. Kahl, B. Kruyt, M. Lehning

A Bayesian Hierarchical Model for Hydropower Dam Accidents Risk

A. Kalinina, M. Spada, P. Burgherr

Physical-based model of a dam failure event

A. Kalinina, M. Spada, P. Burgherr

Seasonal and Diurnal Wind Power

B. Kruyt, M. Lehning

Multi-risk in the Swiss landscape: The case of earthquake-triggered landslides

A. Jafarimanesh, A. Mignan, D. Giardini

Long-term decay and possible reactivation of induced seismicity at the Basel EGS site

M. Herrmann, T. Kraft, T. Tormann, S. Wiemer

Controlling induced seismicity in EGS projects by a model-driven traffic light system

A. Mignan, M. Broccardo, S. Wiemer

ENSAD v2.0 Hydro: a new interactive, GIS-based database for historical hydropower accidents worldwide

P. Burgherr, M. Spada, A. Kalinina, K. Wansub, S. Hirschberg

Accident Risk Assessment for Deep Geothermal Energy Systems for Switzerland: An Update

M. Spada, E. Sutra, P. Burgherr

Induced seismicity risk analysis in OpenQuake. Basel 2009 case study, validation and GIS integration

M. Broccardo, L. Danciu, A. Mignan, S. Wiemer

Nonstructural Damage Tests on Masonry Building Walls: First Phase

M. Didier, M. Broccardo, G. Abbiati, L. Danciu, K. Beyer, B. Stojadinovic, D. Giardini

Social discourses on deep geothermal energy

O. Ejderyan, M. Stauffacher

Task Objectives

- The exploitation of underground energy resources as well as the use and expansion of hydropower, are, like all energy technologies, not risk free. To address this risk, we develop a holistic concept of risk governance and community resilience, advocating a broad picture of risk: not only does it include 'risk management' and 'risk analysis', it also looks at how risk-related decision-making unfolds when a range of actors is involved. This requires coordination and possibly reconciliation between a profusion of roles, perspectives, goals and activities. Developments include: a rigorous common methodology and a consistent modelling approach to hazard, vulnerability, risk, resilience and societal acceptance assessment of energy technologies; a stress test framework and apply it to assess the vulnerability and resilience of individual critical energy infrastructures, as well as to address the first level of interdependencies among these, from local and regional perspectives; standardized protocols, operational guidelines and software for monitoring strategies, for real-time hazard and risk assessment during all project phases, and for mitigation and related communication strategies.

Interaction Between the Partners – Synthesis

- Risk Governance by its very nature is a truly interdisciplinary and integrative activity, with interfaces to science, industry, regulators, and the public / media. The composition of the team behind task 4.1 reflects these needs and provides bridges to the other tasks of the SCCER-SoE, liaising both geo-energy and hydropower research by using a common risk governance language. The fact that the core team at ETHZ is located in a central office, together with the SCCER-SoE exploration and modelling teams promotes exchanges within the broad SCCER-SoE landscape. Participation of PSI additionally provides a natural link with other integrative activities. Exchanges with other SCCERs is also ongoing (e.g. FURIES and CREST). Via the SED, meetings occur on a regular basis with cantonal and industry representatives in order to discuss the application of our R&D for ongoing and future projects. Additional synergies with other projects, funded by both Switzerland and the European Union, exist.

Highlights 2016

- A risk governance workflow for induced seismicity risk has been developed and is being implemented. This workflow will also be tested in connection of the EU project DESTRESS (www.destress-h2020.eu) where the Task 4.1 team is a major contributor.
- An international workshop on induced seismicity will again take place in Davos in March 2017, with more than 150 participants (www.seismo.ethz.ch/schatzalp).
- The team is continuing to contribute actively to the permitting process for future geothermal plants in Switzerland by advising industry and cantonal authorities. A workshop in the context of the GeoBest-CH project for cantonal authorities was

conducted in April 2016
(www.seismo.ethz.ch/eq_swiss/Geothermie/Geothermie_SED/index_EN)

Accounting for uncertainty in the propagation of dam break flood waves in the Rhone River: from hazards to risks

Darcourt, A., Matos, J.P., Schleiss, A.J.
Corresponding author: jose.matos@epfl.ch

Abstract

The safety of large dams is commonly verified resorting to deterministic approaches, according to which a number of scenarios designed to represent the main ways in which the infrastructures may fail.

Such approaches certainly provide valuable qualitative depictions of risk, but by no means quantitative ones. In fact, overall scenario probabilities are commonly unknown and a number of uncertainties neglected.

Here, an inclusive Monte Carlo probabilistic approach in which aleatory and epistemic uncertainties are accounted for is explored. To accomplish it constraining computational challenges associated with dam break flood wave routing were addressed [1].

Numerical model for routing

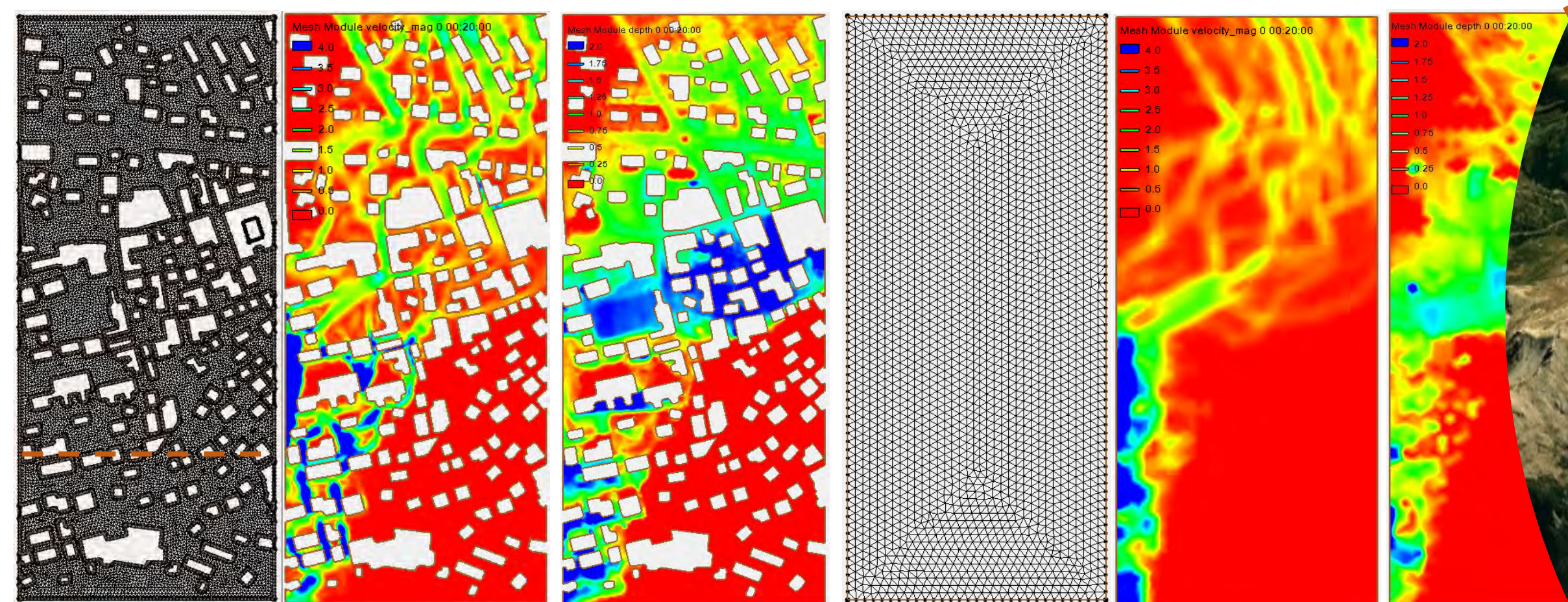
Creation of a 1D/2D coupled numerical model using BASEMENT.

4

Numerical modelling of urban areas

Model roughness correction to obtain acceptable results with a relatively large mesh; thus faster to run.

$$K^* = K \cdot f(\text{built area}) \cdot g(\text{built perimeter})$$



5

Numerical simulations and their interpolation

Detailed BASEMENT simulations are conducted for each breach derived from the failures within the catalogue computed in step (3).

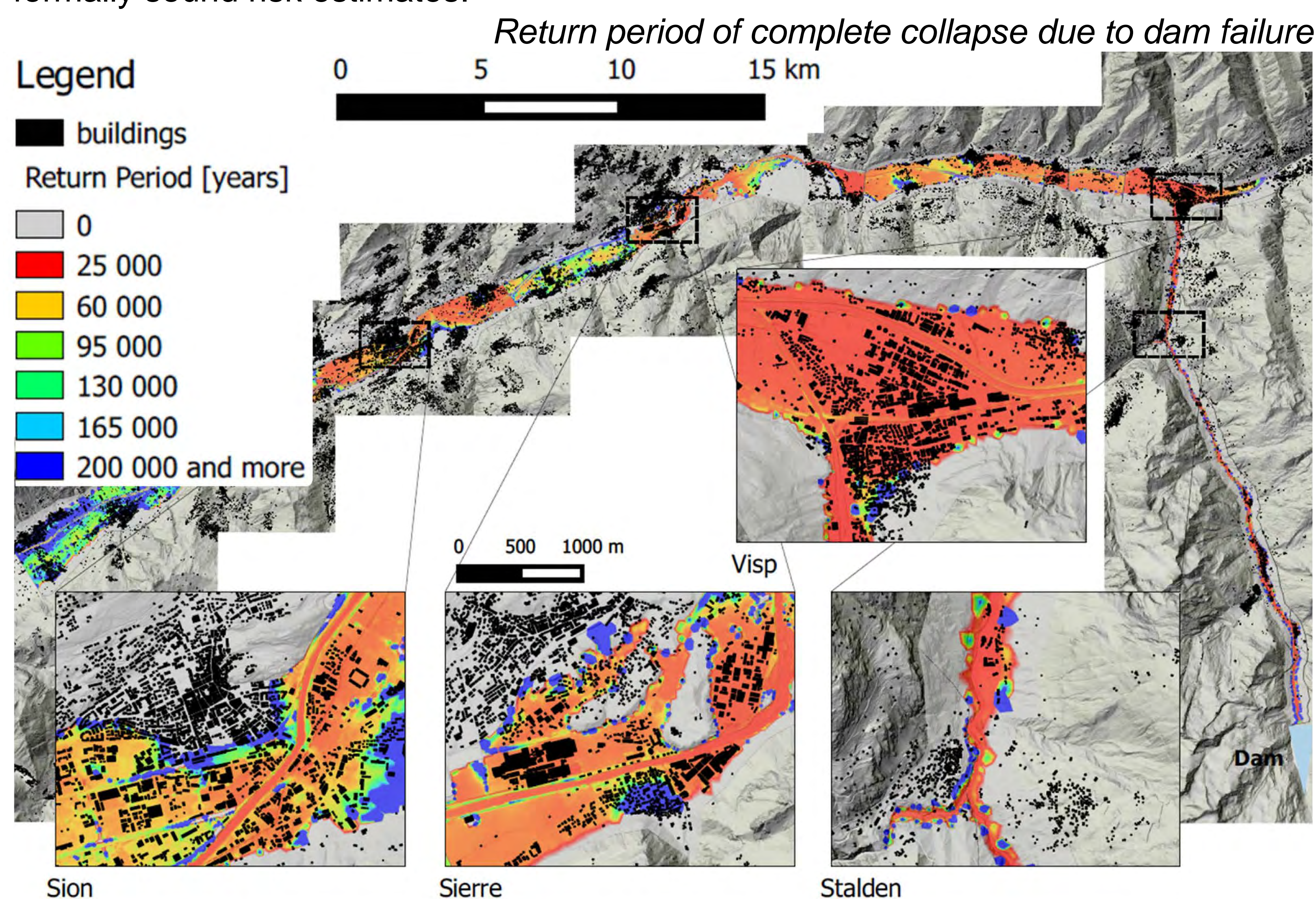
Focusing on each parameter (e.g. max. depth, max. velocity) a regression is made for every possible breach and location over the inundated area.

6

Damage and risk assessment

Using fragility curves specific for building type and size [4] one can estimate damages. With frequency information from step (1) it is possible to compute formally sound risk estimates.

7



Harmonized approach to stress tests for critical infrastructures against natural hazards

www.strest-eu.org. Project funded by the European Community's 7th Framework Programme [FP7/2007-2013] under grant no: 603389.



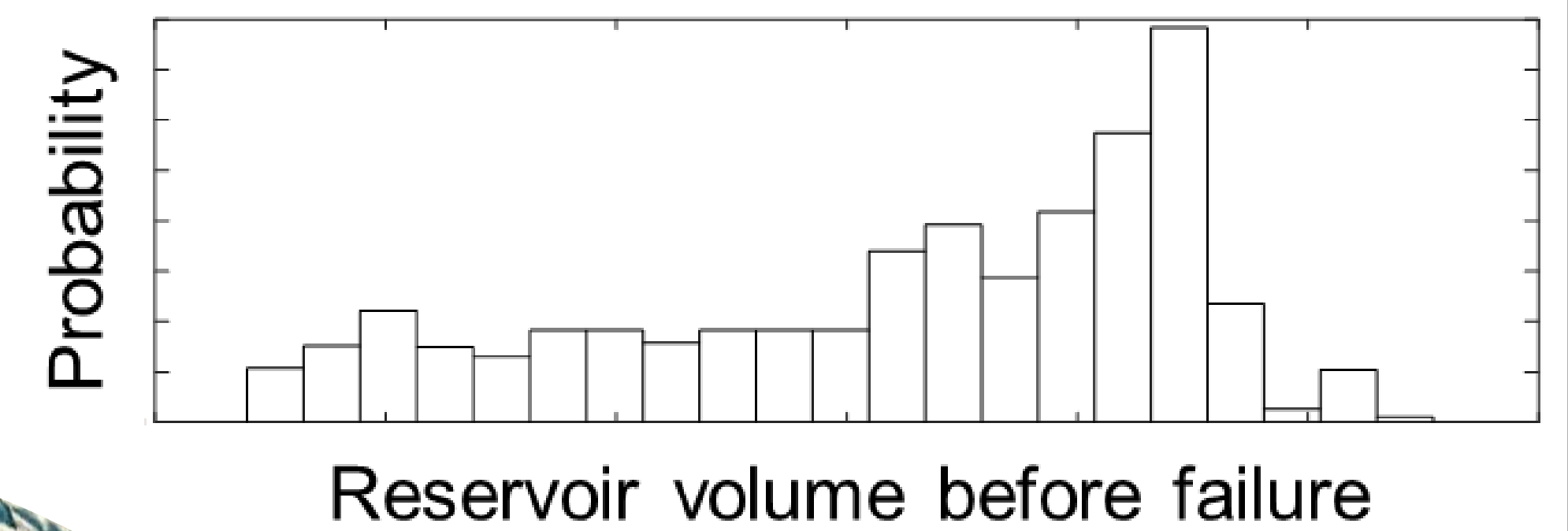
ÉCOLE POLYTECHNIQUE FÉDÉRALE DE LAUSANNE



LABORATOIRE DE CONSTRUCTIONS HYDRAULIQUES

1 Failure occurrence and upstream flood conditions

Millions of years of operation of the system are simulated accounting for epistemic uncertainty, hazard coincidences, interactions, and intra-hazards. Failure probabilities and other data are obtained using the Generic Multi-Risk (GenMR) framework [2].

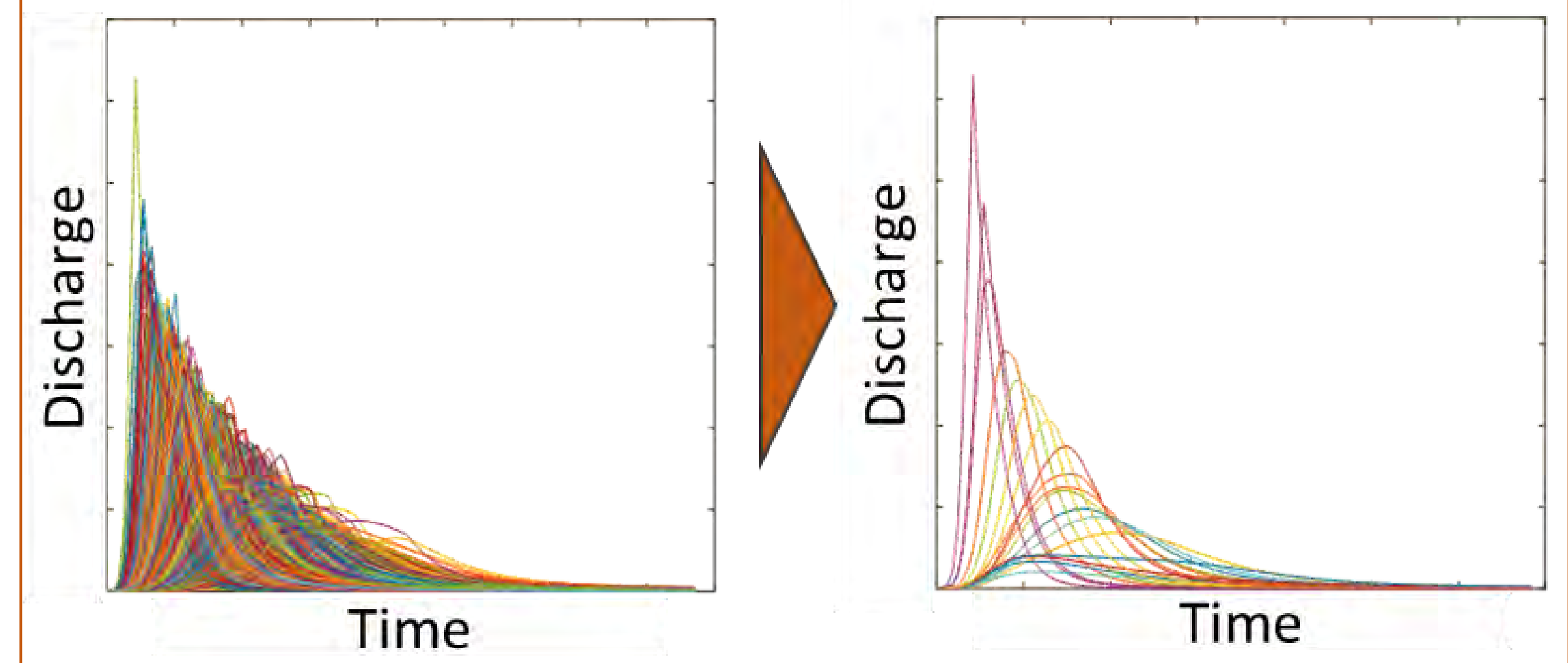


2 Breach formation

The methodology is applied to earthfill dams, where a large degree of uncertainty is associated with the formation of breaches [3].

3 Breach catalogue

Clustering is used to select a representative catalogue of breaches from which any breach can be derived. Detailed hydraulic simulations are only computed for the hydrographs derived from the catalogue.



References

[1] Darcourt, A. 2016. Numerical simulation of dam break flood wave propagation in the Rhone River. From dam breach formation to loss assessment. M.Sc. Thesis. School of Architecture, Civil, and Environmental Engineering, École Polytechnique Fédérale de Lausanne.

[2] Matos, J. P., Mignan, A., Schleiss, A. J. The Generic Multi-Risk GenMR framework. Part B, Vulnerability of large dams considering hazard interactions. Swiss Competence Center on Supply for Electricity Annual Conference 2015. Neuchâtel, 10-11 September 2015.

[3] Froehlich, D. C. 2008. Embankment Dam Breach Parameters and Their Uncertainties. Journal of Hydraulic Engineering doi:10.1061/(ASCE)0733-9429(2008)134:12(1708).

[4] Suppasri, A., E. Mas, I. Charvet, R. Gunasekera, K. Imai, Y. Fukutani, Y. Abe, and F. Imamura. 2013. Building damage characteristics based on surveyed data and fragility curves of the 2011 Great East Japan tsunami. Natural Hazards 66, 319-341. doi:10.1007/s11069-012-0487-8.

Risk GOveRnance of electricity pOrtfolioS (RIGOROUSt): Cross-technology and spatial tradeoffs of multiple risks

Evelina Trutnevyte, Philip Berntsen, Theresa Knoblauch, Sandra Volken
ETH Zurich, Department of Environmental Systems Science (USYS), USYS Transdisciplinarity Lab

RIGOROUSt aims (2015-2018)

- Examine cross-technology and spatial tradeoffs of risks to human safety, health, natural and built environment posed by the Swiss electricity portfolio as a whole (not only individual technologies);
- Adopt a more open view to risk, including uncertain outcomes, likelihoods, and uneven knowledge robustness;
- Build two interactive tools RISKMETERS by linking electricity portfolio model EXPANSE with the risk information;
- Measure expert, stakeholder, and public preferences concerning these risk tradeoffs.

Maps: swisstopo, BFE

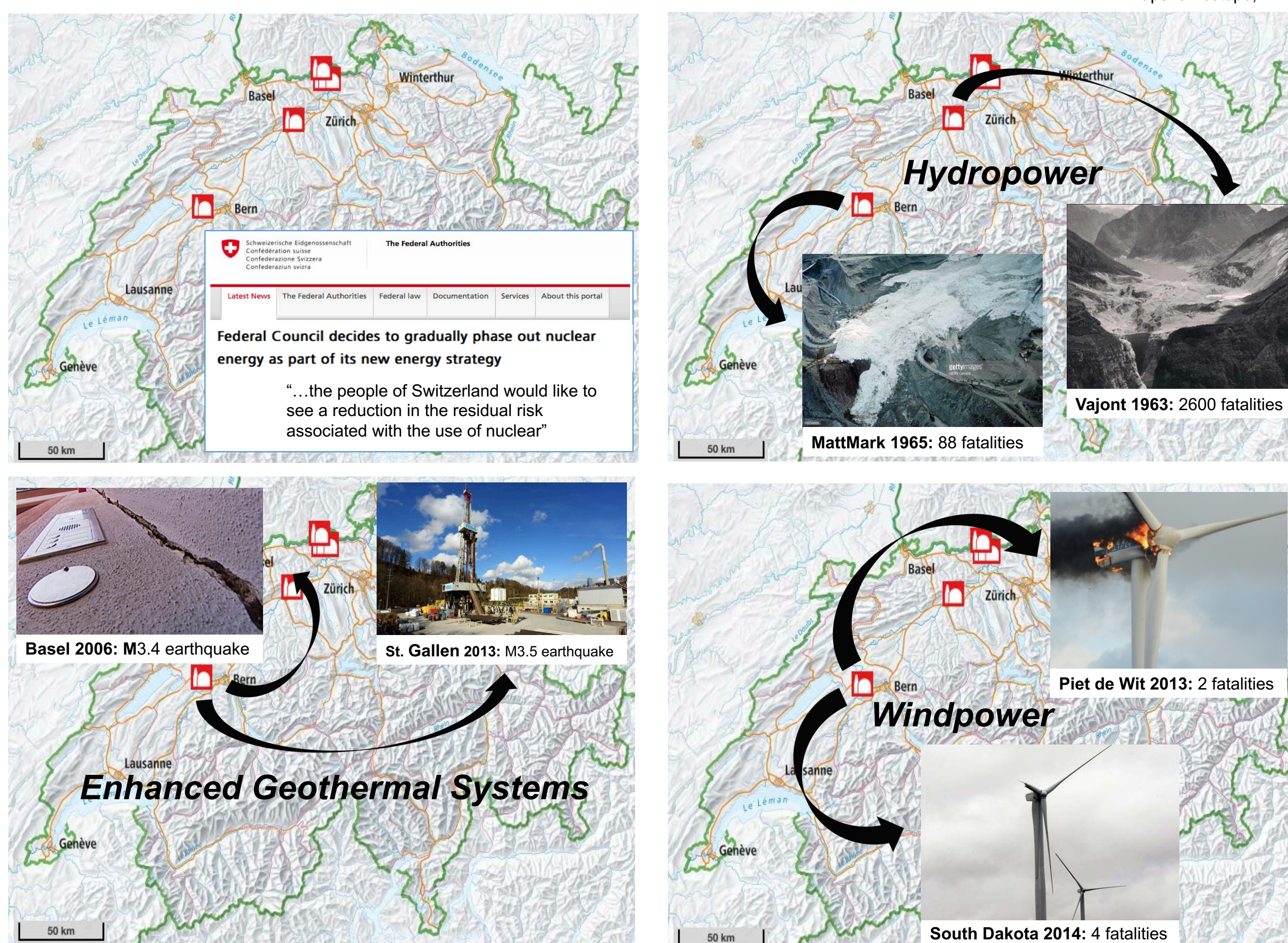


Figure 1. Stylized illustration of risk tradeoffs in the Swiss electricity portfolio.

Highlights from year 1: Expert elicitation on induced seismicity by Enhanced Geothermal Systems (EGS)²

Aim: Evaluate induced seismicity hazard and risk for EGS and characterize uncertainty, using the judgments of knowledgeable experts.

Method: We used the state-of-the-art expert elicitation method¹ that combines technical analysis with insights from behavioural science. In interviews experts were given a harmonized scenario of an EGS plant, its stimulation and operation parameters, geological context, and exposed population and structures. The quantitative judgements were then elicited on: (i) lower bound, upper bound and best-guess exceedance probabilities of $M \geq 3$ and $M \geq 5$ induced events, and (ii) economic loss, injuries and fatalities in the cases of $M=3$ and $M=5$ induced events.

Selected results²: 14 experts from 12 organizations in 6 countries were interviewed, covering 300 years of experience with natural seismicity, 231 years with induced seismicity, and 137 years with seismic risk. Selected results are shown in Figure 2.

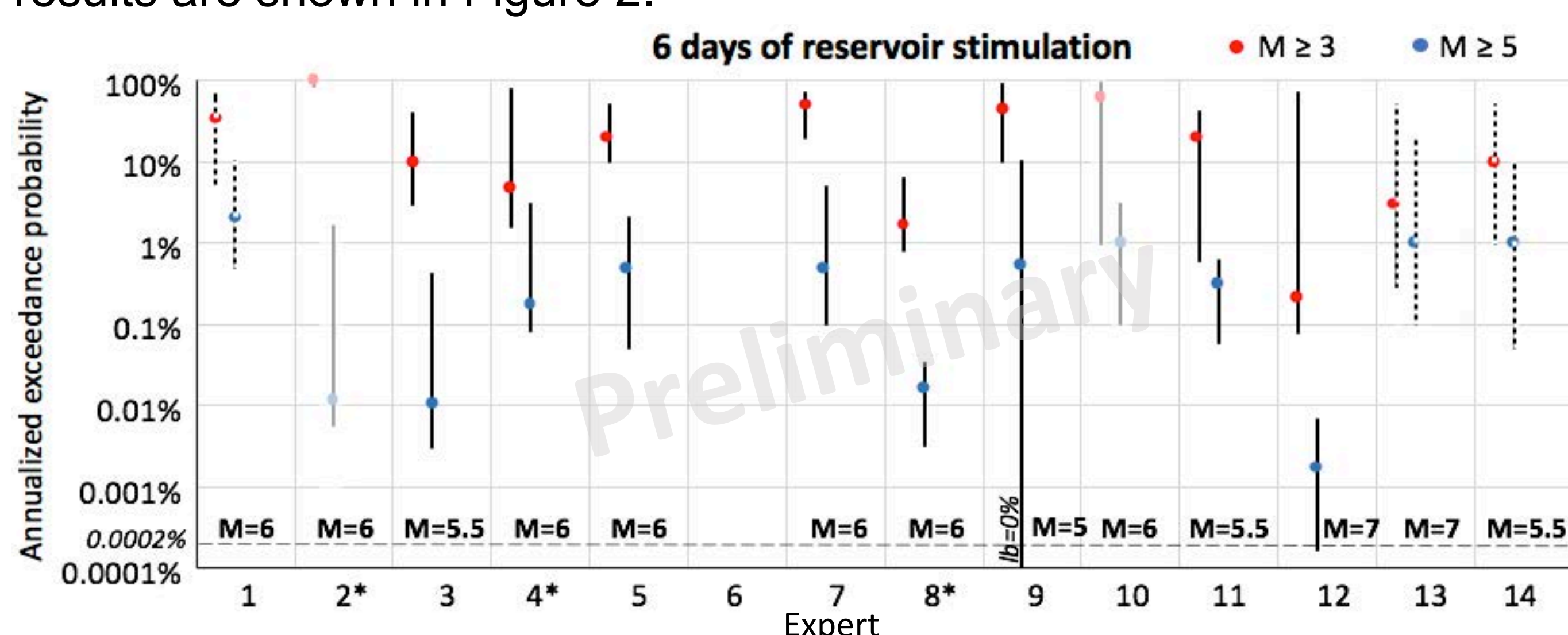


Figure 2. Annualized exceedance probabilities of induced events during EGS reservoir stimulation. For $M \geq 3$ (red circles) and $M \geq 5$ (blue circles) experts provided their lower bound, upper bound and best-guess estimates. For maximum observed magnitude (green triangles) experts estimated the maximum observed magnitude at 0.0002% annualized probability only. These judgements are conditional to the given EGS scenario².

References

- 1 Morgan M.G. 2014. Use (and abuse) of expert elicitation in support of decision making for public policy. Proceedings of the National Academy of Sciences 111(20), 7176-7184.
- 2 Trutnevyte E., Azevedo I.L. 2016. Expert agreements and disagreements about EGS induced seismicity. Under preparation.
- 3 Densing M., Panos E., Hirschberg S. 2016. Meta-analysis of energy scenario studies: example of electricity scenarios for Switzerland, Energy 109, 998-1015.
- 4 Trutnevyte E., 2016. Does cost optimization approximate the real-world energy transition? Energy 106, 182-193.

Highlights from year 1: Assessment of the diversity of existing Swiss electricity supply scenarios⁵

Aim: Assess the diversity of existing Swiss electricity supply scenarios³ and identify the futures that have not been represented in the scenarios.

Method: EXPANSE model⁴ (EXploration of PATterns in Near-optimal energy ScEnarios) was built for the Swiss electricity supply sector in 2035 and 2050. EXPANSE is a technology-rich, bottom-up energy system model with 1-hour dispatch. EXPANSE uses Modelling to Generate Alternatives technique to produce and analyze large ensembles of diverse, technically-feasible electricity supply scenarios.

Selected results⁵: EXPANSE reproduced the breadth of technology deployment levels in the existing Swiss scenarios (Figure 3). Existing scenarios thus sufficiently cover the individual technology contributions. Looking at the scenarios as a whole, we identified lack of scenarios that: (i) in 2035 assume higher electricity demand and higher penetration of solar PV, wind, and biomass, and (ii) in 2050 assume lower penetration of renewable technologies.

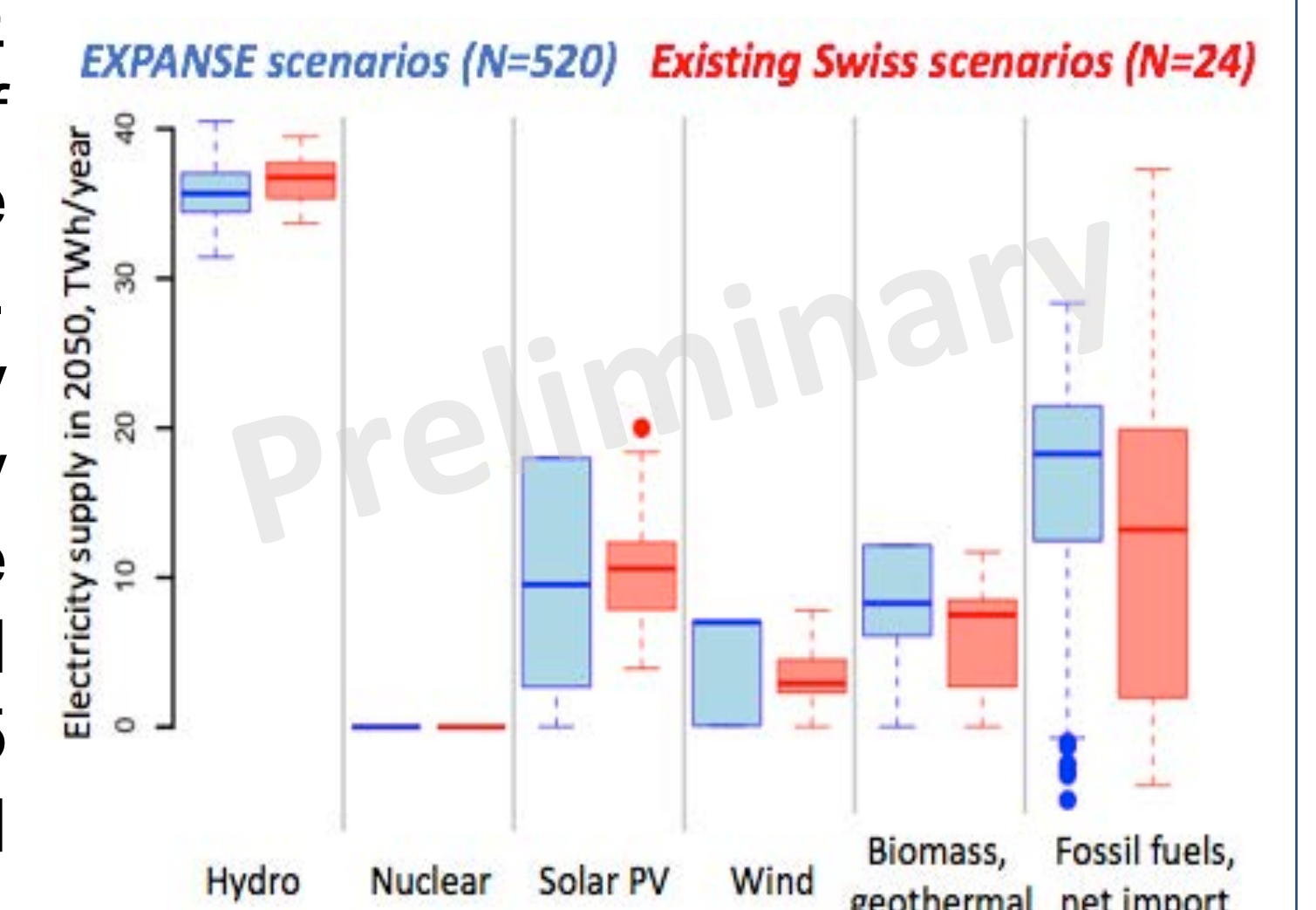


Figure 3. Technology-by-technology comparison of EXPANSE and existing Swiss electricity scenarios⁵.

Highlights from year 1: Laypeople's beliefs and perceptions of risks posed by the Swiss electricity generation⁷

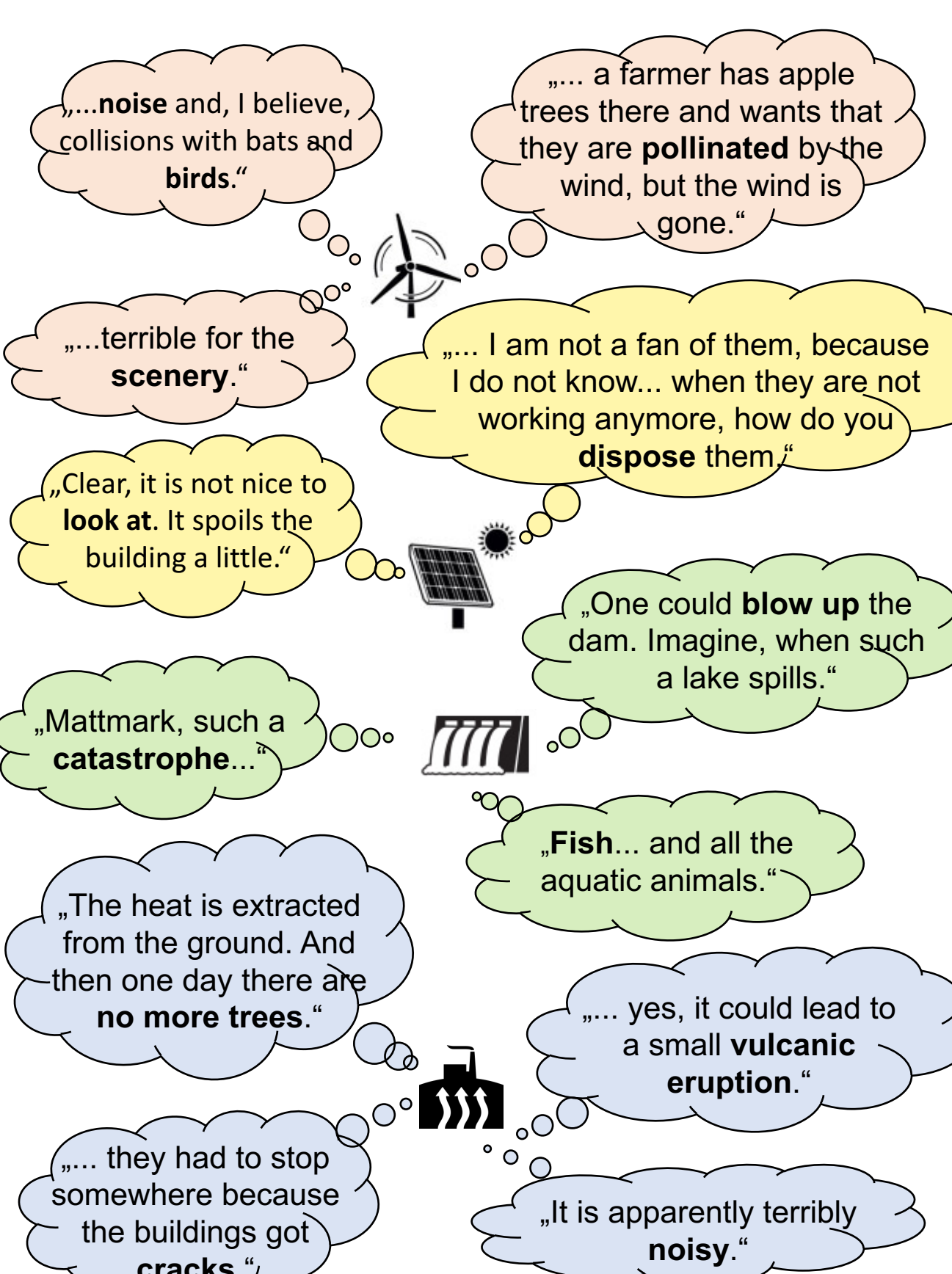


Figure 4. Examples of laypeople awareness and misconceptions of electricity generation risks⁷.

Aim: "Strategically listen"⁶ to the beliefs and perceptions of the Swiss population about electricity generation risks in order to identify information needs and prepare for RISKMETERS.

Method: We conducted 12 semi-structured laypeople interviews on (i) their subjective knowledge about electricity technologies, (ii) types, likelihoods and consequences of associated risks, and (iii) trust, concern and acceptance of the risks.

Selected results⁷: We found that most of the interviewees could think in risk tradeoffs, e.g. that nuclear phase-out requires new technologies with own risks to be deployed. Some misconceptions were identified too (Figure 4).

Highlights from year 1: Risk communication for low-probability high-consequence EGS induced seismicity⁸

Aim: Test how different formats of information about EGS induced seismicity affect the public's perception of this information in terms of understandability, trust, and concern? Compare EGS and shale gas.

Method: A representative online survey (N=590) was conducted. Using an experimental design, 6 groups of respondents received the same EGS induced seismicity risk information in different formats: qualitative, quantitative, quantitative with risk comparison, and all these with or without a commentary about uncertainties and limited expert confidence. The same procedure was repeated for the potentially-contested shale gas.

Selected results⁸: We found that technology (EGS vs. shale gas) has a significant effect on how the identical risk information is perceived in terms of trust and concern. Additional commentary about uncertainties and limited expert confidence significantly reduced the clarity and understandability of information as well as increased concern.

⁵ Berntsen P., Trutnevyte E. 2016. Ensuring the diversity of national energy scenarios: Bottom-up energy system model with Modeling to Generate Alternatives. Under review.
⁶ Pidgeon N., Fischhoff B. 2011. The role of social and decision sciences in communicating uncertain climate risks. Nature Climate Change 1(1): 35-41.
⁷ Volken S., Wong-Parodi G., Trutnevyte E. 2016. Laypeople's beliefs and acceptance of risks of electricity generation technologies. Under preparation.
⁸ Knoblauch T., Stauffacher M., Trutnevyte E. 2016. Communicating low-probability high-consequence risk, uncertainty and expert confidence: Induced seismicity of deep geothermal energy and shale gas. Under review.

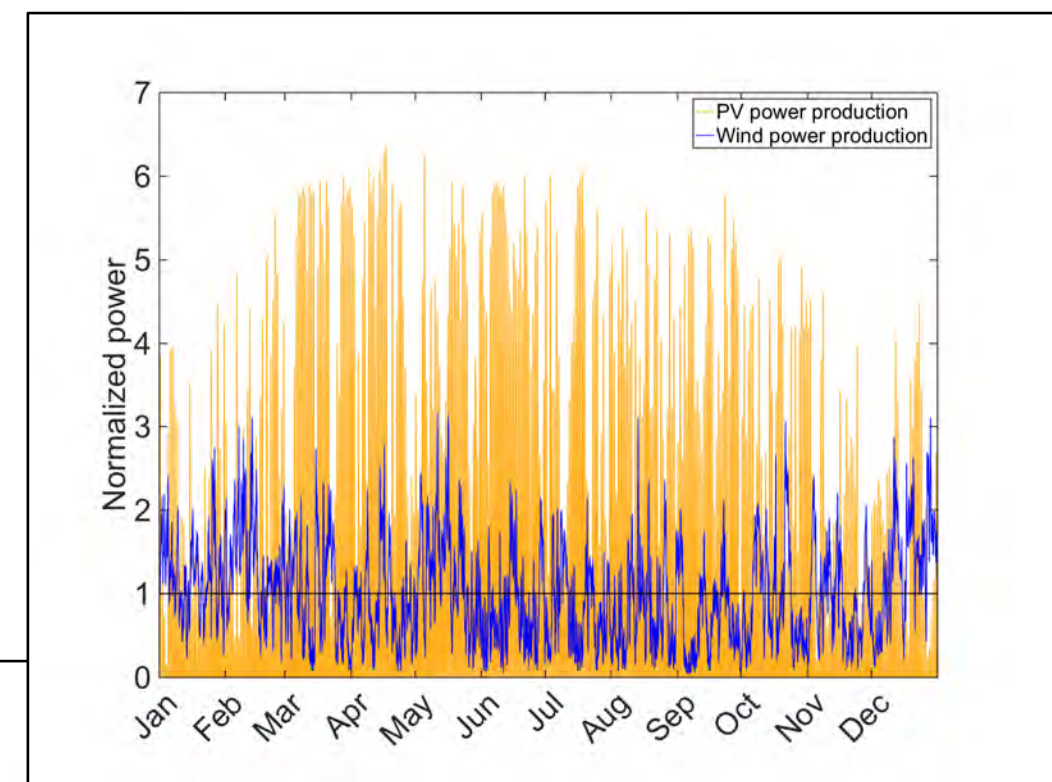
Impact of combined wind and solar energy on the Swiss electricity system

Jérôme Dujardin ⁽¹⁾, Annelen Kahl ⁽¹⁾, Bert Kruyt ^{(1) (2)}, Michael Lehning ^{(1) (2)}
(1) ENAC, EPFL, Lausanne, (2) WSL Institute for Snow and Avalanche Research, Davos

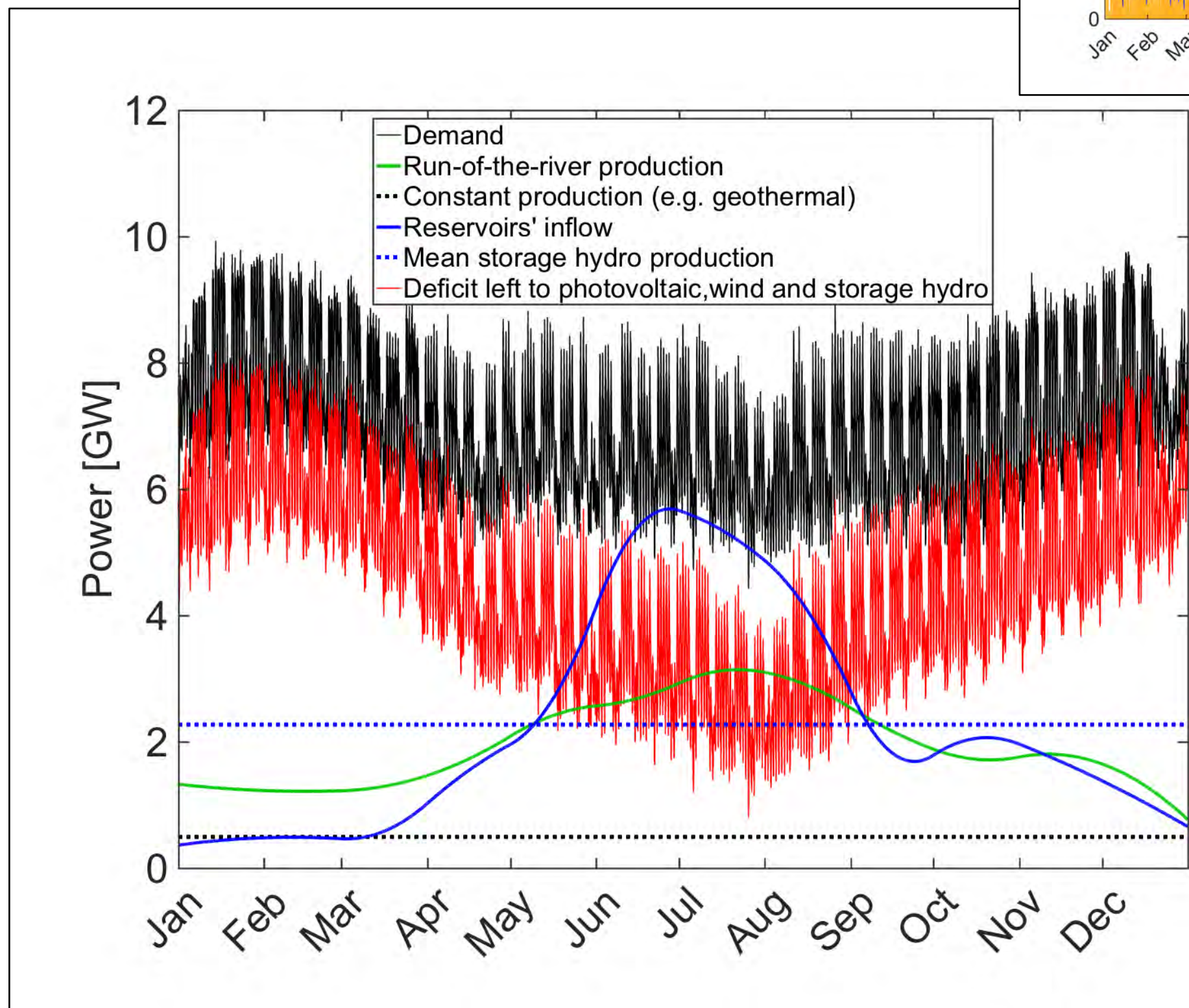


1. Introduction

- Electricity in Switzerland in 2014:
 - Demand: 61787 GWh
 - Storage hydropower: 19888 GWh
 - Run-of-the-river: 17243 GWh
 - Nuclear + Other: 30325 GWh



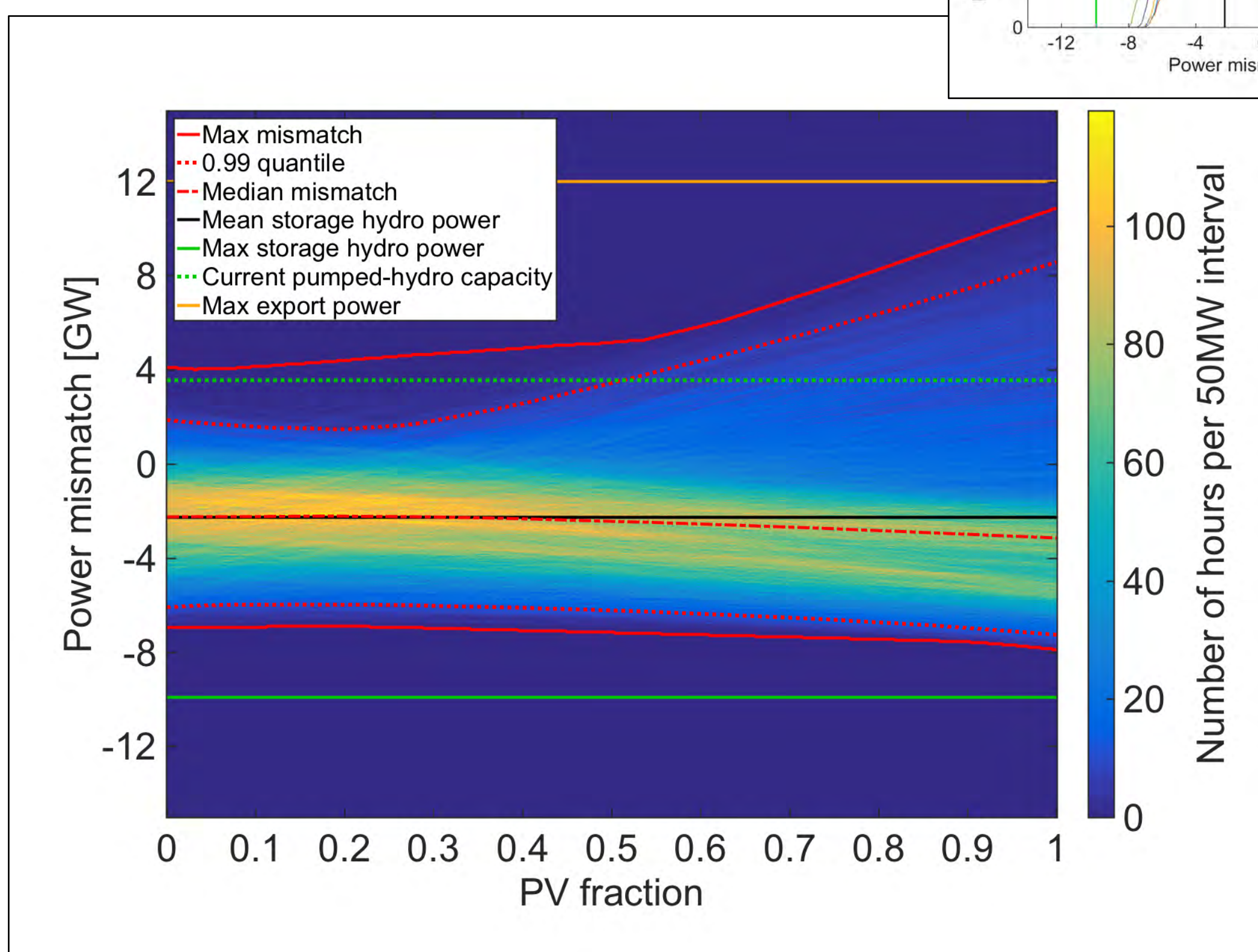
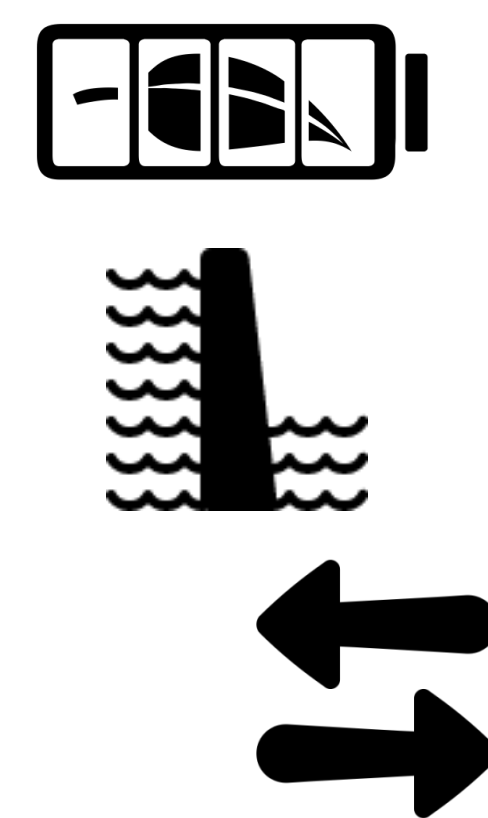
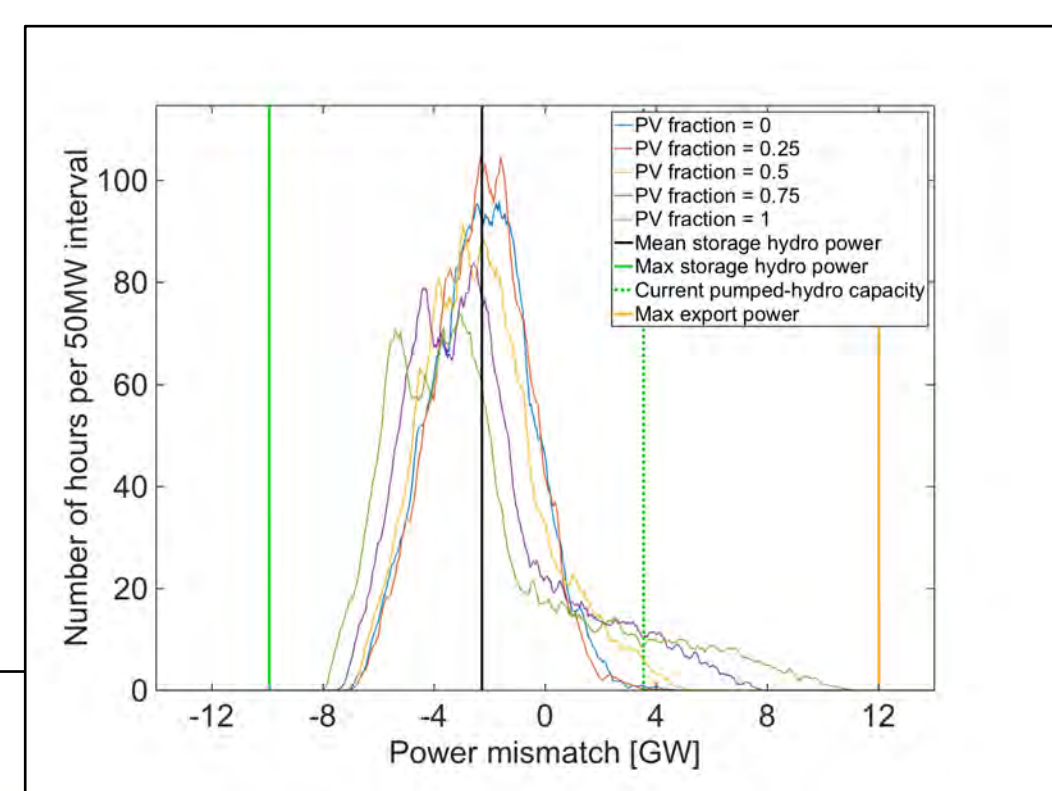
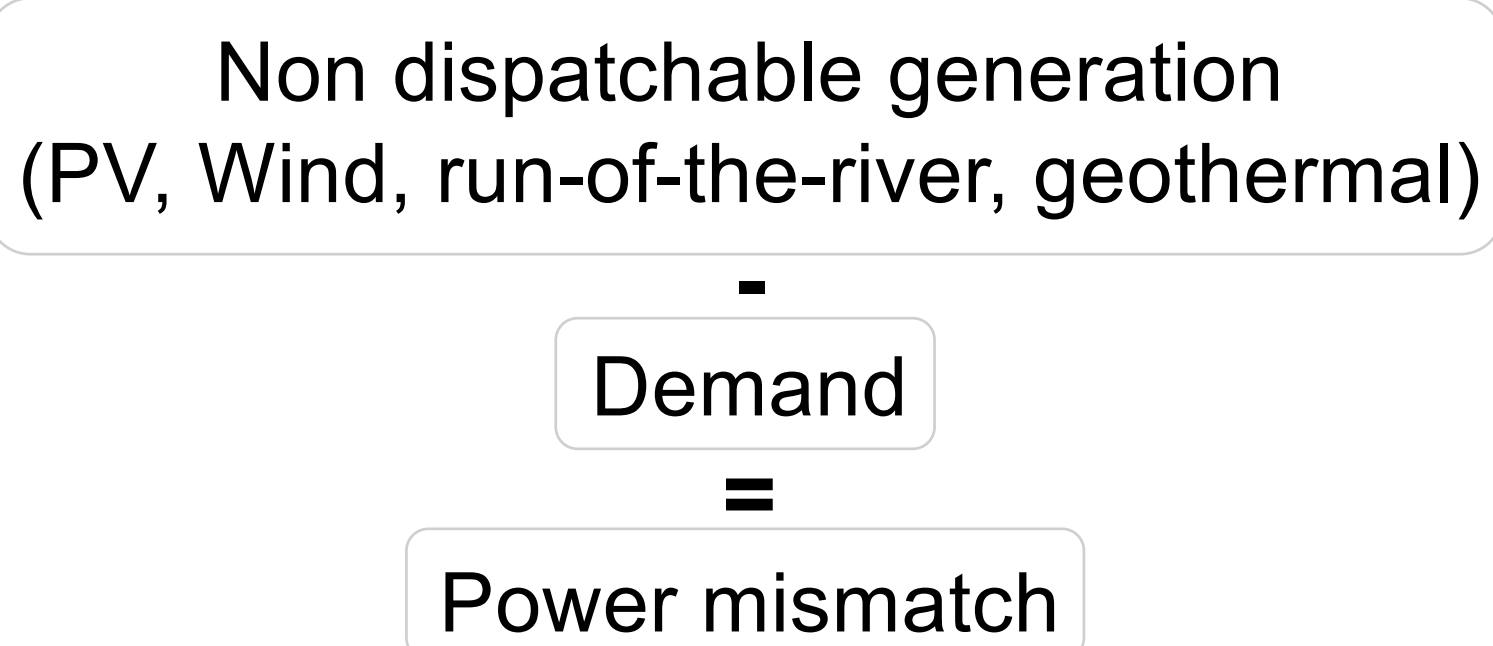
- Impact of a fully renewable production?



Swiss power production and demand in 2014

- Replace 24656 GWh with:
 - Geothermal: 4325 GWh
 - PV+Wind: 20331 GWh
- Correlation Hydro / PV and anticorrelation with demand
 - Seasonal storage?
 - Role of storage hydro?
- High share of PV+Wind and high variability
 - Short term storage?
 - Role of storage hydro?

2. Methods



Distribution of power mismatch (non dispatchable generation – demand)

Balancing mismatches:

- Deficits:
 - Dispatchable generation (storage hydropower)
- Overproduction:
 - Short term storage
 - + Export

- Balancing of instantaneous power mismatch through short term storage (within capacity limits)
- Incorporating reservoir inflow and stored energy
- Analyzing energy balance of the entire system

- Optimal use of storage hydropower
- Required import/export

4. Conclusion

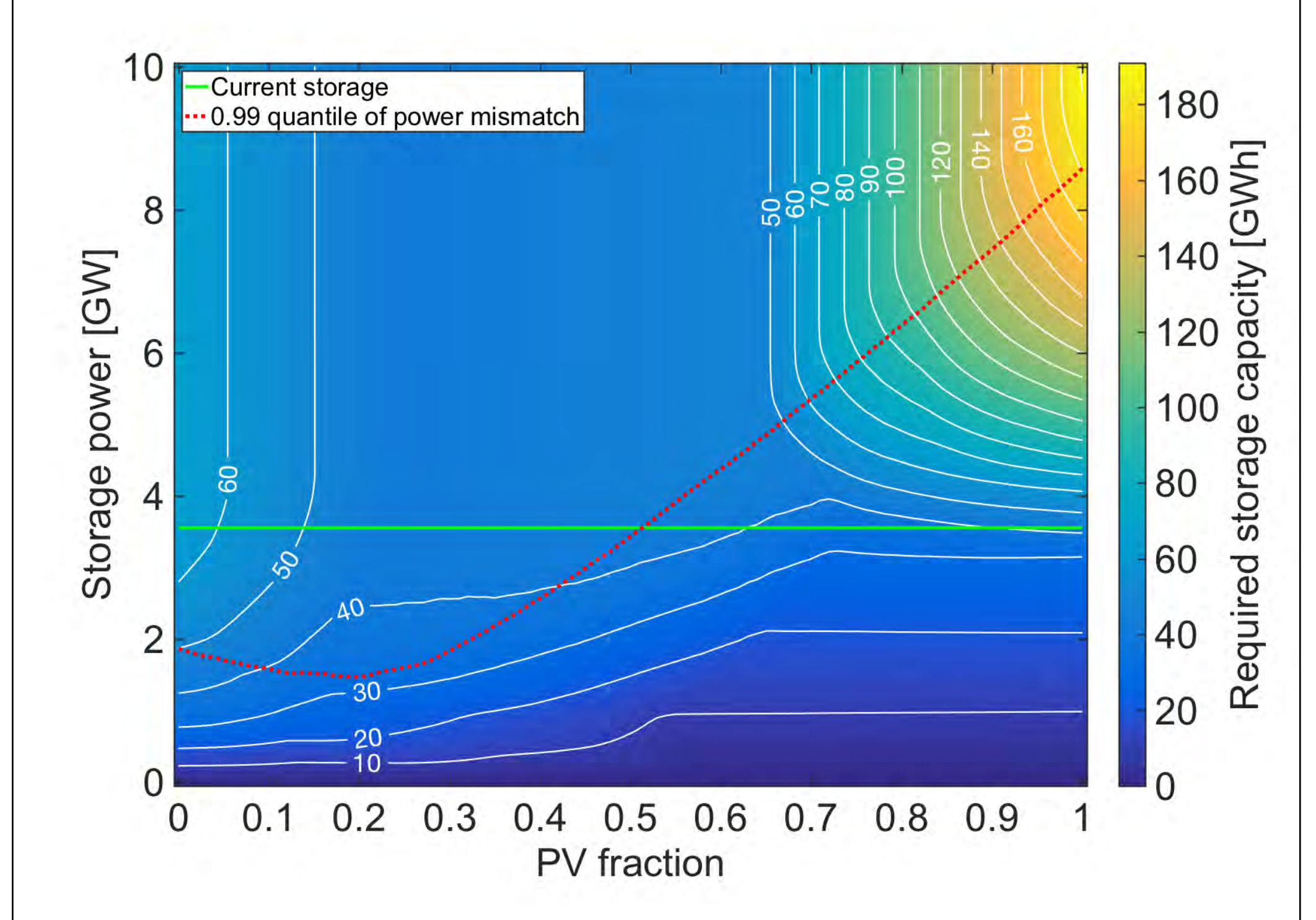
- With the current pumped hydro capacity (including Nant de Drance and Limmern) :
- PV should contribute 20 – 60 % (4 – 12 TWh/year or 2.9 – 8.6 GW capacity)
 - Wind should contribute 40 – 80% (8 – 16 TWh/year or 4.4 – 10.2 GW capacity)
 - 3.9 – 5.2 TWh of required import if reservoir capacity is not increased
 - 10 – 30% of increased reservoir capacity to stay at current import

Data

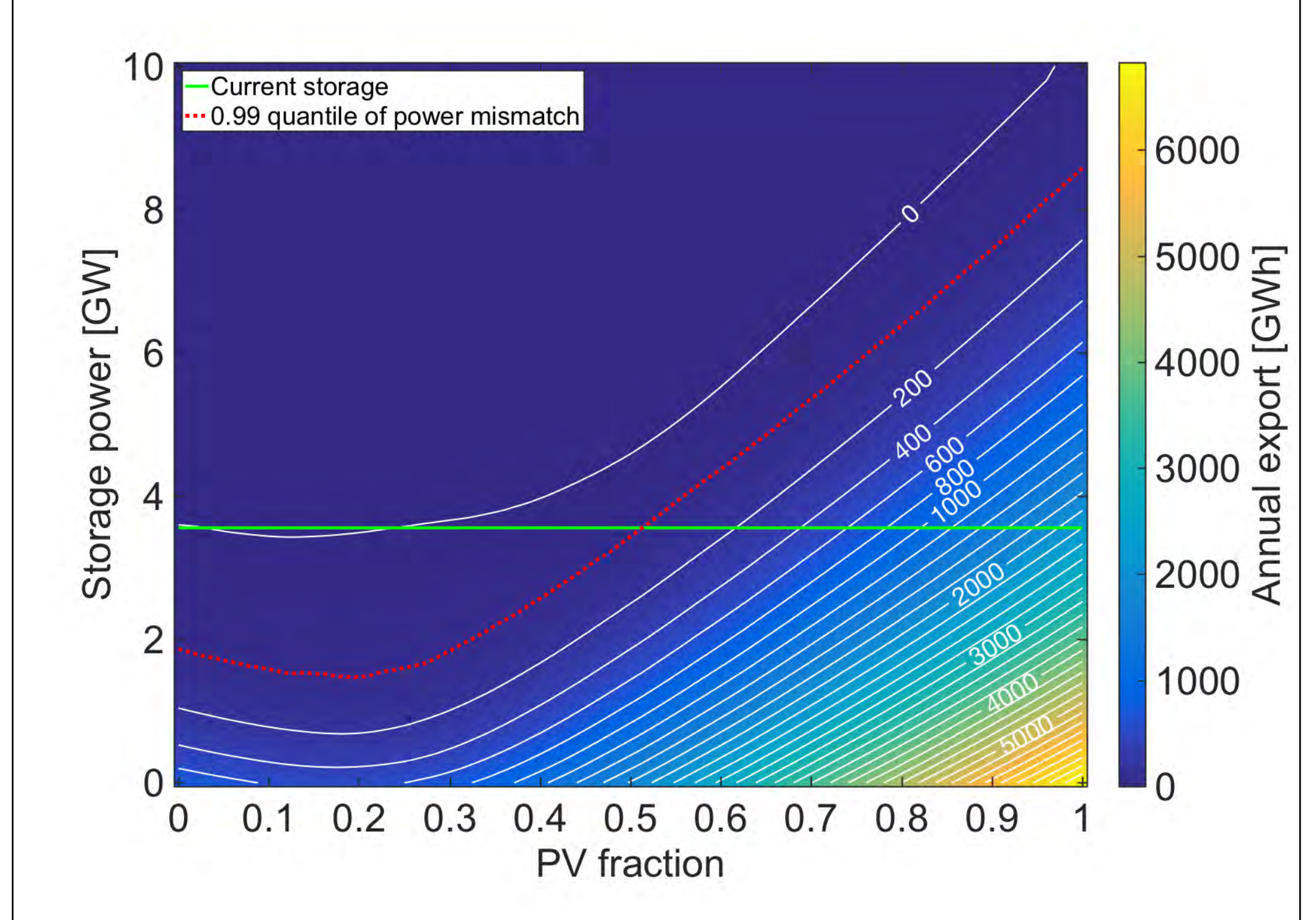
- PV production time series based on satellite-derived irradiance (MeteoSwiss)
- Wind production time series based on wind speed measurements (MeteoSwiss)
- Demand time series from Swissgrid (publicly available on their website)
- Run-of-the-river monthly production and reservoirs' inflow from the Swiss Federal Office of Energy (SFOE)
- Storage hydropower and pumped hydro characteristics from WASTA database (SFOE)

3. Results

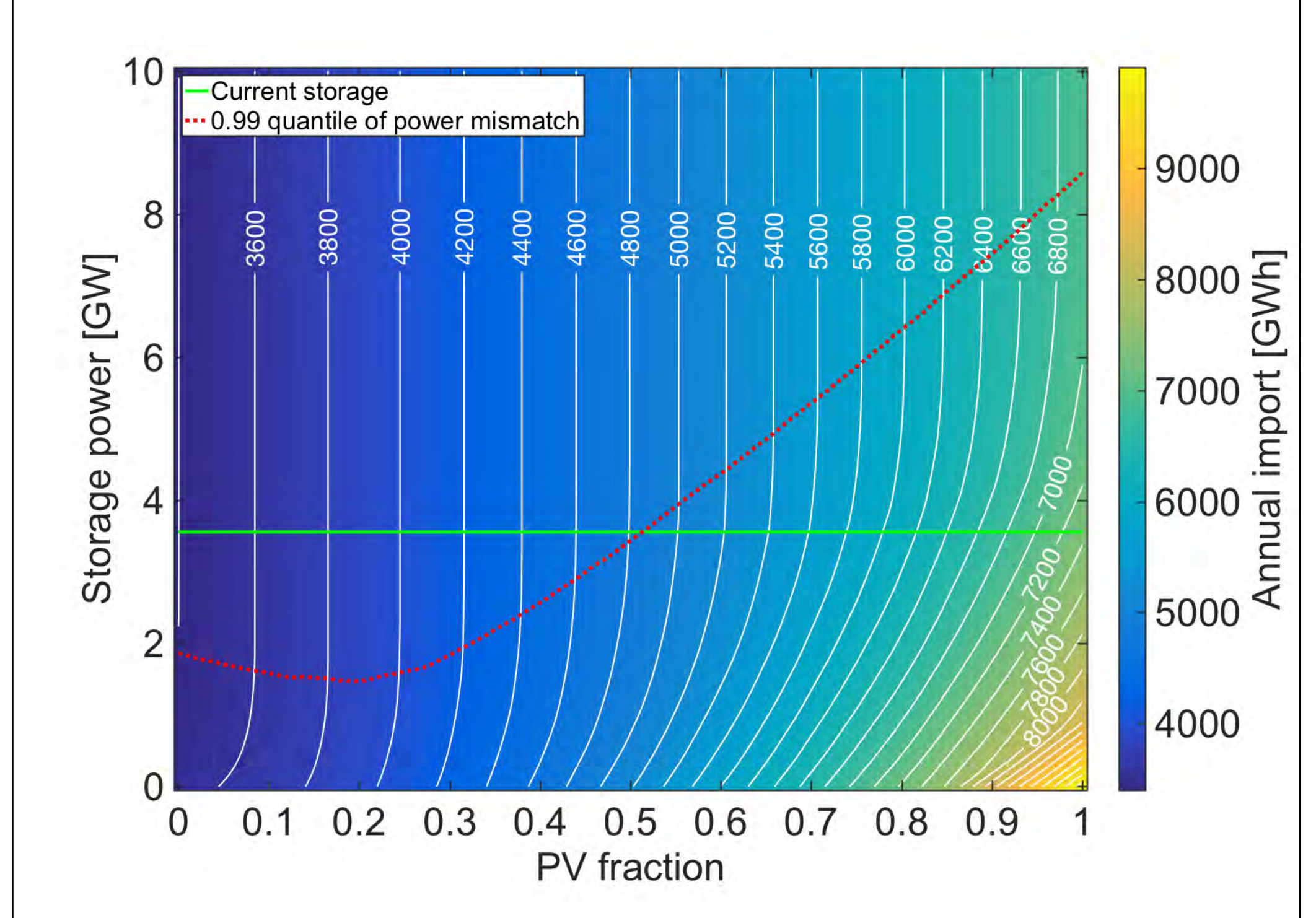
Required storage capacity



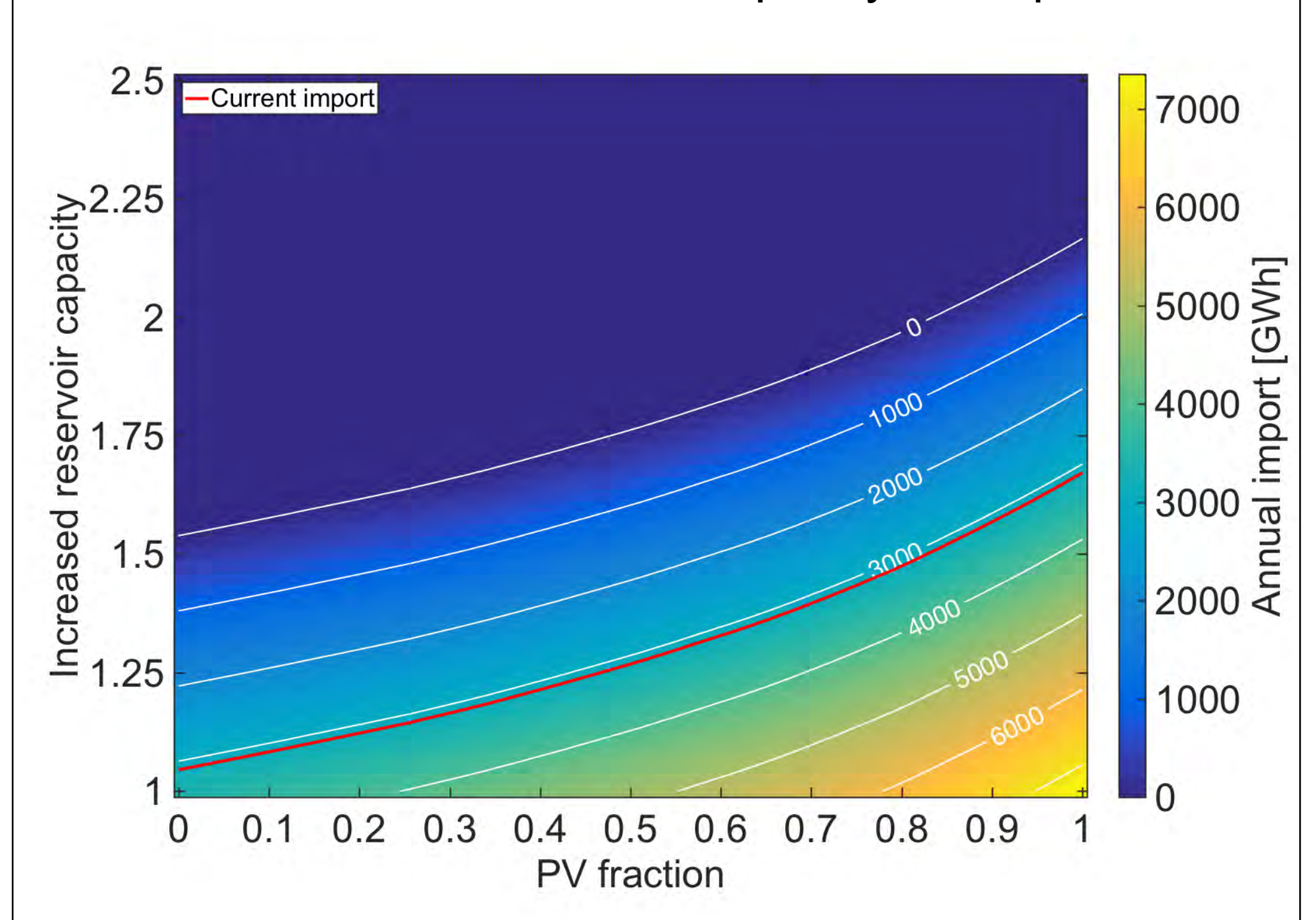
Annual forced export induced by overproduction



Annual required import



Effect of increased reservoir capacity on import



A Bayesian Hierarchical Model for Hydropower Dam Accidents Risk

Anna Kalinina (anna.kalinina@psi.ch), Matteo Spada, Peter Burgherr
Technology Assessment Group, Paul Scherrer Institute, CH-5232, Villigen, Switzerland

Motivation

- Provide a comprehensive **update and extension** both in terms of available **historical experience** and advanced **statistical methods for the actual analysis of the hydropower accident data**.
- The aim is to demonstrate the advantages of a **Bayesian Hierarchical approach** to model **generic and representative frequency and severity distributions for different characteristics of the hydropower accident data**.

Data

For this study PSI's Energy-related Severe Accidents Database (ENSAD) was updated with new information about worldwide hydropower dam accidents. Data in the time frame 1896-2014 were analyzed. **Figure 1** presents the distribution of accidents per year, whereas the number of fatalities associated with each accident is given in **Figure 2**. To allow comparative evaluation of accident frequencies for hydropower dams among different characteristics, frequencies were normalized by the unit of operational dam-year, yielding the number of accidents per dam-year. A cumulative plot of the operational dam years is given in **Figure 3**.

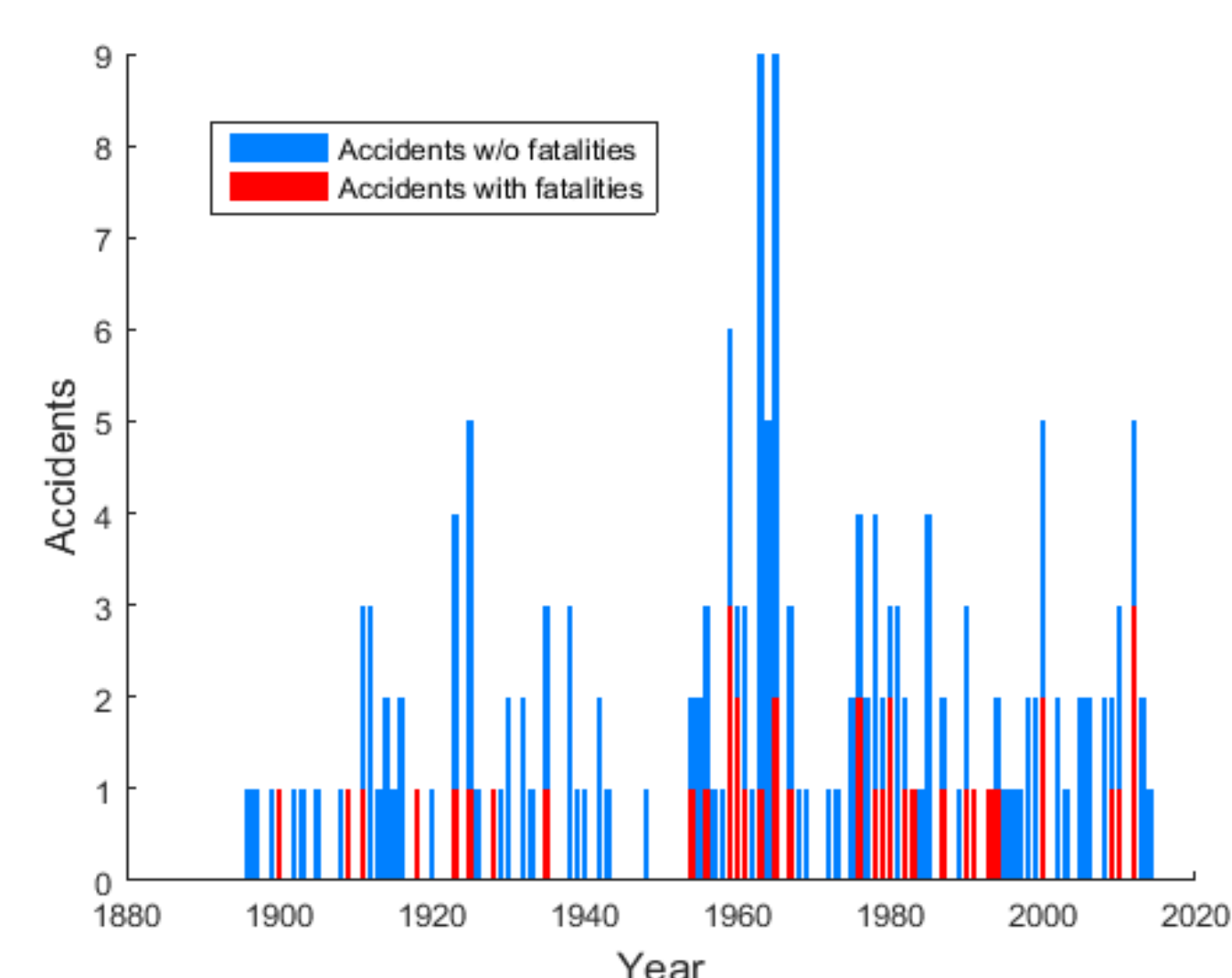


Figure 1. Accidents per Year

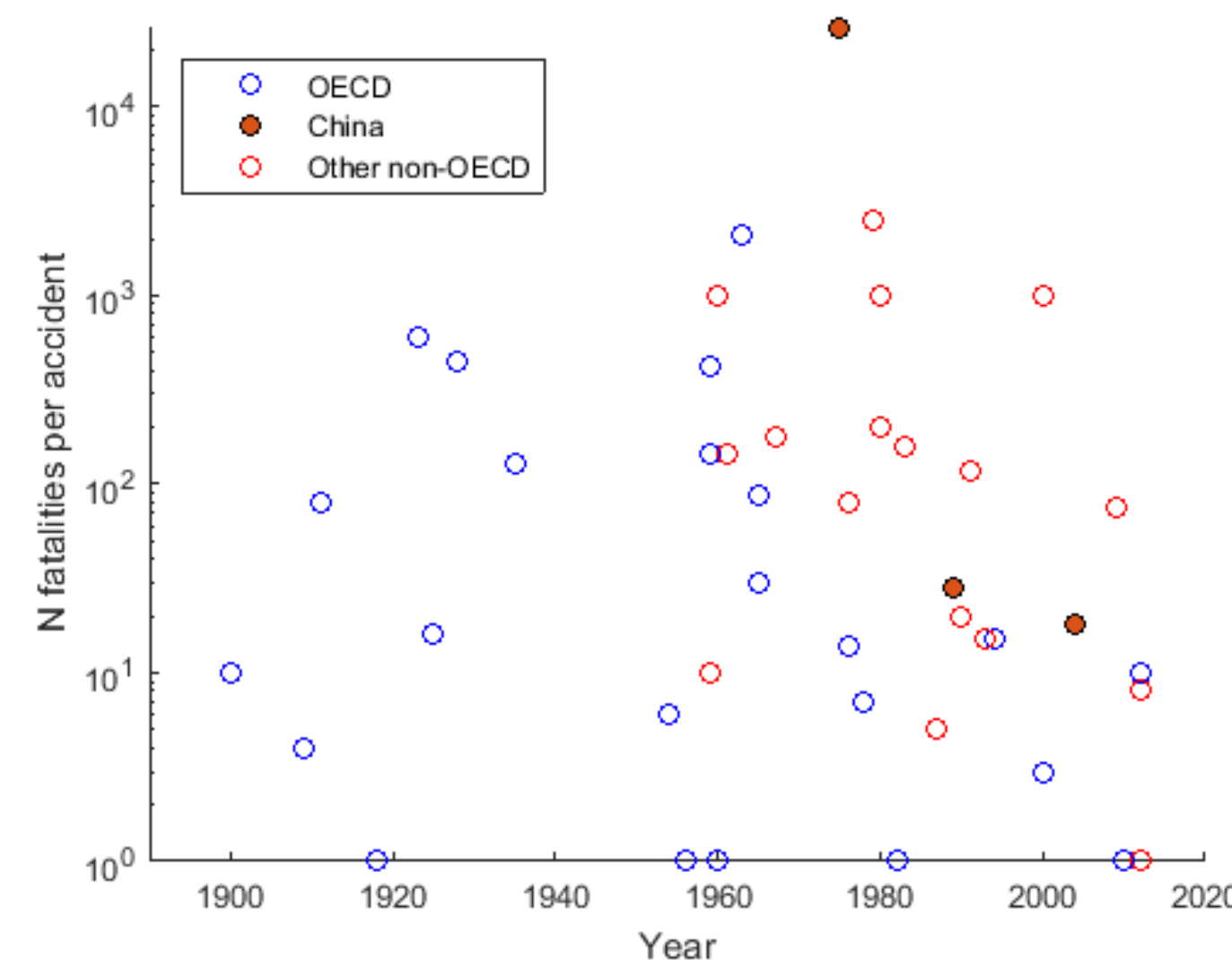


Figure 2. Fatalities per Accident

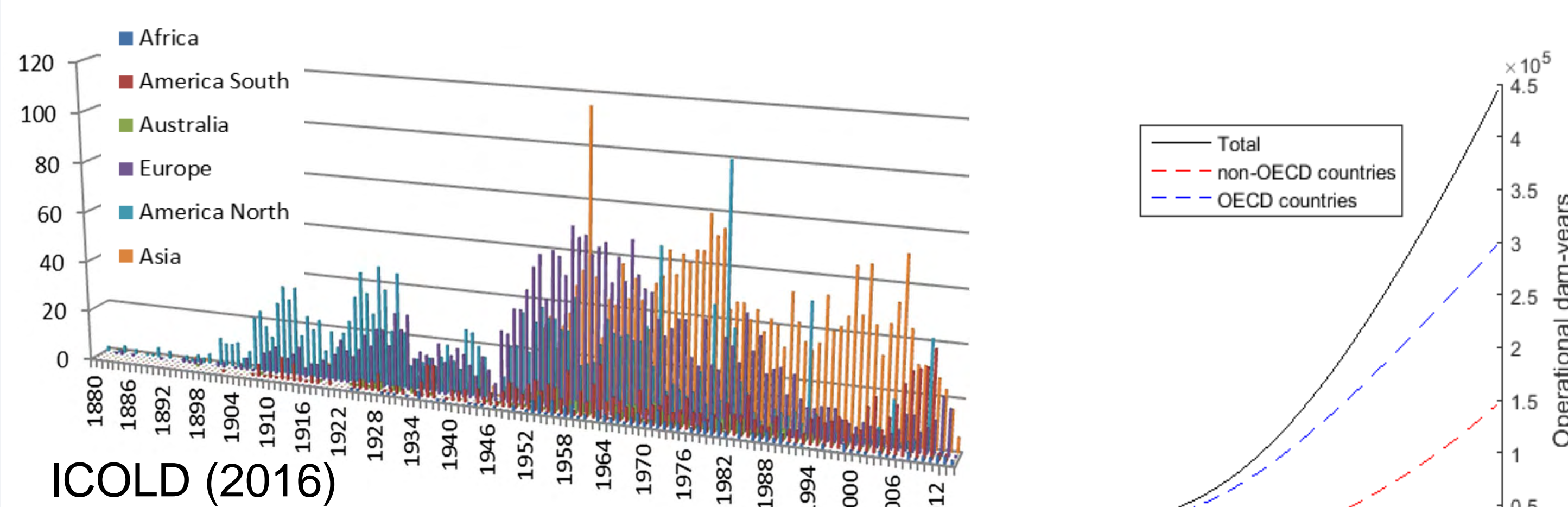


Figure 4. Number of Hydropower Plants

Figure 3. Operational Dam Years

Subcategorization

The distinction of the accident data between categories has proven to be meaningful. One example can be the distinction between OECD and non-OECD countries, because of the substantial differences in management and regulatory frameworks between countries (Hirschberg et al., 1998). Another example is the distinction between time sub-periods due to the unequal development of the large hydropower industry in different geographical locations (e.g., see Figure 4).

Considered categories in this study:

- Country clusters (OECD, non-OECD)
- Types of the accident cause (Natural, Technical, Man-Made)
- Dam types (Buttress, Embankment, Arch/Multiple Arch, Gravity)
- Physical parameters of the dam (dam height: <15 m, >15 m)
- Stage of the dam life cycle (Construction, First Filling, <5 % >5years)
- Time sub-periods
- Failure vs. non-Failure of the dam

References

- Eckle, P. & Burgherr, P. 2013. Bayesian data analysis of severe fatal accident risk in the oil chain. Risk Analysis, 33: 146-60.
- Gelman, A., Carlin, J. B., Stern, H. S. & Rubin, D. B. 2003. Bayesian Data Analysis, Chapman & Hall/CRC.
- Hirschberg S., Spiekerman G. and Dones R. 1998. Severe Accidents in the Energy Sector.
- ICOLD 2016. The World Register of Dams. Online database.

Methodology

A Bayesian Hierarchical modelling framework is employed, which allows creating an exhaustive model of the system with all hydropower dam accidents. This model, along with the multilevel structure, consists of modules or subsets which share certain characteristics (see **Subcategorization** section). The applied accident frequency and severity models with all assigned distributions are given in **Figure 6**.

The Bayesian Hierarchical model pools information from the entire dataset. Employing knowledge about the entire system and interdependence between characteristics of the system, it models frequency and severity values for individual characteristics (see **Figure 5**). In this way the approach compensates the lack of data for individual characteristics, which for other methods leads to a challenge in estimating the likelihood (Gelman et al., 2003). The Bayesian Hierarchical modelling has been successfully applied for the analyses of other energy chains (e.g., Eckle and Burgherr, 2013).

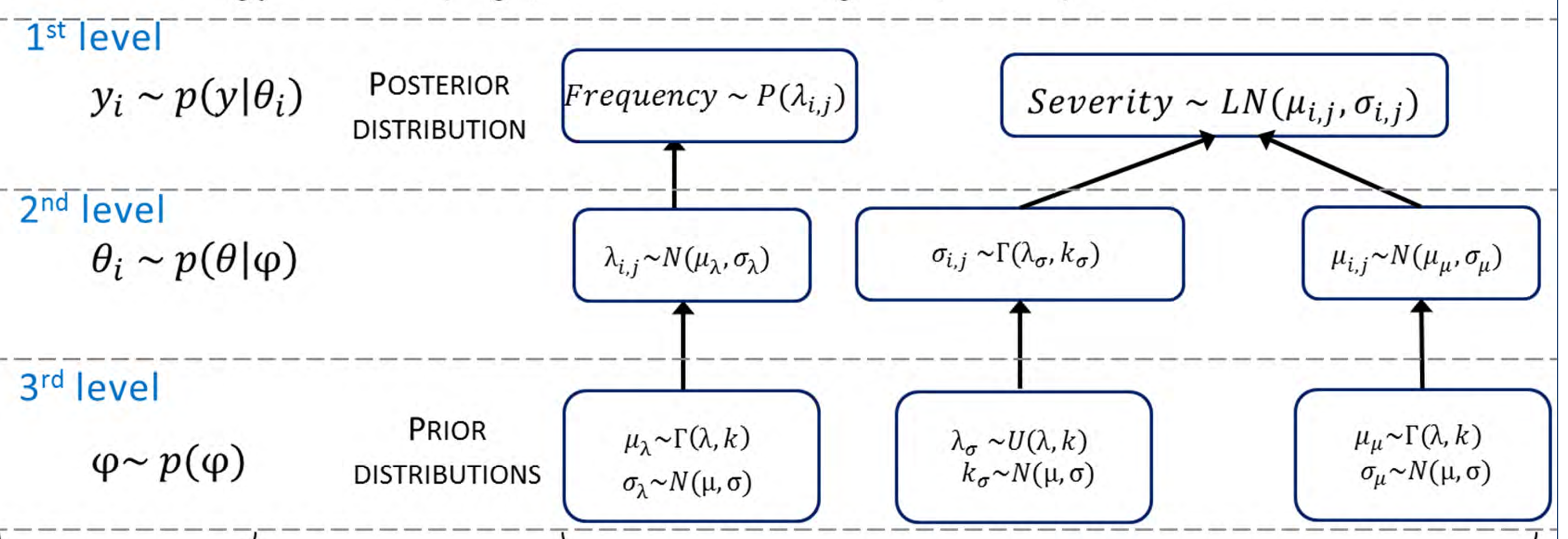


Figure 5. General representation of the Bayesian hierarchy

Figure 6. Applied hydropower risk model

This is a hierarchical model, where:

- y_i represents the observed data;
- $\theta = (\theta_1, \dots, \theta_n)$ and ϕ are parameters, only ϕ has a prior that is set;
- i, j are indexes of the considered categories;
- Software used for computations: MATLAB and OPENBUGS

Preliminary Results

Figure 7 shows the computed frequencies per dam-year and mean number of fatalities per an accident for different dam types and failure vs. non-failure events in OECD and non-OECD countries in the period 1896-2014. Historically the hydropower dam accidents are more rare in OECD than non-OECD countries (with exception of the gravity dam failures), whereas severity of the dam accidents is highly dependent on the type of the dam. The latter can be due to differences in the proportions of the dam types in the country clusters or differences in the structural behavior of dams of different types.

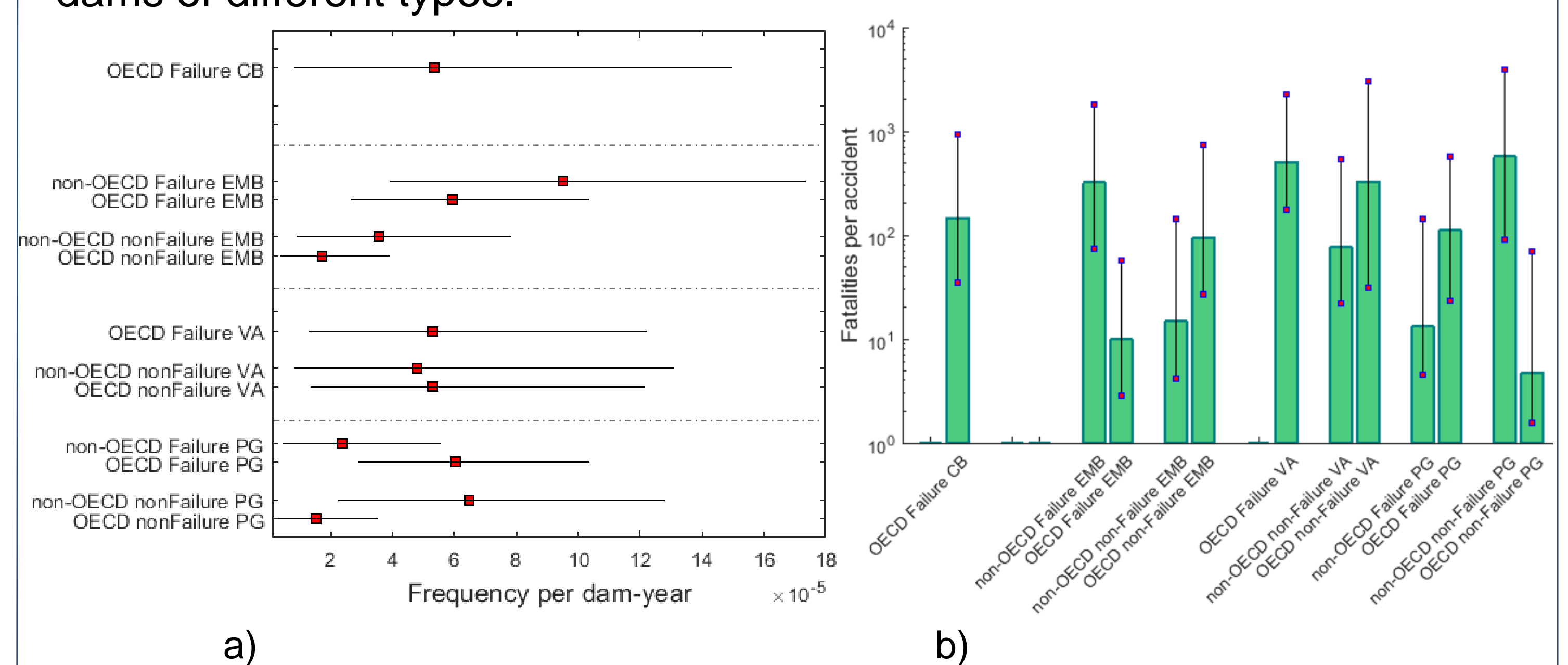


Figure 7. Representation of a) the frequency and b) severity results (mean values with 5% and 95% quantiles of the mean). Where CB = Buttress, EMB = Embankment (Earth fill, Rock fill), VA = Arch and Multiple Arch, PG = Gravity.

Acknowledgment

This work has been completed within the Swiss Competence Center on Energy Research – Supply of Electricity, with the support of the Energy Turnaround National Research Programme (NRP70) of the Swiss National Science Foundation.

The authors express their sincere thanks to Bruno Sudret and Stefano Marelli, Chair of Risk, Safety and Uncertainty Quantification ETH, Zurich, Switzerland, for valuable comments and assistance to the undertaking of the research summarized here.

Physical-based model of a dam failure event

Anna Kalinina (anna.kalinina@psi.ch), Matteo Spada, Peter Burgherr
Technology Assessment Group, Paul Scherrer Institute, CH-5232, Villigen, Switzerland

Motivation

- Establish a comprehensive **framework for the modelling of dam-break consequences** (e.g., life loss) with the help of state-of-the-art techniques.
- Identify **the sources of uncertainty** in each phase of the modelling.
- Propagate those uncertainties through the established model to determine **uncertainty in the output**.

Physical Model of the Dam Break Event

Basic Assumptions:

- Large arch concrete dam (height ca. 100 m, reservoir volume ca. 100 Mio m³):
 - Representative type for large hydropower dams in Switzerland
 - Extensively addressed in literature
- Complete and instantaneous failure of the dam:
 - Worst-case scenario as well as sensitivity cases
 - We are not interested in the cause of the dam failure
- Consideration of aspects within structural safety is outside the focus, since it is more relevant for embankment dams

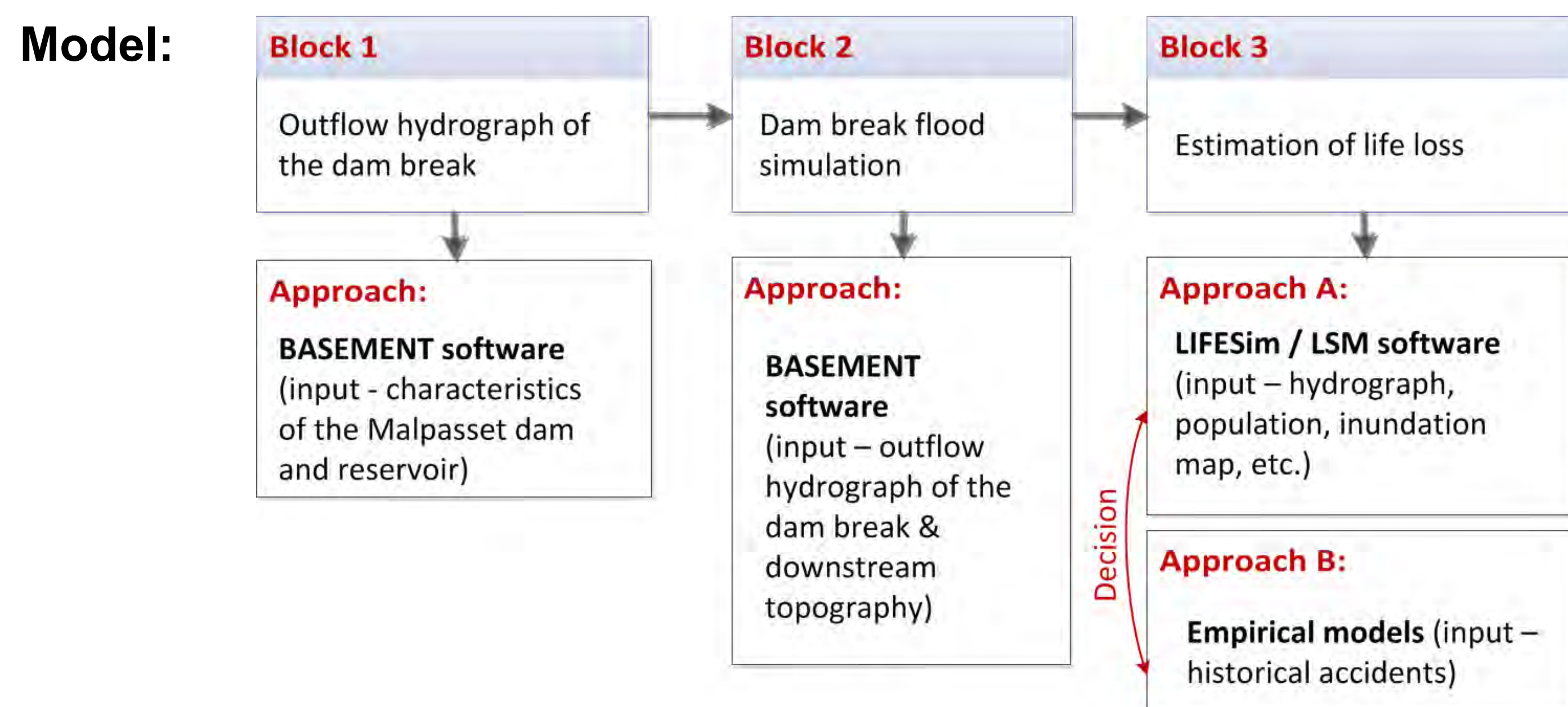


Figure 1. Three blocks of the physical model of a dam failure event proposed in this study

Block 1: Outflow hydrograph of the dam break

Model: An outflow hydrograph of the dam break will be computed using the BASEMENT software (Vetsch et al., 2015). The initial conditions are assumed as those for the Malpasset dam break. The computed results at different control points (in particular P2, see **Figure 2**) can be validated with field data and data available from case studies (Valiani et al., 2002).

History: The Malpasset dam break occurred in Southern France, in 1959. This event caused 421 fatalities. Prior to its failure the dam was 66.5 m high with a reservoir of 55 Mio m³. The collapse of the wall was sudden and complete, which makes this event unique.

Assumptions: The initial water surface elevation in the reservoir is set to +100 m.a.s.l. and in the downstream area 0 m.a.s.l. Initially the downstream area is assumed to be dry. At t=0, the dam is removed. The hydraulic code developed by VAW at ETH Zurich solves the sudden wet-dry change (discontinuity problem, Riemann problem), see **Figure 3**.

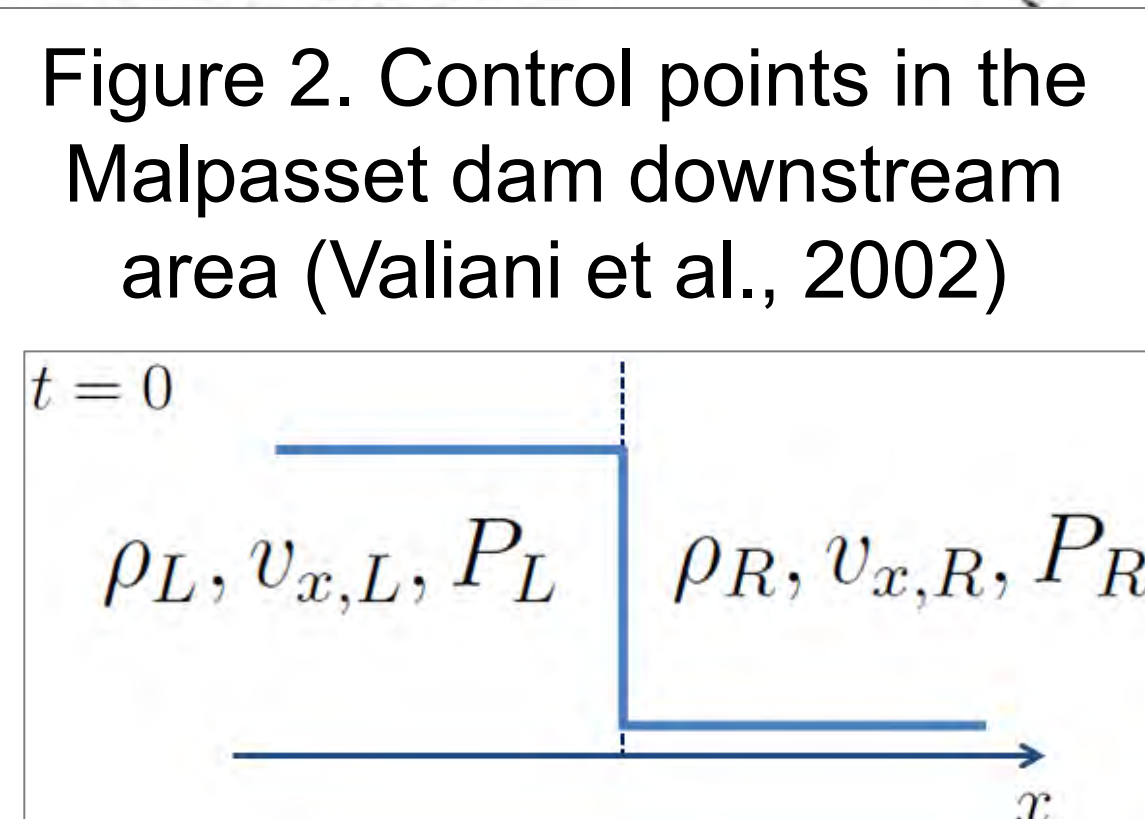
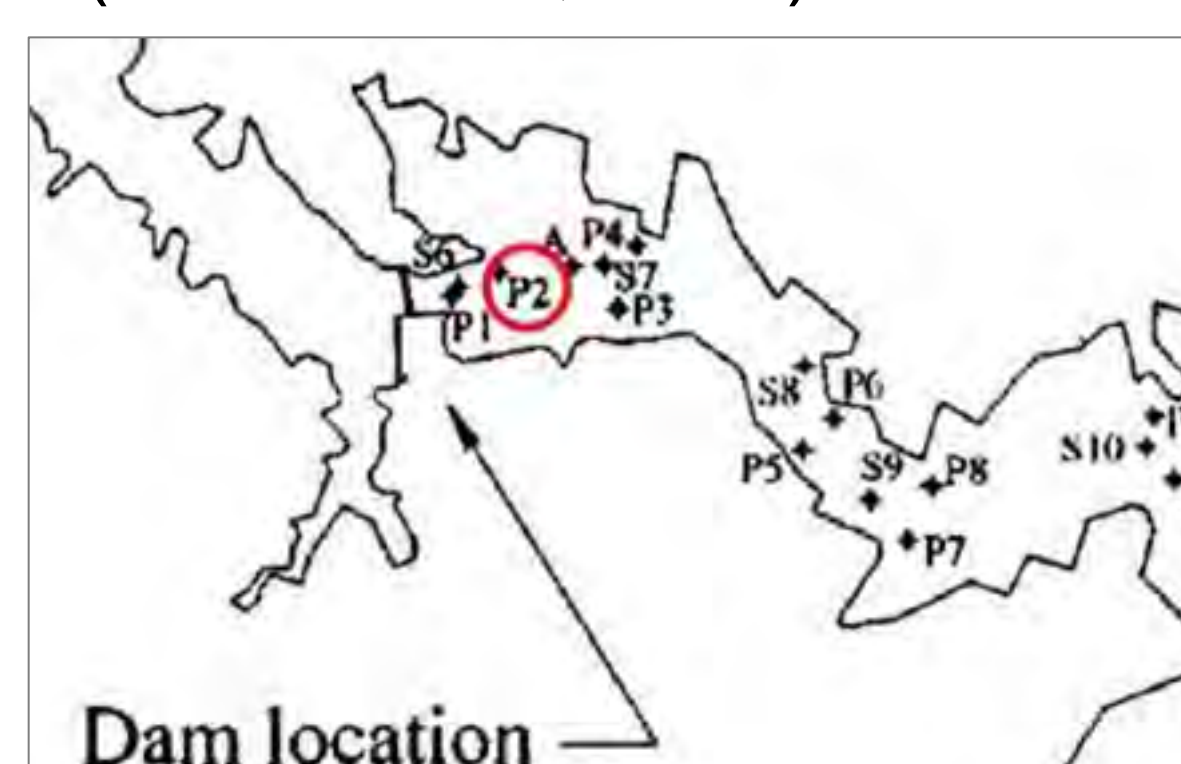


Figure 2. Riemann problem (e.g., Mocz, 2013)

References: Dubourg, V., Sudret, B. & Deheeger, F. 2013. Metamodel-based importance sampling for structural reliability analysis. *Prob. Eng. Mech.*, 33: 47-57. II Mocz, P. 2013. 1D Euler and MHD Shocks. Retrieved on 07.09.2016 <https://www.cfa.harvard.edu/~pmocz/shocks/index.html> II Sudret, B. 2012. Meta-models for structural reliability and uncertainty quantification. In: In K. K. Phoon, M. B., S. T. Quek, and S. D. Pang (Eds.) (ed.) *Proc. 5th Asian-Pacific Symp. Struct. Reliab. (APSSRA'2012)*. Singapore. II Valiani, A., Caleffi, V. & Zanni, A. 2002. Case Study: Malpasset Dam-Break Simulation using a Two-Dimensional Finite Volume Method. *Journal of Hydraulic Engineering*, 128. II Vetsch, D., A. Siviglia, D. Ehrbar, M. Facchini, M. Gerber, S. Kammerer, S. Peter, L. Vonwiller, C. Volz, D. Farshi, R. Mueller, P. Rousselot, R. Veprek, and R. Faeh (2006-2015). BASEMENT.

Framework for Uncertainty Quantification

Uncertainty in the modeling of the dam-failure consequences will be addressed quantitatively. A global framework for uncertainty quantification will be employed (Sudret, 2007) (see **Figure 4**).

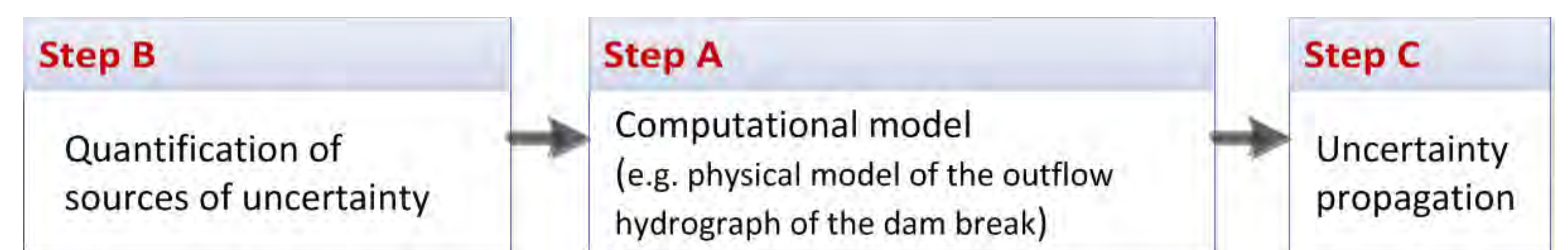


Figure 4. Global Framework for Uncertainty Quantification

The use of the finite-volume method for the flood propagation makes a crude Monte Carlo approach non-applicable for uncertainty quantification in the flood propagation model, since computational costs will be too high. Meta-modelling approaches (Dubourg et al., 2013) offer an opportunity to reduce the computational cost of evaluating the expensive-to-evaluate computational model. For this purpose, the computational model is approximated by a meta-model.

The Polynomial Chaos Expansion (PCE) technique will be employed as a meta-modelling tool. PCE is a non-intrusive method treating the computational model as a black box and representing it with a sum of multivariate polynomials:

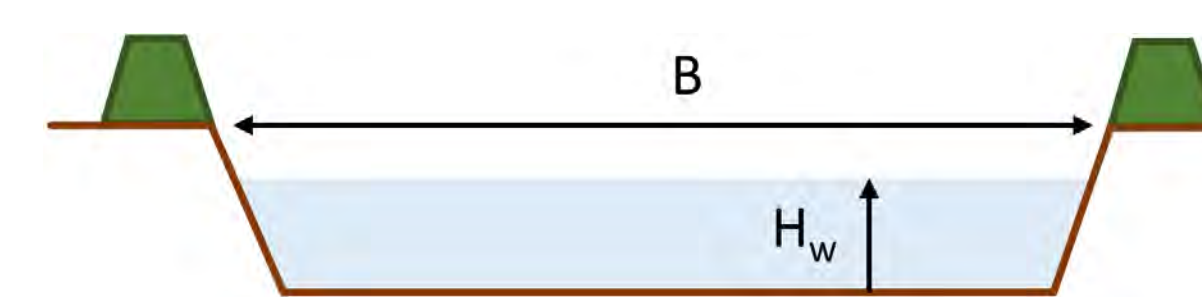
$$Y = \sum_{\alpha \in A} y_{\alpha} \Psi_{\alpha}$$

Where Y is our PCE Model response, the multi-indices $\alpha = \{\alpha_Q, \alpha_{K_s}, \alpha_B, \alpha_{\alpha_{dike}}\}$ determine the degree of the underlying polynomials, y_{α} is the coefficient for the actual term of the sum, the multivariate polynomial Ψ_{α} are the product of the underlying orthonormal polynomials and X is the input parameter vector.

Example: Dike Problem

Example from the Group Project work completed within the Uncertainty Quantification in Engineering course (ETH FS 2016) given by Prof. B. Sudret and Dr. S. Marelli, the computational model describes a water level of the river nearby the dike H_w :

Step A: Parametrization of the model, so called "black box"



$$H_w = (Q, K_s, B, \alpha)$$

Step B: Identification of sources of uncertainties

Variable	Type of PDF	μ	σ	Parameters of PDF
Maximal annual flow Q [m ³ /s]	Uniform	1330	50	[1243.4, 1416.6]
Strickler coefficient K_s [m ^{1/3} /s]	Uniform	30	0.75	[28.7, 31.3]
River width B [m]	Uniform	200	1	[198.3, 201.7]
River slope α_{dike} [-]	Uniform	10 ⁻³	10 ⁻⁵	[9.82E-04, 1E-03]

Step C: Propagation of the uncertainty through the model

The PCE was built on a sample set of size 100. Afterwards, the PCE was evaluated on a validation set of size 100,000 built applying the Latin Hypercube sampling technique. The computed deviation of the mean values of the validation set and of the meta-model response vs. the increasing polynomial degree (see **Figure 5**) shows a good agreement between both models.

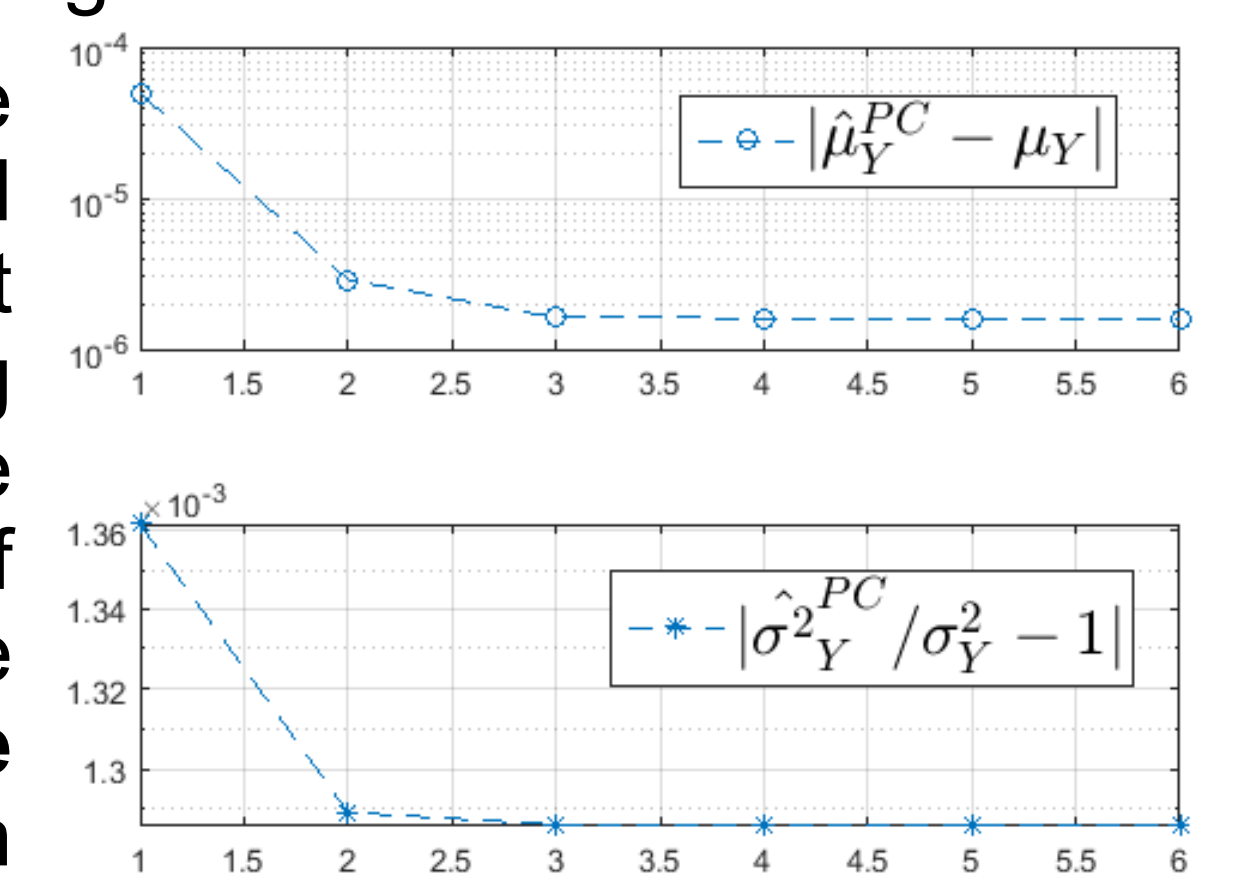


Figure 5. Convergence of moments vs. Polynomial Degree

Outlook

The on-going work is focused on Block 1 (see **Figure 1**). The hydraulic code by VAW, ETHZ for the model of the outflow hydrograph in BASEMENT (Step A) has been implemented. Step B, namely building a probabilistic model input, is currently on-going.

Acknowledgment

This work has been completed within the Swiss Competence Center on Energy Research – Supply of Electricity, with the support of the Energy Turnaround National Research Programme (NRP70) of the Swiss National Science Foundation.

The authors express their sincere thanks to Bruno Sudret and Stefano Marelli, Chair of Risk, Safety and Uncertainty Quantification ETH, Zurich, Switzerland, for valuable comments and assistance to the undertaking of the research summarized here.



Seasonal and Diurnal Wind Power

Bert Kruyt and Michael Lehning

Ecole Polytechnique Fédérale de Lausanne, Laboratory for Cryospheric Sciences CRYOS, Lausanne, Switzerland
WSL Institute for snow- and avalanche research SLF, Davos, Switzerland



Abstract & main Conclusions

- Wind speeds & wind power are **higher in winter**, and as such well suited to complement hydro power.
- Sustained **low wind power periods** are less persistent in winter and less likely at higher elevation.
- Valley winds cause **strong diurnal evolution** of wind speeds in summer.
- **Local terrain features** are the main influence on wind climate, although
- Wind speeds & power production **increase with elevation**.

Introduction

- Switzerland has a **power deficit** in winter, due to increased demand and the **seasonality of hydropower production**.
- In a future, highly renewable Swiss power system, ideally renewable electricity sources will be able to **complement** the hydro cycle.

Results

- On average **56% higher** wind power in winter (Nov - April).
- Lower **return levels for persistent low wind conditions** in winter months and with increasing elevation.

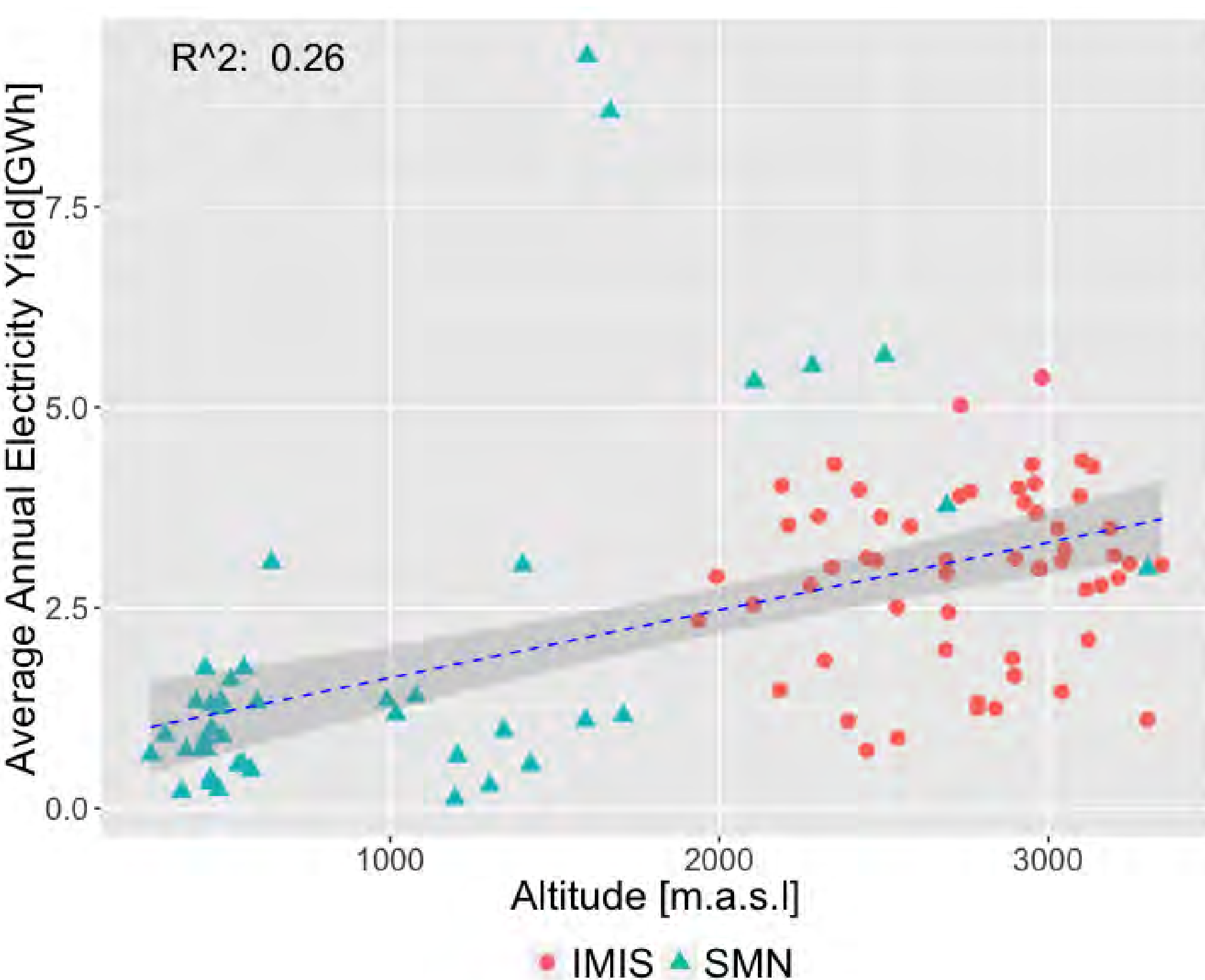


Fig 1: Average yearly power production (simulated) increases with elevation, but local terrain effects play an important role.

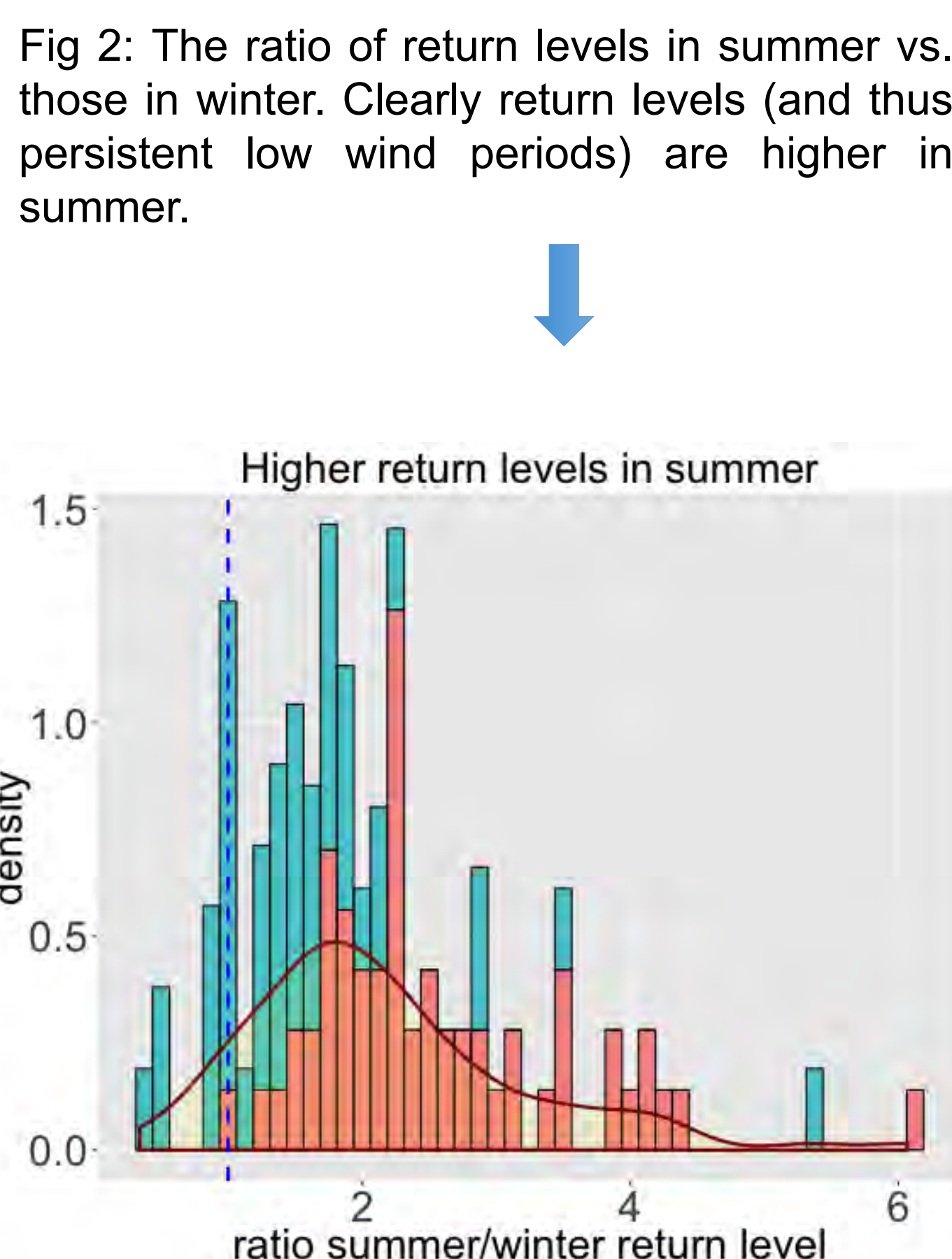


Fig 2: The ratio of return levels in summer vs. those in winter. Clearly return levels (and thus persistent low wind periods) are higher in summer.

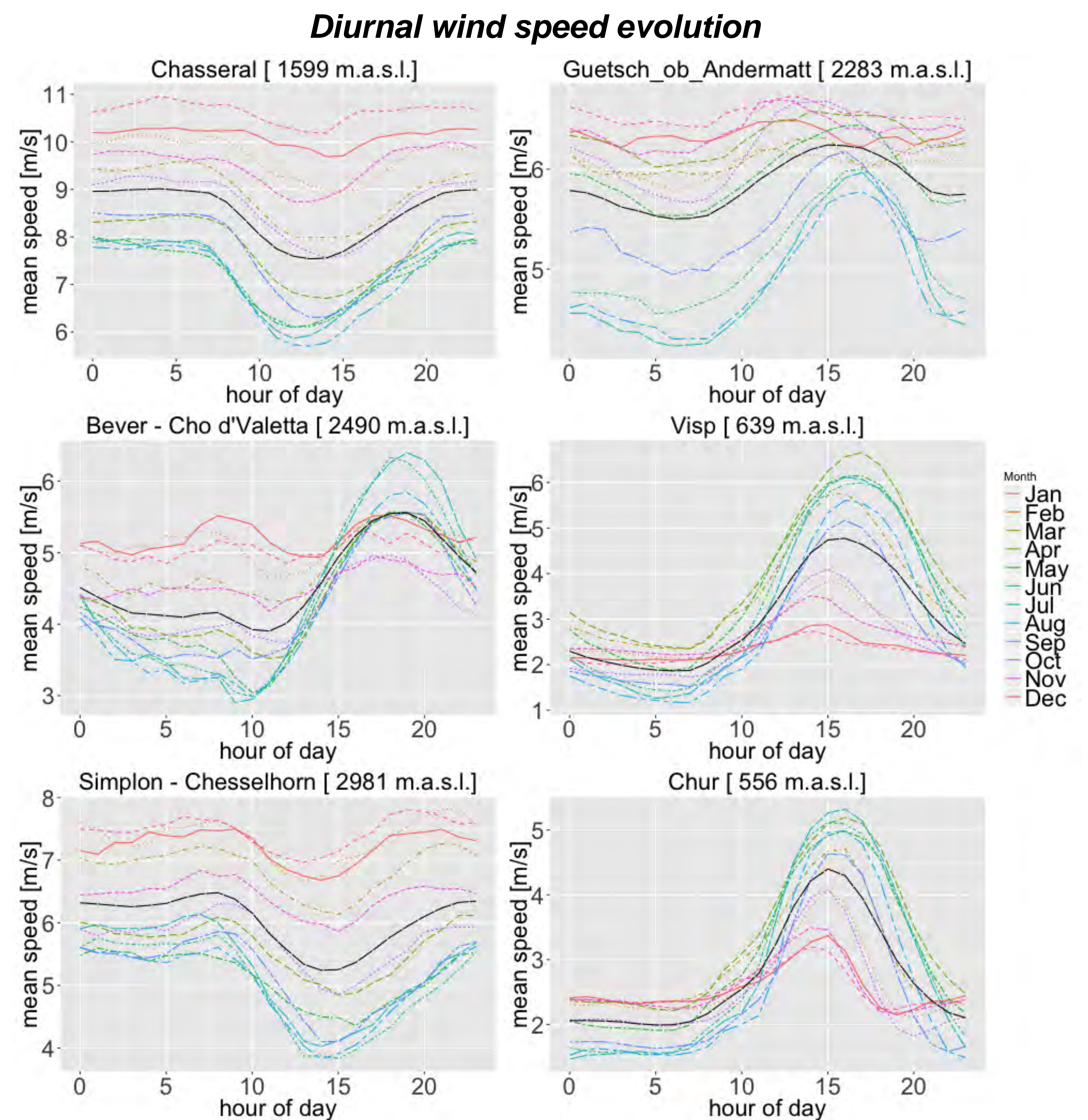


Fig 4: Daily evolution of wind speeds in different terrains. Monthly averages over several years. The black solid line represents the annual mean. Valley winds and boundary layer growth have opposite effects on afternoon wind production in valleys and ridges respectively. Time is UTC: +1 for winter and +2 for summer time.

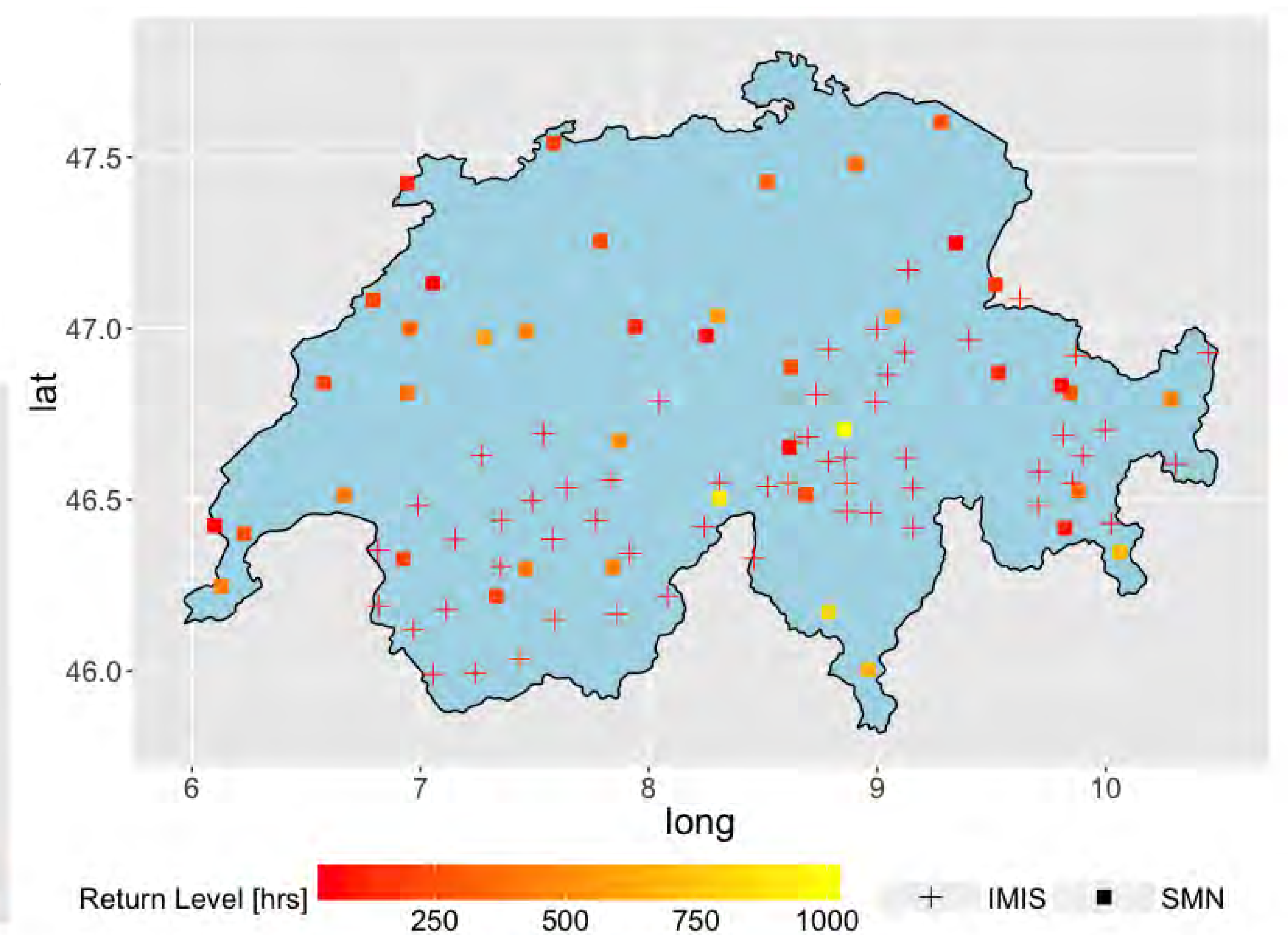


Fig 3: Return levels of no-wind power persistence, for a return period of 10 year. This can be interpreted as the level to be exceeded once every 10 years.

Methods & Data

- Hourly wind speeds from the Swiss MetNet (SMN) and IMIS **measurement stations**.
- **Imputation** of missing values with the Amelia package.
- Translation of speeds to 80m hub height.
- **Extreme Value Analysis** of interval length below cut-in (above cut-out).
- Calculate **power production** based on Enercon E82 2MW turbine.
- Correction for lower **air density** at altitude.

Outlook

- Investigate energy **potential from complex terrain** features by hi-res CFD modelling of flows over gaps, glaciers and valleys
- Simulate interactions of **different spatial configurations** of wind & PV to **complement hydropower** (also see poster on "Impact of combined wind & solar on the Swiss electricity system")
- **Optimal** spatial configuration to match diurnal and seasonal **demand**?



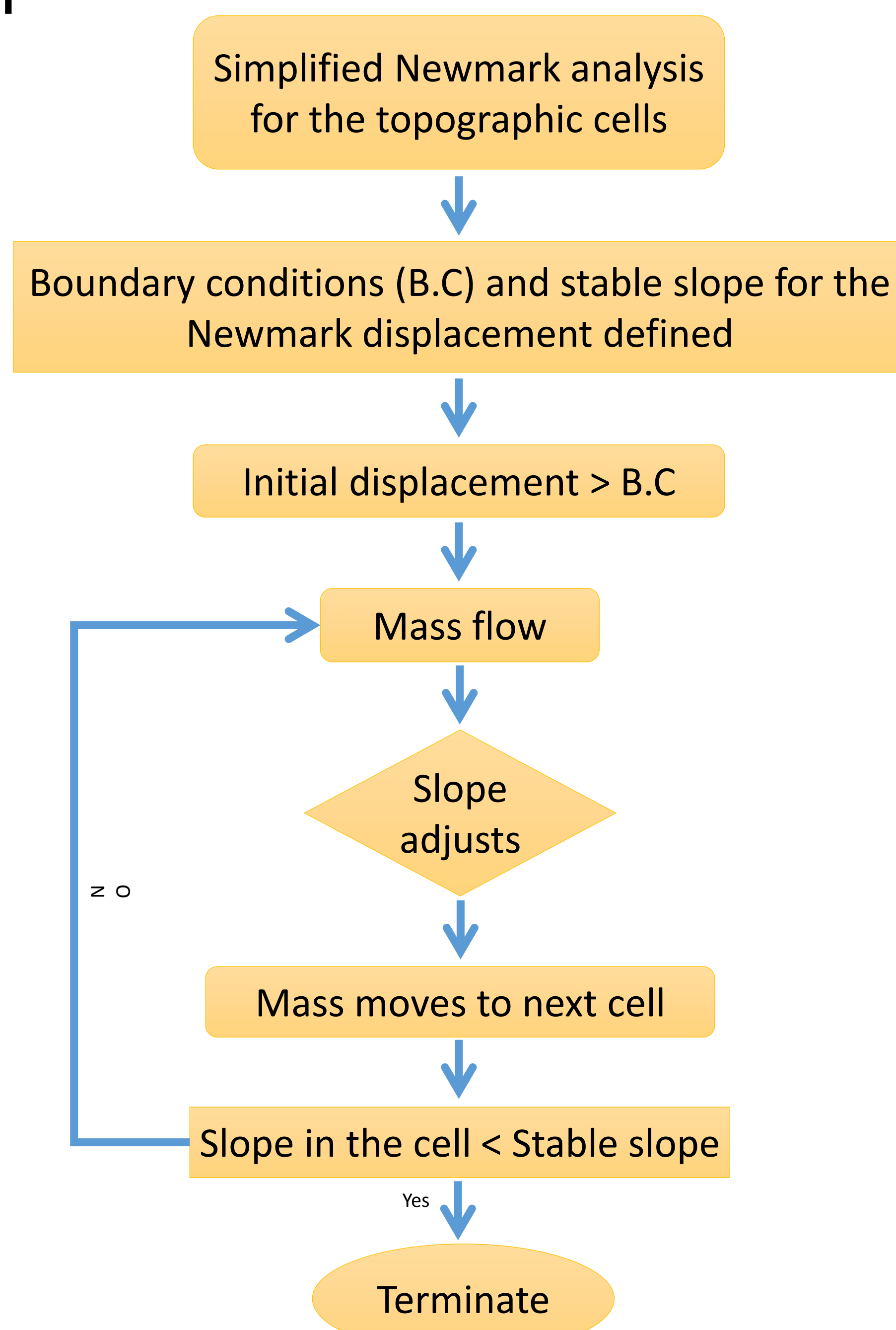
Multi-risk in the Swiss landscape: The case of earthquake-triggered landslides

Ahoura Jafarimanesh, Arnaud Mignan and Domenico Giardini

Abstract

We present a simple cellular automaton to simulate landslide footprints triggered by both rain and earthquakes. The method is based on the Sandpile model, which dynamics is here controlled by the ground slope. Rain levels are approximated by ground water saturation and earthquake-landslide triggering is evaluated using the concept of Newmark displacement. That concept is then modified to estimate stable slopes during shaking at which locations the landslide stops. The cellular automaton is first tested in a virtual area where a parameter sensitivity analysis is made. Then it is tested in a region of Switzerland, where historic landslides triggered by earthquakes are known to have occurred. The model is finally validated based on power-law fitting.

Algorithm



Modelling

A. Generic aspects of earthquake- and rain-triggered landslide in a virtual region

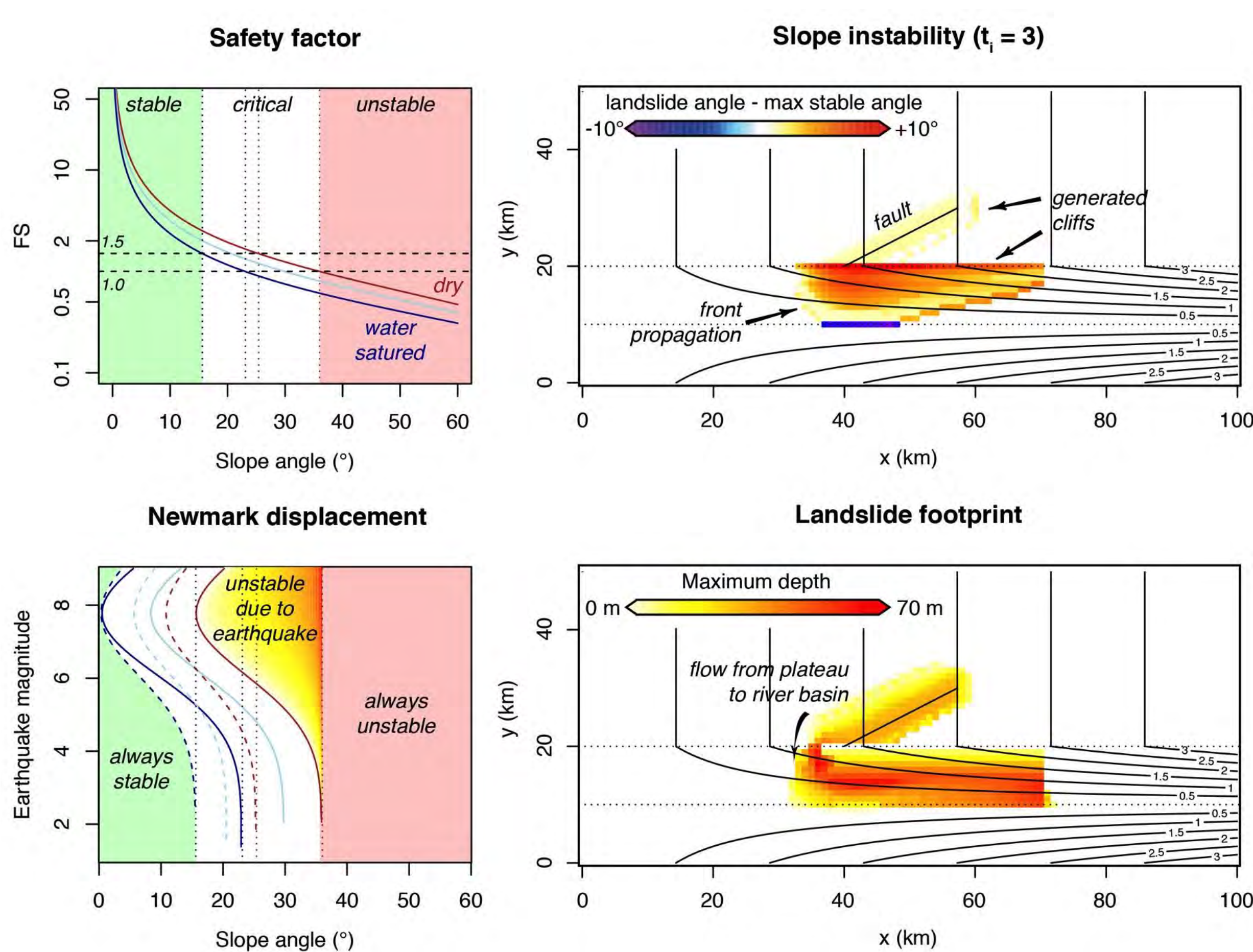


Fig. 1: landslide triggering model tested in a virtual region for a magnitude 6.5 earthquake under saturated soil (10m thick).

B. Application of the model at the site-specific level (Switzerland)

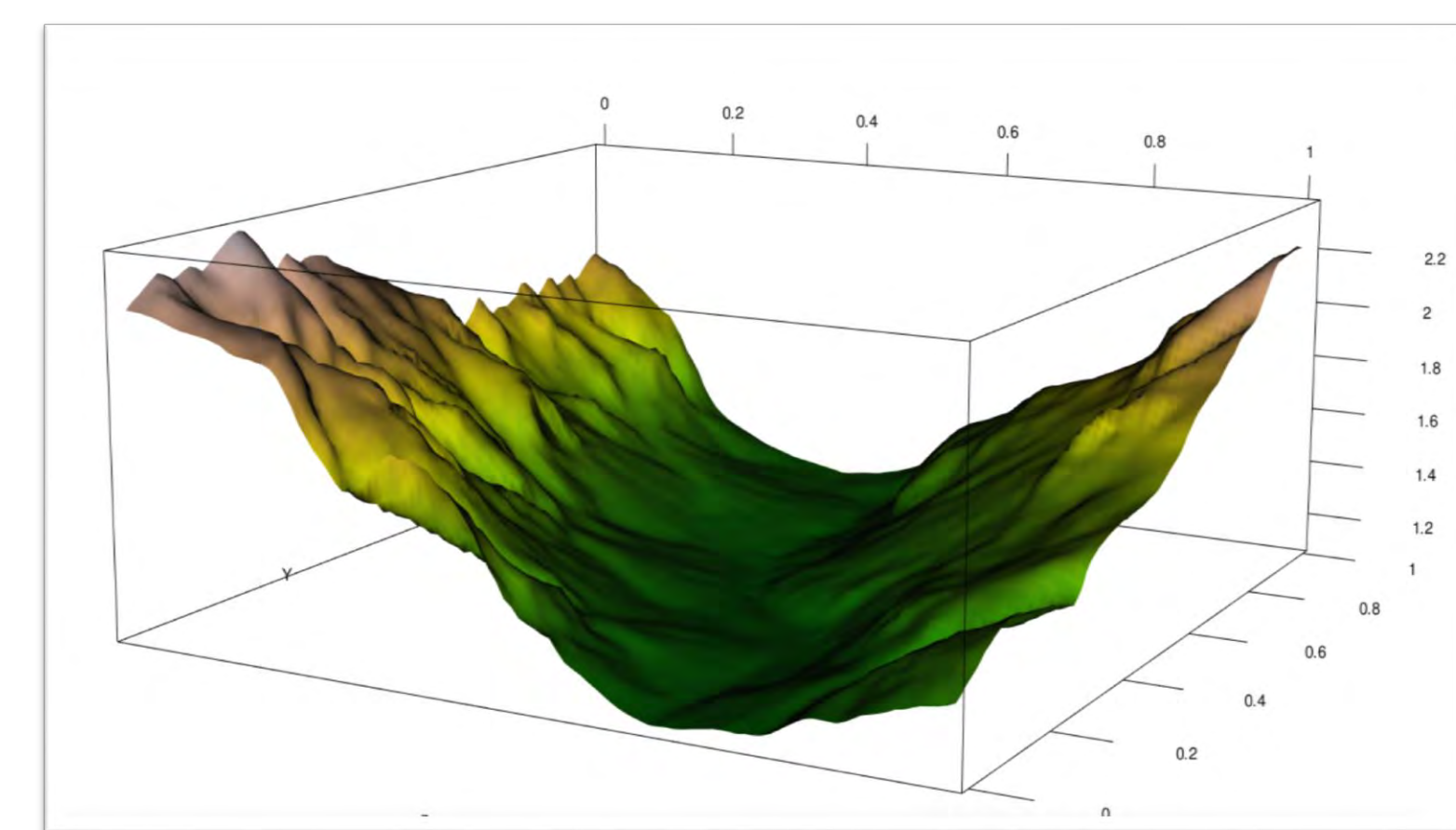


Fig. 2: Elevation map of the Mattered Valley, Valais.

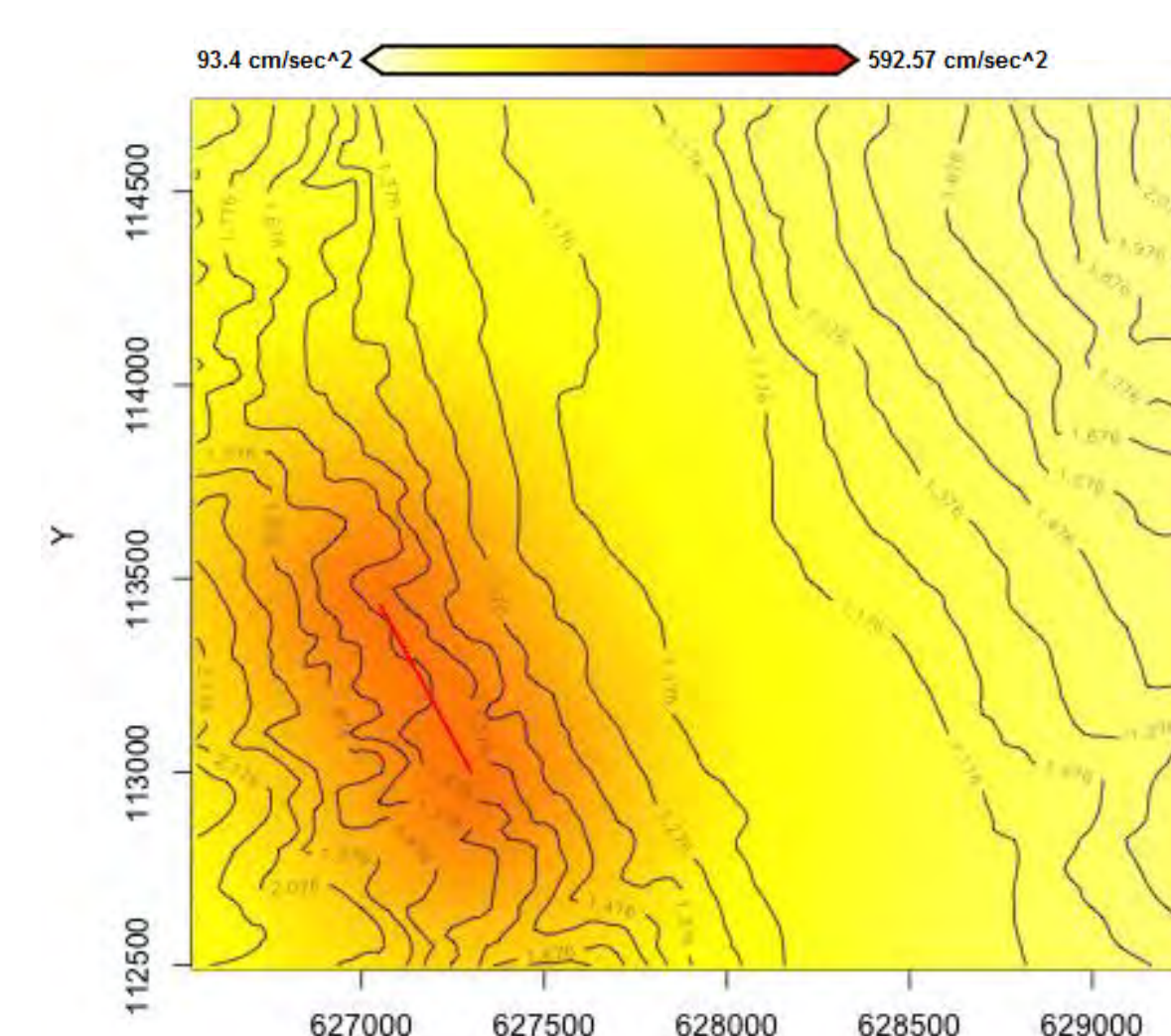


Fig. 3: Ground acceleration map due to a hypothetical earthquake (Mw = 6.5) in Mattered Valley

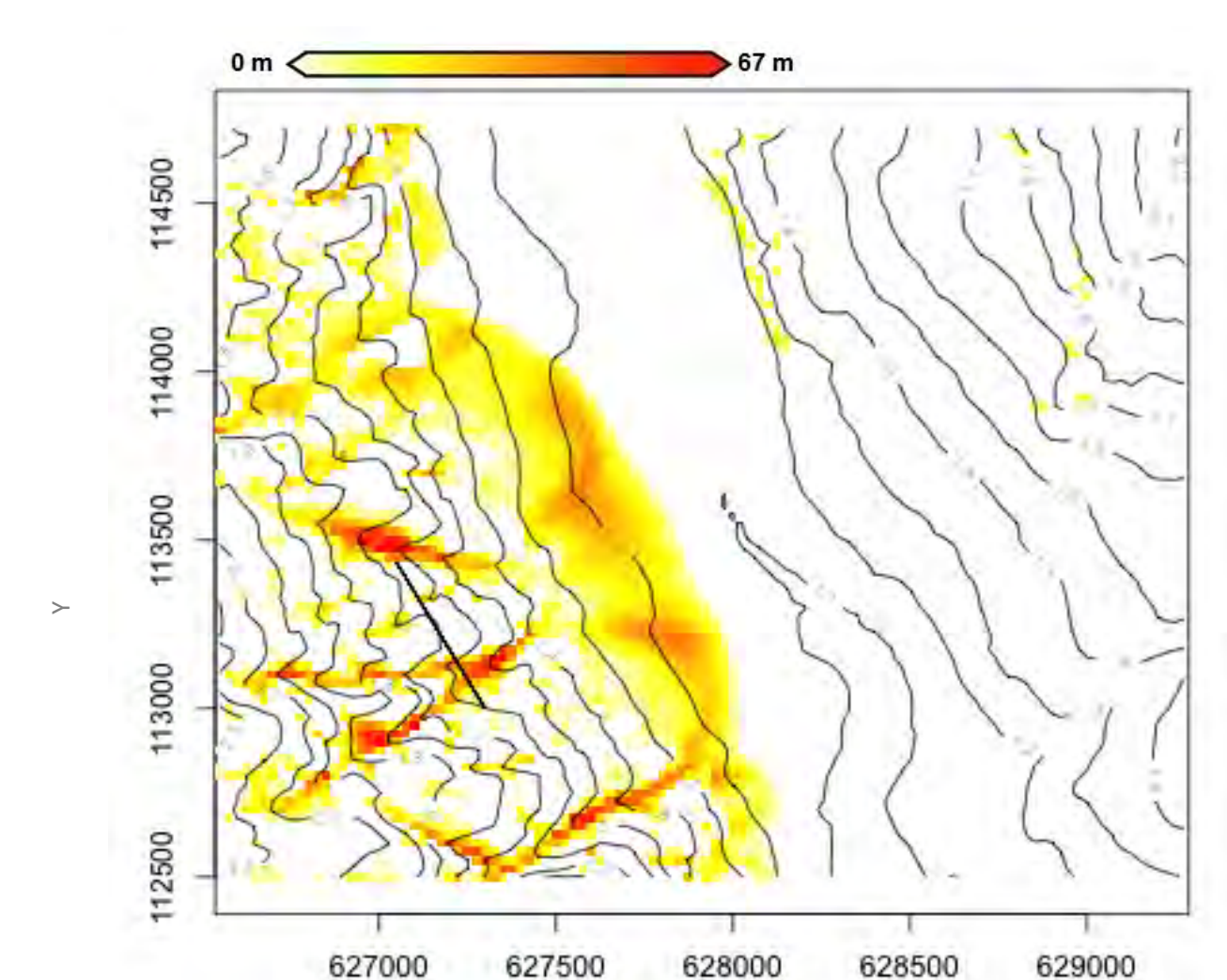


Fig. 4: Landslide footprint and debris accumulation pattern in Mattered valley following the earthquake of Fig. 3.

Validation

To validate the proposed cellular automaton model, the frequency-area distribution of the simulated landslides was analysed in terms of power-law slope and compared to distributions observed in nature, determined from published landslide inventories (Harp and Jibson, 1995; Xu et al., 2015).

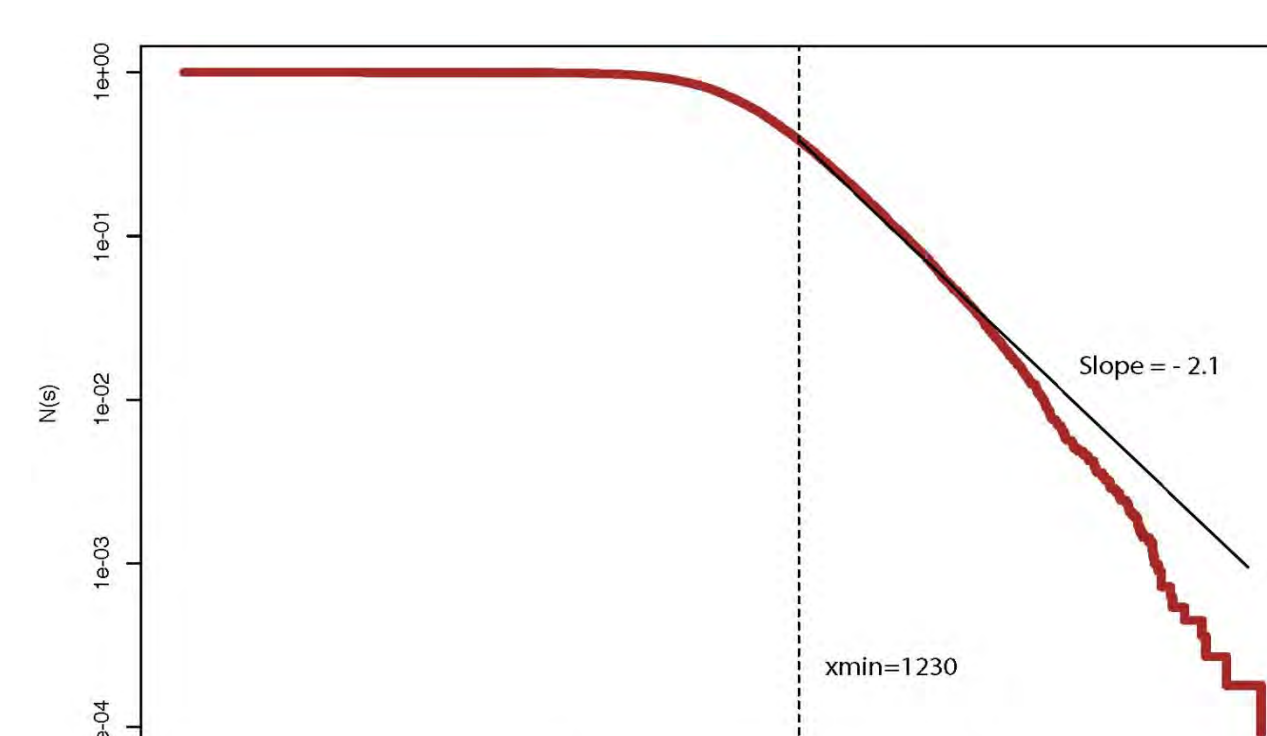


Fig. 5: Frequency-area distribution of the landslides due to the 1994 Northridge earthquake, California, USA.

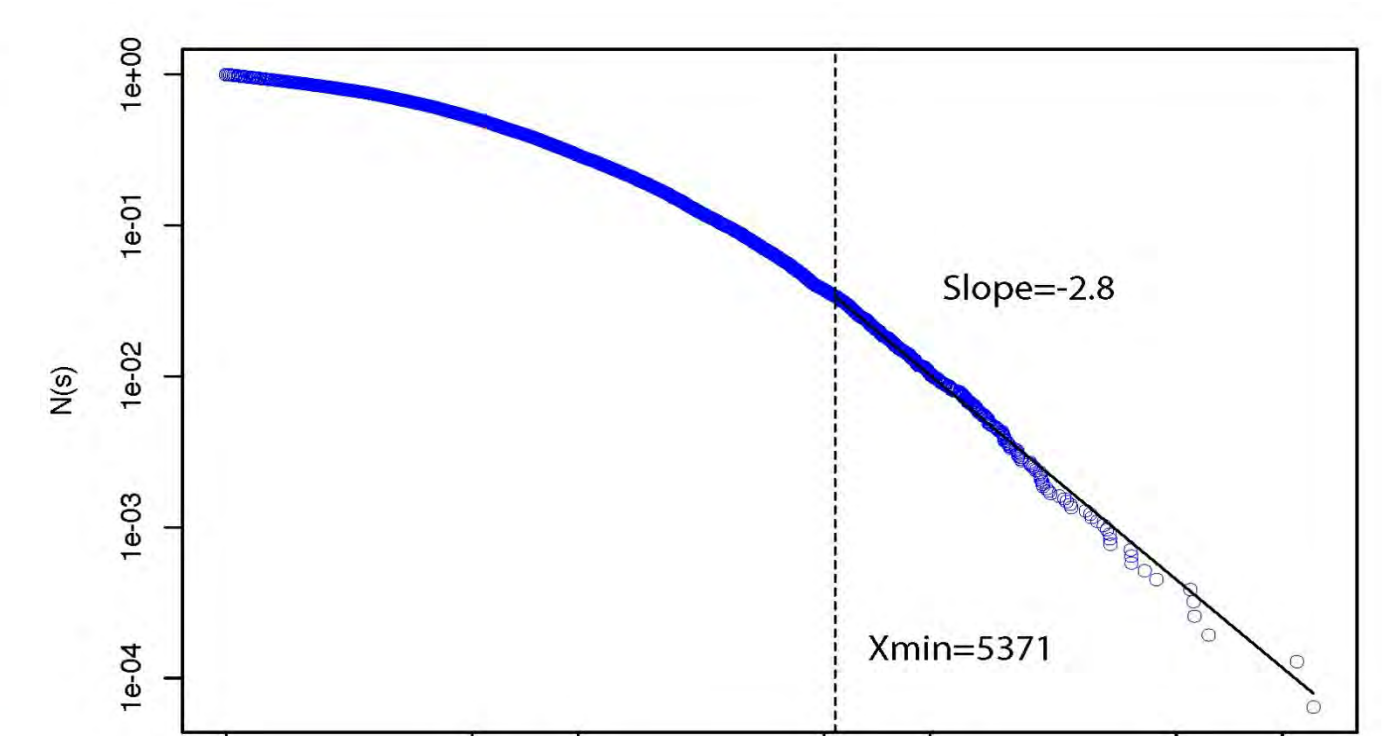


Fig. 6: Frequency-area distribution of the landslides due to the 2013 Lushan earthquake, China.

The slope of the power law obtained in the proposed model is $s = 2.3$ is compatible with the range $2.1 < s < 2.8$ observed for the landslide inventories of Northridge (Harp and Jibson 1995) and Lushan (Xu et al. 2015), in contrast with $s = 1$ usually emerging in simple Sandpile models, hence validating this new model.

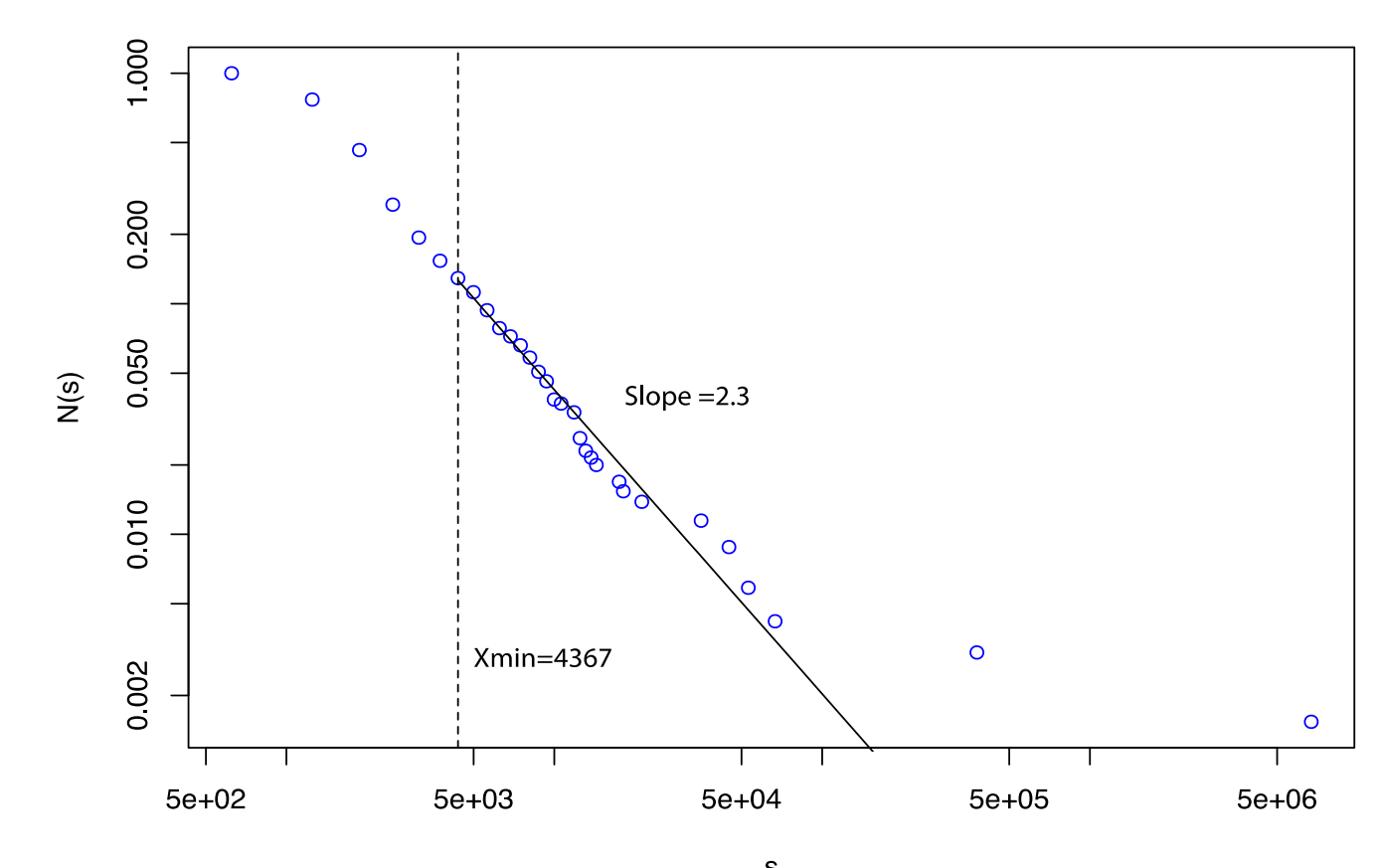


Fig. 7: Frequency-area distribution of simulated landslides due to M6.5 earthquake in the Mattered region

Database references

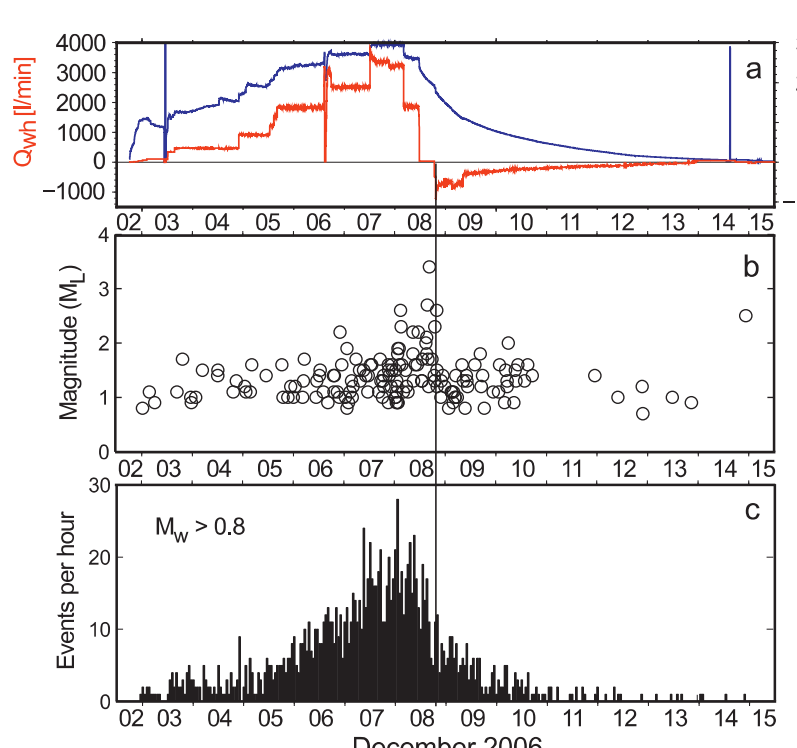
Harp, E. L. and R. W. Jibson (1995), *USGS report*
Xu, C., X. Xu and J. B. H. Shyu (2015), *Geomorphology* **248**

Long-term decay and possible reactivation of induced seismicity at the Basel EGS site

Background & Problem Statement

In December 2006, an extensive fluid injection was carried out below the city of Basel, Switzerland, to stimulate a reservoir for an Enhanced Geothermal System (EGS). Some details:

- ~11,500 m³ water injected into crystalline rock, 5km deep
- After 6 days, M_L 2.6 event exceeded safety threshold
 - reduced injection rate, then stopped completely
 - shut-in (closure of borehole)
- Hours later: widely felt M_L 3.4 event
 - well opened, rapid decay of seismicity
- Originally detected ~13,000 EQs (located ~3,500)
- Dez. 2009: project canceled – a seismic risk study suggested substantial risk of further felt and potentially damaging events [Baisch 2009]
- Mid-2010: ultimate shut-in & pressure increase at well-head
- Mid-2012: “revive” of seismic activity (M_L > 1.0)



The well-monitored and well-studied induced sequence allowed many new insights in terms of reservoir creation. Until now, a **detailed analysis of the long-term behavior** remained unexplored since a consistent catalog did not exist. We want to create one.

Highlights & Outlook

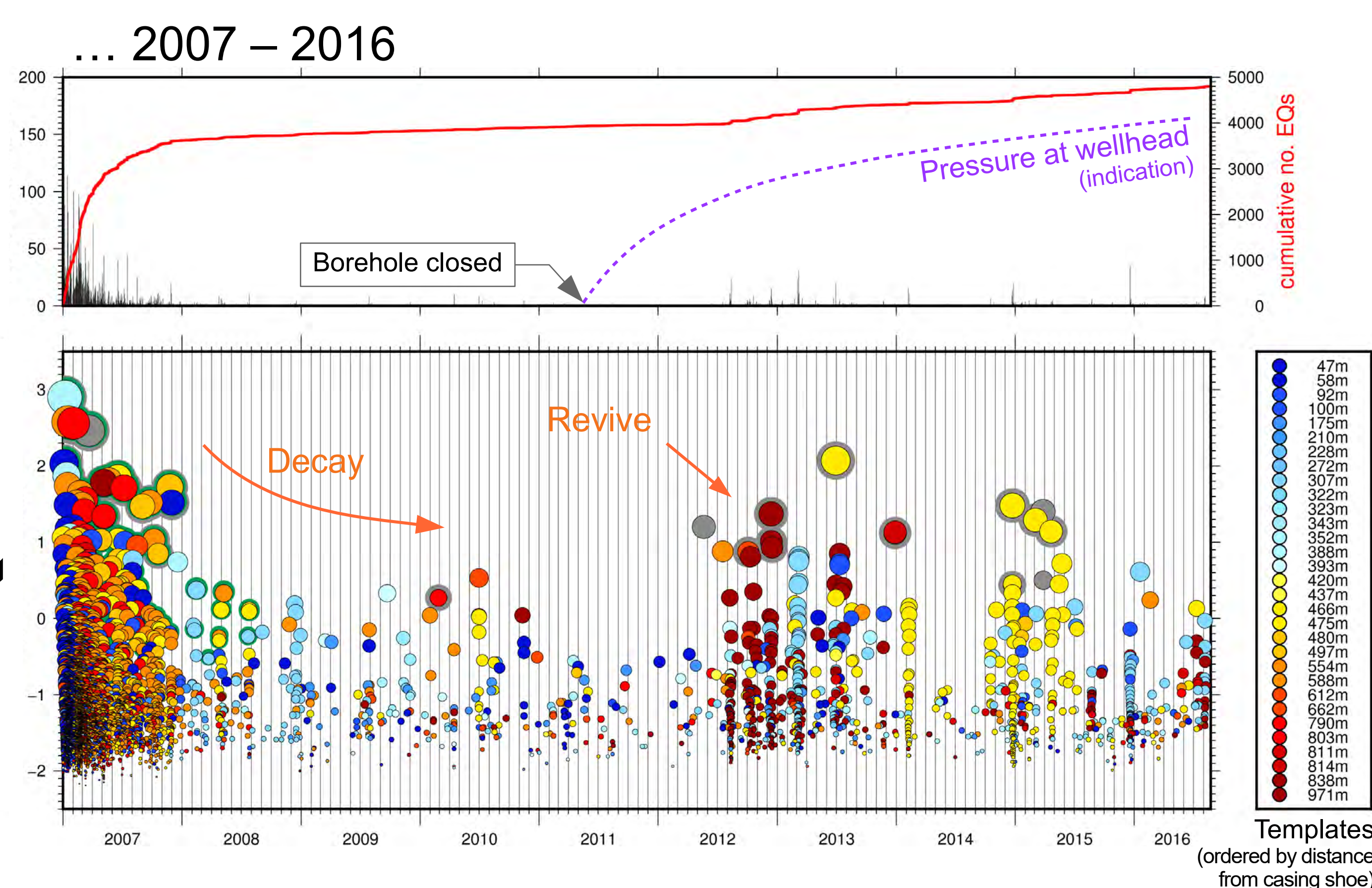
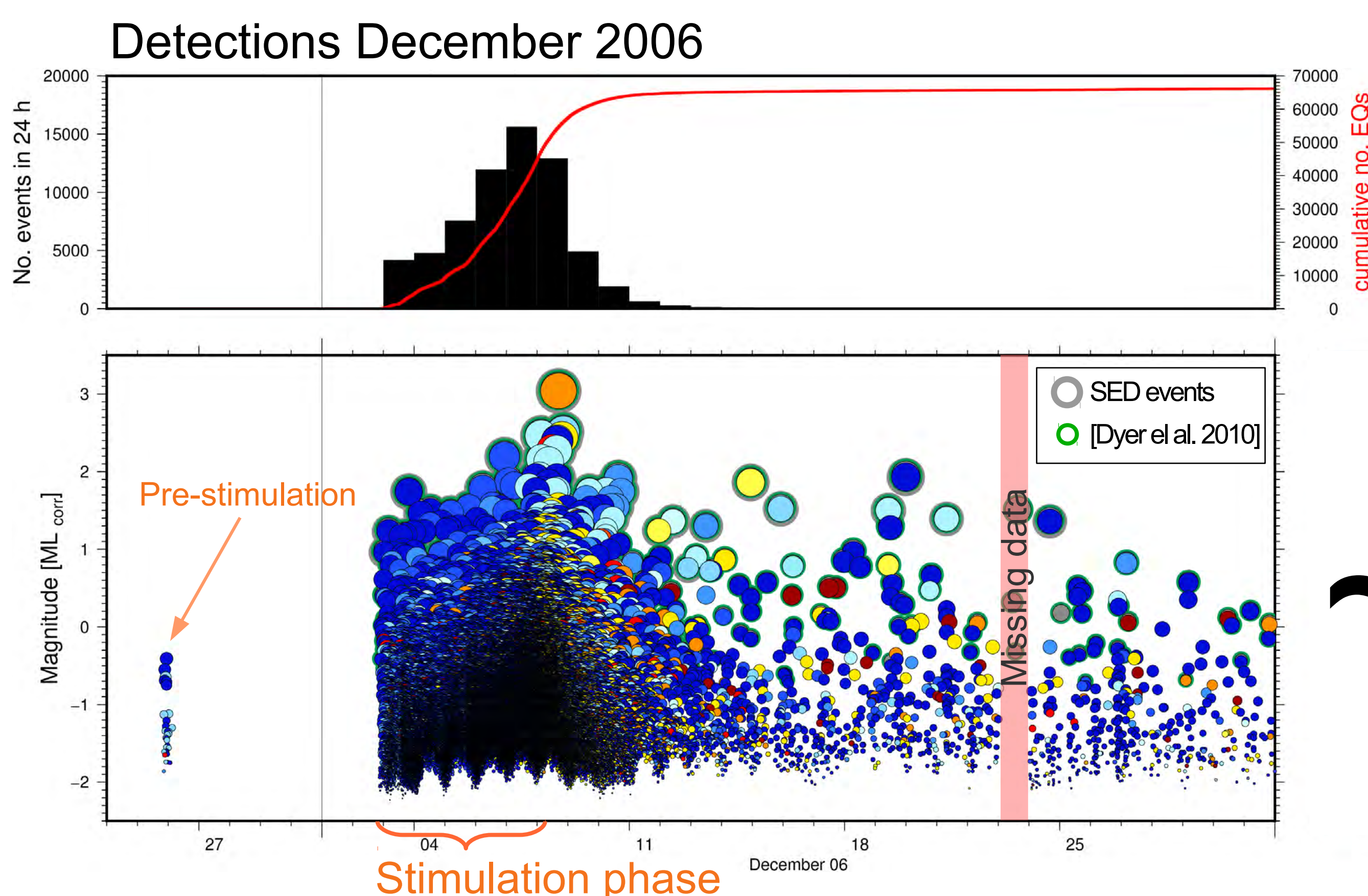
- Detections confirm clearly the (re-)activity several years after injection; they tend to cluster
- Possible connection: pressure increase ↔ re-activation?
 - Questions:
 - Should the borehole be opened again?
 - How long do we have to monitor a closed EGS project?
- We not only found previously missed events, but also more smaller seismic events, especially at later times when manual inspection became rare
 - decreased the detection limit (~1 magnitude unit)
 - increased spatio-temporal resolution; more information
 - allows better statistical analysis
 - allows to determine structures better (constrain fault plane)
- We observed a change in template association over time
 - migration of seismicity
- Our newly obtained catalog spans over more than nine years and features a uniform (and low) detection threshold
- The improved resolution of the long-term behavior and the later seismicity increase will help to understand involved mechanisms better
- More induced or natural sequences will be investigated with our procedure
- Automation for real-time processing

Findings of a multi-template approach

We scanned the recordings of the deepest installed borehole station (2.7km). This station is very close (1.5–2.5km) to deep reservoir, completely in the granite bedrock. It has the highest signal-to-noise ratio among all (borehole-)stations.

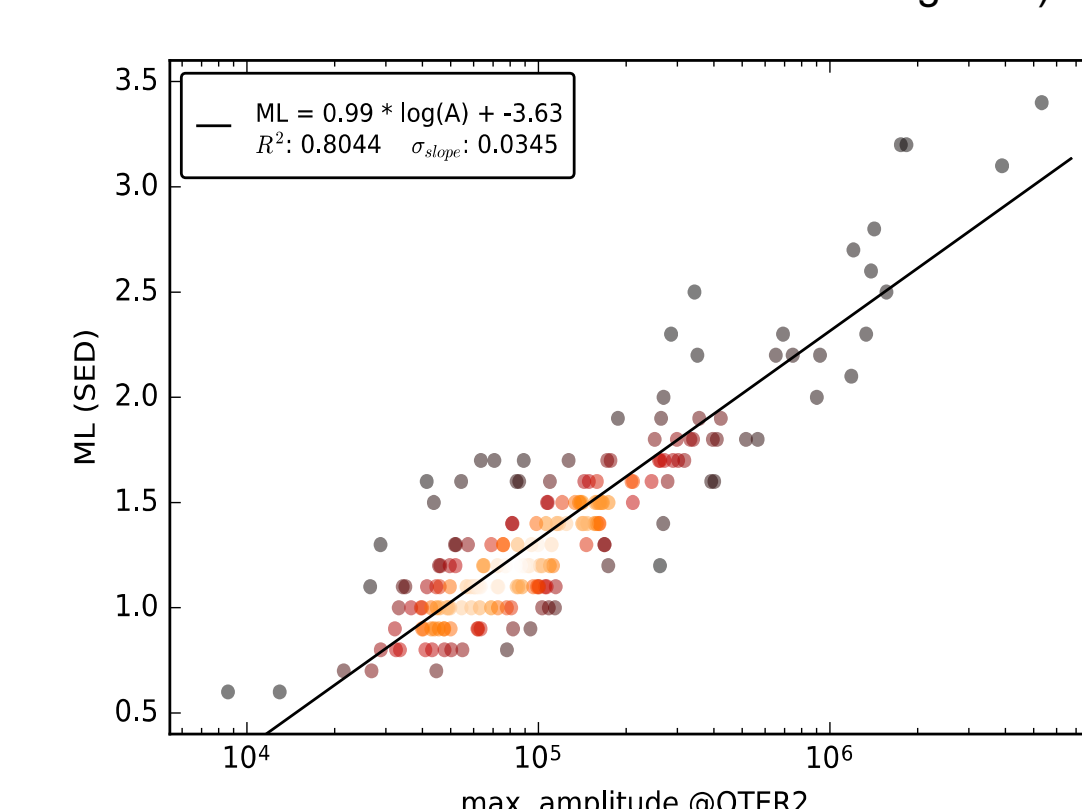
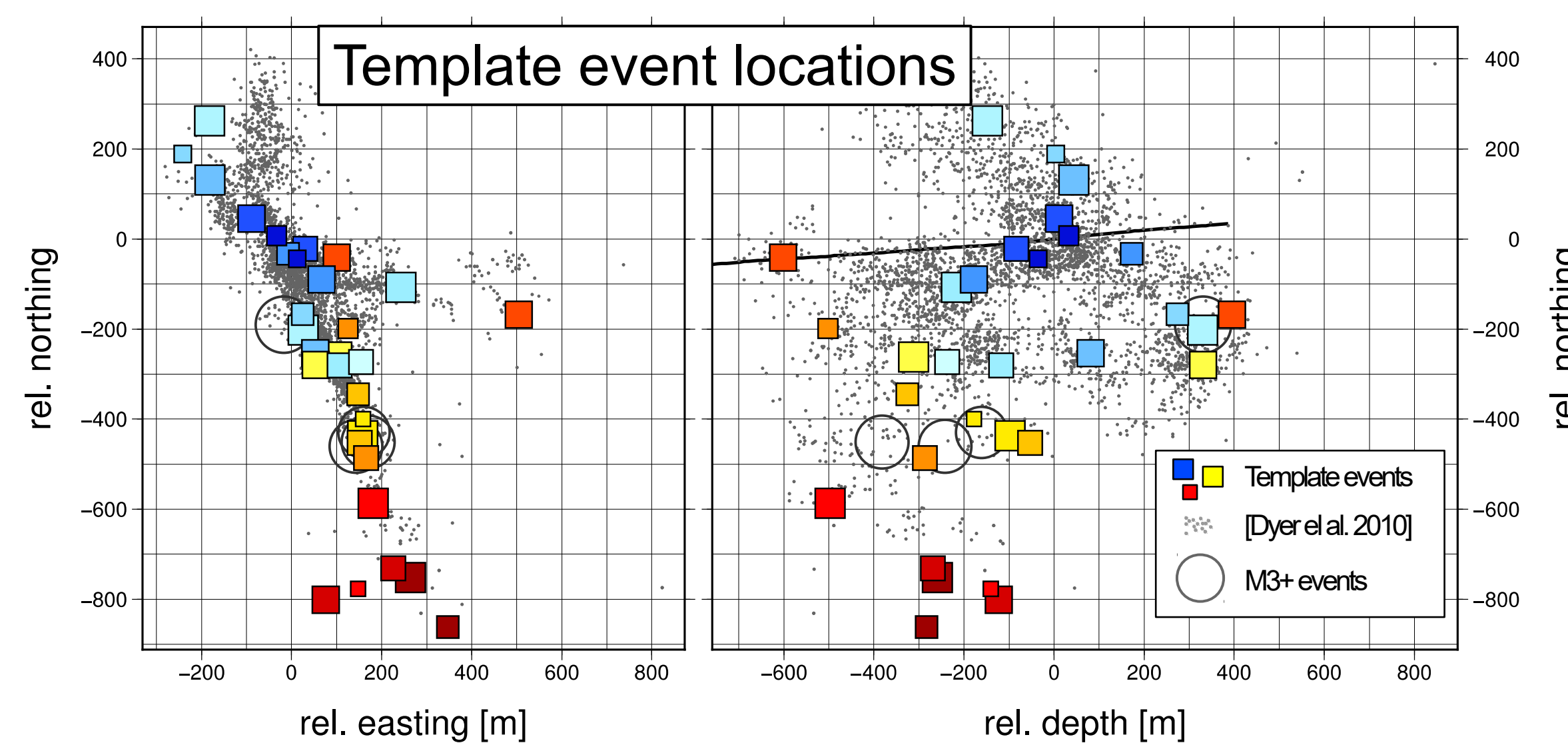
Notes on the scanning process:

- Since we can only detect events that are similar to the used template(s), the template set has to be updated over time.
- We updated the template set if a known event was not detected by already used templates
- Since the Z-channel failed in 2010 we only used the 2 horizontal channels to be consistent. This can lead to wrong template associations.



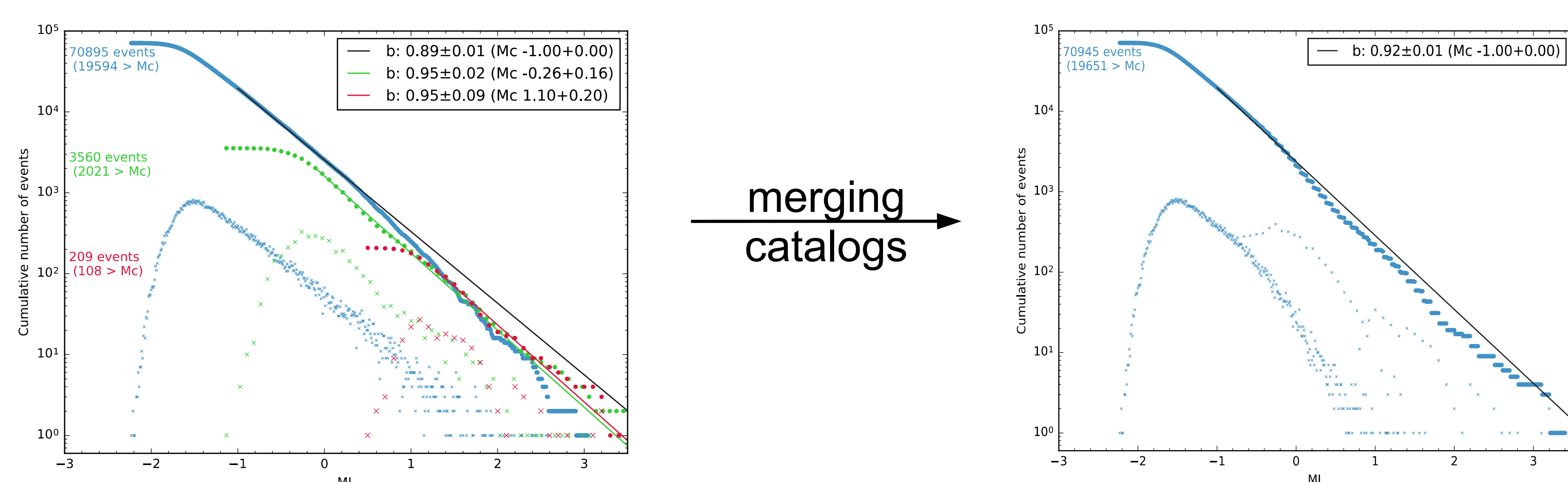
The **color** of a detection indicates to which template it is most similar.

The orientation of the individual faults varies and deviate from the general orientation “seismic cloud” [Deichmann et al. 2014]. This makes it necessary to use numerous template events to “sample” the underground. Later events tend to occur and cluster more outwards. But also older (inner) fault patches get reactivated again.



Amplitude–Magnitude regression. To suppress high-frequency contributions in the amplitude, we filtered the waveform with a 1-20Hz Bandpass filter.

Earthquake statistics / Frequency–magnitude–distribution (FMD)



FMDs of 3 catalogs: ours based on template matching, Dyer et al. 2010, and observed by Swiss Seismological Service (SED)

Associating the same events taking the preferred magnitude, i.e. the magnitudes based on Dyer or even on SED

Acknowledgements

We thank GeoEnergie Swiss AG and GeoExplorers Ltd. for providing the seismometer recordings of the Basel Geothermal Project. The research leading to these results has received funding from the European Community's Seventh Framework Programme under grant agreement No. 608553 (Project IMAGE).

References

- Baisch, S., Carbon, D., Dannwolf, U. S., Delacou, B., Devaux, M., Dunand, F., ... Vörös, R. (2009). Deep Heat Mining Basel: Seismic Risk Analysis.
- Dyer, B.C., et al., 2010. Application of microseismic multiplet analysis to the Basel geothermal reservoir stimulation events. Geophys. Prospect. 58.
- Deichmann, et al., 2014. Identification of faults activated during the stimulation of the Basel geothermal project from cluster analysis and fault mechanisms for the larger magnitude events. Geothermics.

Controlling induced seismicity in EGS projects by a model-driven traffic light system

Arnaud Mignan, Marco Broccardo and Stefan Wiemer

Abstract

The stimulation phase of Enhanced Geothermal Systems (EGS) induces earthquakes, hence posing problems to the feasibility of geo-energy projects. Although traffic light systems (TLS) exist to mitigate the risk of anthropogenic seismicity, they are on-the-fly tools with so far no forecasting capability. We show in 6 stimulation experiments that a piecewise model describes the observed data with a good degree of confidence. The model is driven first by the injection profile followed by post-injection normal diffusion, and completely defined by a three-parameter set $\theta = [b, a_{fb}, \tau]$ (earthquake size ratio, activation feedback and mean relaxation time, respectively). This allows defining as TLS the magnitude threshold m_{th} at which injection must be stopped to respect a given probabilistic safety target. The proposed model can be used during project planning to estimate the likelihood of failing based on an *a priori* θ and during stimulation phase to respect the safety target.

Induced Seismicity Model

We propose the following piecewise induced seismicity temporal rate $\mu(t)$ model:

$$\begin{cases} \mu(t) = 10^{a_{fb}} 10^{-bM_c} \Delta V(t) & ; t \leq t_{shut-in} \\ \mu(t) = \mu(t_{shut-in}) \exp\left(-\frac{t-t_{shut-in}}{\tau}\right) & ; t > t_{shut-in} \end{cases} \quad (1)$$

where the injection phase (before shut-in time $t_{shut-in}$) is described by a linear relationship between $\mu(t)$ and the injected flow rate $\Delta V(t)$, in agreement with previous observations (Dinske and Shapiro, 2013; Mignan, 2016; van der Elst et al., 2016), and where the post-injection phase is described by a pure exponential decay representative of a normal diffusion process (Mignan, 2015; 2016) (Fig. 1).

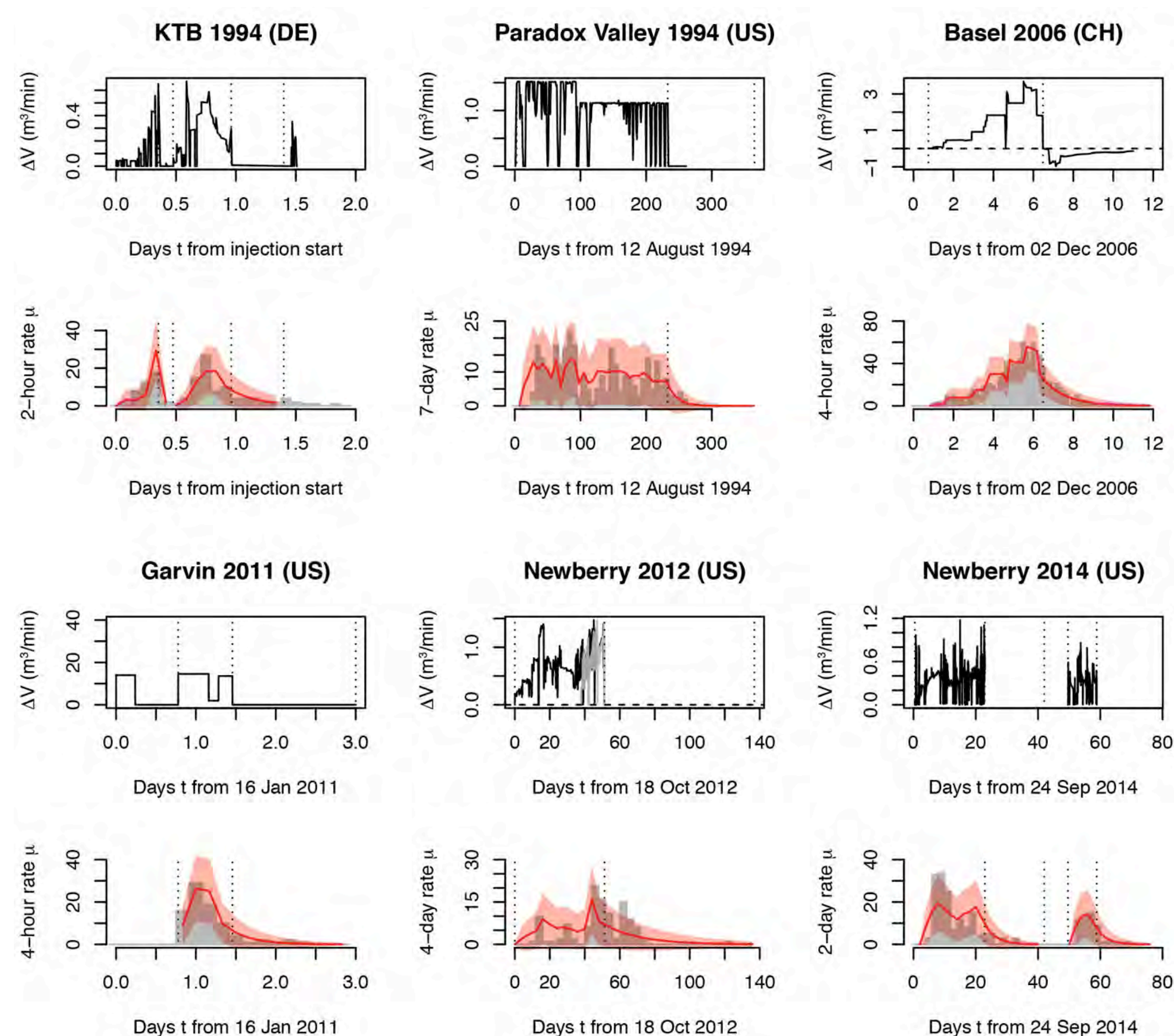


Fig. 1: Induced seismicity model fitting of six stimulation experiments (all publicly available): Kontinentale Tiefbohrung (KTB), Germany, 1994; Paradox Valley, United States, 1994; Basel, Switzerland, 2006; Garvin, United States, 2011; Newberry, United States, 2012 and 2014. For both KTB and 2014 Newberry, experiments are broken down into two separate stimulations, each with its own post-injection tail. The model (Eq. 1) is represented by the red curves on the induced seismicity time series with the $\pm 3\sigma$ uncertainty envelope shown in light red. Vertical lines indicate the shut-in time and the sub-stimulation separations. The model uses as input the induced seismicity time series and the injection profile characterized by the flow rate ΔV .

TLS use during EGS project planning

A safety criterion is recommended that defines acceptable levels of probabilities of exceedance Y , for a prescribed safety threshold X (e.g., magnitude threshold m_n). Assuming a non-homogeneous Poisson process, we have $\Pr(m \geq m_n, T) = 1 - \exp(-\Lambda_{m \geq m_n}(T)) = Y$ with $\Lambda_{m \geq m_n}$ the mean cumulative number of events obtained by integrating Eq. 1. It finally yields:

$$\Lambda_{m \geq m_n}(T) = 10^{a_{fb}} 10^{-b m_n} [V(t_{shut-in}) + \tau \dot{V}(t_{shut-in})] \quad (2)$$

where V is the total fluid volume injected during the project. Hence, for a given set θ (e.g., previous experiments like Fig. 1) and a planned injection profile, one can determine if the project would *a priori* pass or fail the fixed safety threshold (Fig. 2).

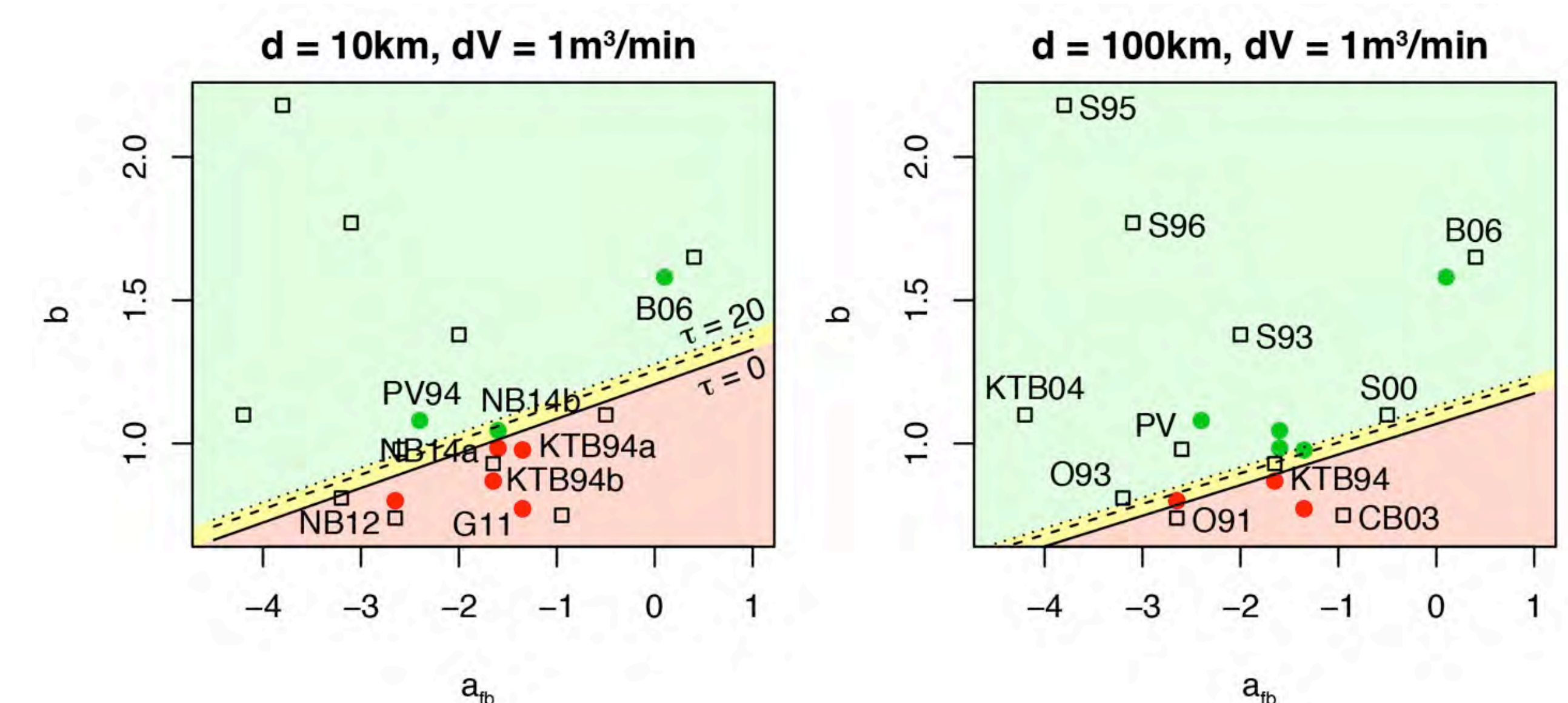


Fig. 2: Acceptable domain for a fixed limit state function with $V = 10,000 m^3$, $\Delta V = 1 m^3/min$, 2 building distances d from borehole (10 or 100 km) & $\Pr(\text{building collapse}) = 10^{-6}$ (see Mignan et al. (2015) for damage to m_n conversion), considering the set θ obtained in previous projects (circles: this study; squares: Dinske and Shapiro, 2013). NB: Preliminary results, subject to changes.

TLS use during EGS stimulation phase

Once the project has the green tag, one can define the TLS using the operational magnitude threshold m_{th} at which the injection is stopped in order to meet the safety target. From

$$\begin{cases} 10^{a_{fb}} 10^{-b m_n} [V(t_{shut-in}) + \tau \dot{V}(t_{shut-in})] \sim Y \\ 10^{a_{fb}} 10^{-b m_{th}} V(t_{shut-in}) = 1 \end{cases} \quad (3)$$

$$\text{we get } m_{th} = \frac{1}{b} \log_{10} [Y - 10^{a_{fb}} 10^{-b m_n} \tau \dot{V}(t_{shut-in})] + m_n \quad (4)$$

which validity is verified in Fig. 3.

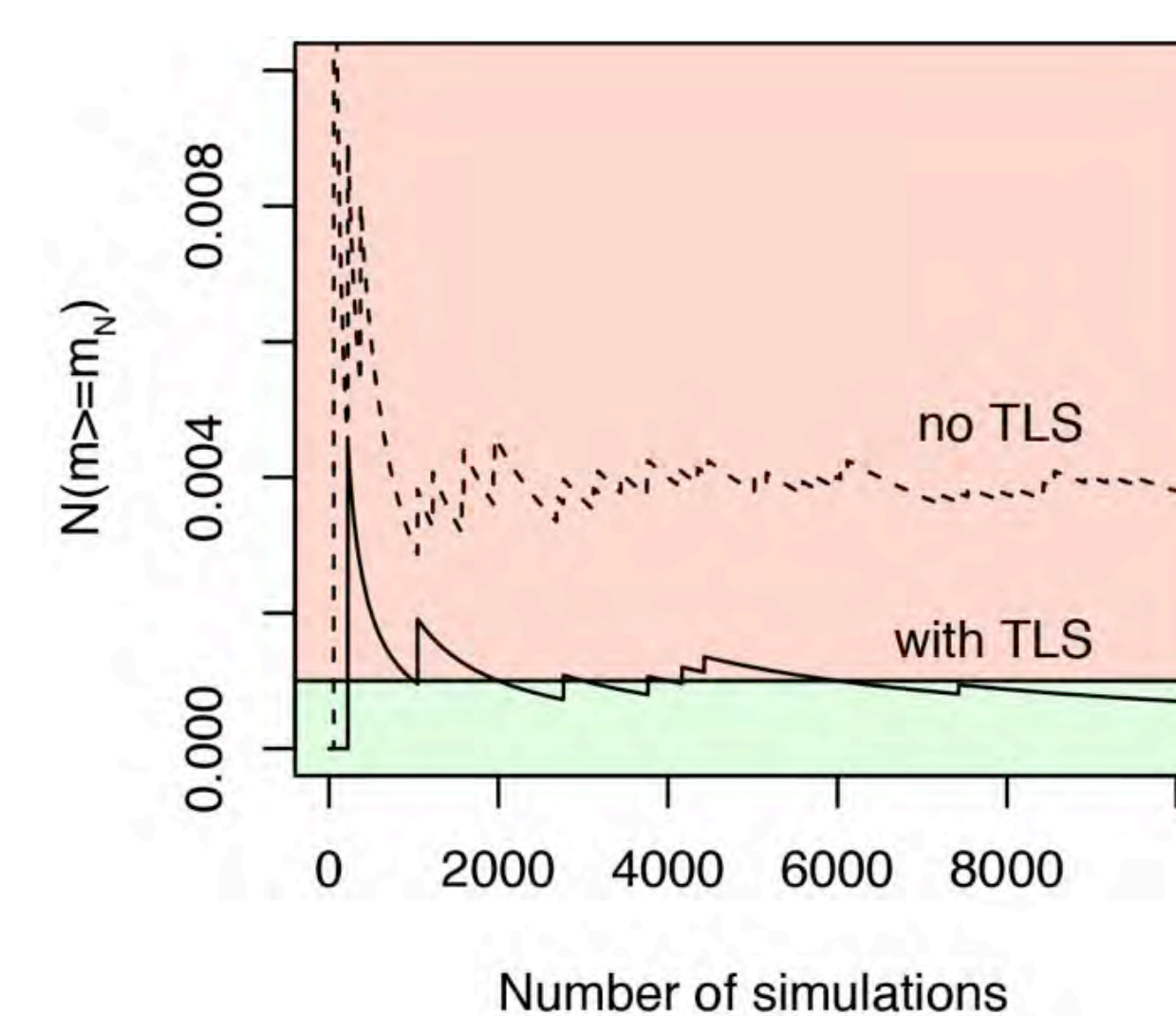


Fig. 3: Number of m_n events observed per simulation for a fixed set θ and fixed injection profile following Eq. 1. In this example, the safety threshold is not respected if no TLS is used. Using the TLS of Eq. 4 stops the stimulation in time in order to respect the safety threshold, in average.

References

- Dinske, C. and S. A. Shapiro (2013), *J. Seismol.* **17**
- Mignan, A. et al. (2015), *Geothermics* **53**
- Mignan, A. (2015), *Geophys. Res. Lett.* **42**
- Mignan, A. (2016), *Nonlin. Processes Geophys.* **23**
- van der Elst, N. et al. (2016), *J. Geophys. Res.* in press

ENSAD v2.0 Hydro: a new interactive, GIS-based database for historical hydropower accidents worldwide

P. Burgherr¹, M. Spada¹, A. Kalinina¹, K. Wansub², S. Hirschberg¹

¹Technology Assessment Group, Paul Scherrer Institut, Villigen PSI, Switzerland

²Future Resilient Systems (FRS), Singapore-ETH Centre, Singapore

(FRS) FUTURE RESILIENT SYSTEMS 未来韧性系统

In cooperation with the CTI
Energy Swiss Competence Centers for Energy Research
Schweizerische Eidgenossenschaft
Confédération suisse
Confederazione Svizzera
Confederaziun Svizra
Swiss Confederation
Commission for Technology and Innovation CTI

Introduction

The historical risk assessment of hydropower accidents is based on data from PSI's Energy-related Severe Accident Database (ENSAD). For this purpose, ENSAD was updated, using data from a broad variety of primary information sources, including various databases, technical reports, case studies, as well as information retrieved from news portals and newspapers (Kalinina et al., 2016, in press).

New accidents were collected up to the current year, and existing accident records thoroughly reviewed and if necessary updated. Data collection was limited to accidental events attributable to hydropower dams, whereas intentional attacks on hydropower infrastructures were excluded. Three types of accident causes were considered, i.e. technical (e.g. material failure, weakness of foundation), natural (e.g. flood, landslide), and man-made (e.g. human error).

Furthermore, the current Microsoft (MS)-Access version of ENSAD is replaced by a newly developed, interactive, GIS-based database named ENSAD v2.0. The compilation of updated hydropower accidents is used for the prototype implementation.

Current ENSAD Database

Since its initial release (Hirschberg et al., 1998), the ENSAD database has been continuously updated and extended: (1) in content to keep up with the growing historical experience, and (2) in functionality and scope to provide high-quality decision support to stakeholders (Burgherr & Hirschberg, 2014). Figure 1 provides a schematic overview of the basic accident record structure as used in ENSAD.

Despite its well-established and proven structure, the ENSAD database has certain limitations (e.g. standalone application, static geo-referencing, no user-role management etc.). Therefore, it has been decided to radically change the foundation of ENSAD towards a web-based system, using state-of-the-art, open-source technologies.

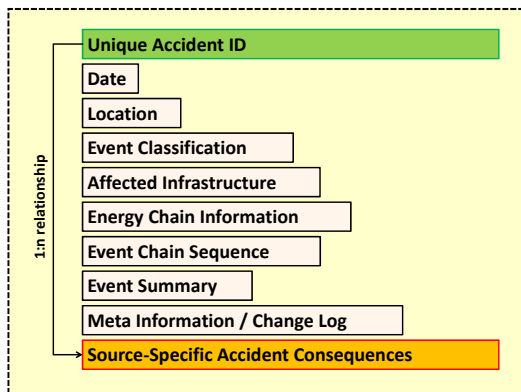


Figure 1: Overview of the accident record structure in ENSAD.

New ENSAD v2.0

Figure 2 shows the data flow and system architecture of the new ENSAD v2.0. First, the MS Access database of the existing ENSAD is migrated and transformed into a spatial database. In a next step, the connection to the GeoServer is made, and finally, the web application server generates the content for the web client.

Since the complete ENSAD database contains 32'705 data records, the migration process is carried out stepwise, i.e. individually for the different energy chains. They hydropower chain has been selected for the prototype development because the number of records is relatively small, and it is also currently updated and extended within the NRP70 joint project "Hydropower and geo-energy".

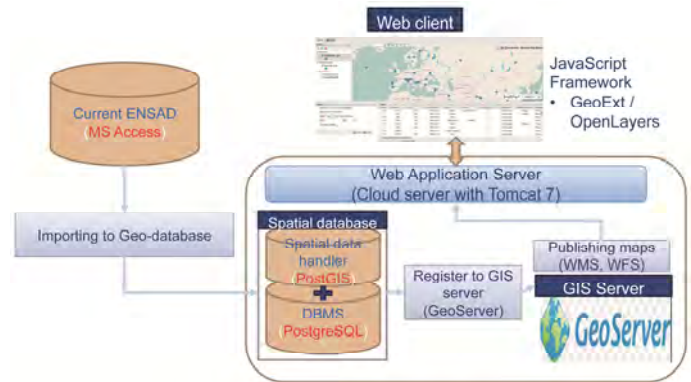


Figure 2: Schematic representation of the data flow and system architecture in ENSAD v2.0

The web client allows defining various user roles with specific properties and access rights, e.g. only data viewing or also editing, export and analysis of data. Accidents can be visualized on a world map. Additional layers with background data (e.g. dam and reservoir properties) or specific environmental and socio-economic information are available and can be combined with the actual accident data.

The hydropower prototype has been implemented in collaboration with PSI's risk team in the Future Resilient Systems (FRS) program of the Singapore ETH Centre (SEC). Figure 3 gives an overview of the current features and functionality of the prototype. It already includes the complete hydropower accident data set as well as a "register wizard" to add new accident records. The next steps comprise extensive internal testing, adding a track change management to log changes to a data record, and setting up the various user roles (user management).

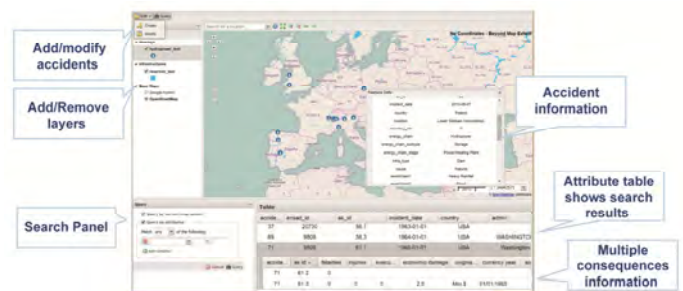


Figure 3: Current implementation status of ENSAD v2.0 hydropower prototype.

The "desktop version" of ENSAD v2.0 will be complemented with a "mobile version" that offers a reduced functionality, focusing on displaying specific accident information. Furthermore, the app will allow users to directly report new accidents to the developer team of ENSAD.

Acknowledgments

This work has been carried out within the Swiss Competence Center on Energy Research – Supply of Electricity, and the Energy Turnaround National Research Programme (NRP70) of the Swiss National Science Foundation, with support by the Future Resilient Systems (FRS) project of the Singapore-ETH Centre (SEC).

References

- Burgherr, P., Hirschberg, S. (2014) Comparative risk assessment of severe accidents in the energy sector. Energy Policy, 74, S45-S56.
- Hirschberg, S., Spiekerman, G., Dones, R. (1998) Severe accidents in the energy sector – 1st ed. PSI Report No. 98-16. Villigen PSI, Switzerland.
- Kalinina, A., Spada, M., Burgherr, P., Marelli, S., Sudret, B. (2016, in press) A Bayesian hierarchical modelling for hydropower risk assessment. European Safety and Reliability Conference (ESREL 2016), Glasgow, UK.

Accident Risk Assessment for Deep Geothermal Energy Systems for Switzerland: An Update



Matteo Spada, Emilie Sutra, Peter Burgherr

Technology Assessment Group, Laboratory for Energy Systems Analysis, Paul Scherrer Institut (PSI)

Introduction

This work is built upon the approach developed in the TA Swiss study (Spada & Burgherr, 2015), which was refined and significantly extended in SCCER-SoE.

Deep geothermal energy systems are, like all energy technologies, not fully risk free. Although the risk of induced seismicity is frequently pointed out, geothermal systems present additional potentially risky aspects such as borehole blowouts or chemical related incidents. In this study, different technological risks associated with deep geothermal energy systems are identified, characterized and quantitatively analyzed. In particular, three major updates have been achieved in this phase, which are the introduction of accidents related to the release of hydrogen sulphide during the drilling and stimulation phases, the update of historical accidents in the period 1990-2015 and, finally, the calculation for all the deep geothermal power plant capacities defined in Task 4.2 "Global Observatory". Results are shown in terms of normalized risk indicators (e.g. fatality rate, injury rate) in order to compare risks of blowouts and release of hydrogen sulphide in the drilling and stimulation phases, and the use of hazardous substances in drilling, stimulation and operational phases.

Data

Since deep geothermal systems have not been yet installed at many sites, historical experience in terms of accidents is rather limited. Therefore, the estimation of risk indicators is based on historical experience of other industries that can be considered a meaningful proxy for deep geothermal systems. In all considered cases, accident data for the time period 1990-2015 from OECD countries were used because they can be considered sufficiently representative for Switzerland. However, when dealing with hazardous substances, it was necessary to focus on the chemicals that could be possibly used in Switzerland. In addition to PSI's Energy-related Severe Accident Database (ENSAD) several other databases were used in order to collect accidents related to the use of hazardous substances, i.e. ERNS, ARIA, HSE, MHAID, FACTS, eMars and HINT.

Hazardous Substance	Accidents/Fatalities	Accidents/Injuries	Accidents/Evacuees
Caustic Soda	13/30	142/1149	30/14863
Hydrogen Chloride (HCl)	2/4	94/697	106/15534
Hydrogen Fluoride (HF)	2/2	26/83	24/10123
Benzene	2/3	33/562	29/87026
Toluene	16/20	66/679	46/2015
Hydrogen Sulphide (H2S)	4/4	9/18	5/743

Summary of the numbers of accidents and associated consequences for the Hazardous Substances analyzed in this study.

Blowouts	Accidents/Fatalities	Accidents/Injuries	Accidents/Evacuees
	4/4	11/25	11/3820

Summary of onshore blowout accidents in the natural gas industry, collected for USA and Alberta, since no specific historical experience for deep geothermal systems is available.

Method

The risk indicators are normalized to the unit of energy production (i.e. Gigawatt-electric-year, GWeyr) using specific normalization factors for each substance and blowout.

$$NF_{Caustic\ Soda} = \frac{CS_{Well} * WD * NW}{total\ production\ 1990 - 2015} * \frac{1}{P_{GWeyr}}$$

$$NF_{Stimulation} = \frac{HS_{Well} * NW}{total\ production\ 1990 - 2015} * \frac{1}{P_{GWeyr}}$$

$$NF_{Working\ Fluid} = \frac{WF_{Year1} + (kg\ of\ substance\ refilled * LT)}{total\ production\ 1990 - 2015} * \frac{1}{P_{GWeyr}}$$

$$NF_{Drill+Stim} = \frac{NW}{total\ number\ of\ natural\ gas\ drilled\ wells\ 1990 - 2015} * \frac{1}{P_{GWeyr}}$$

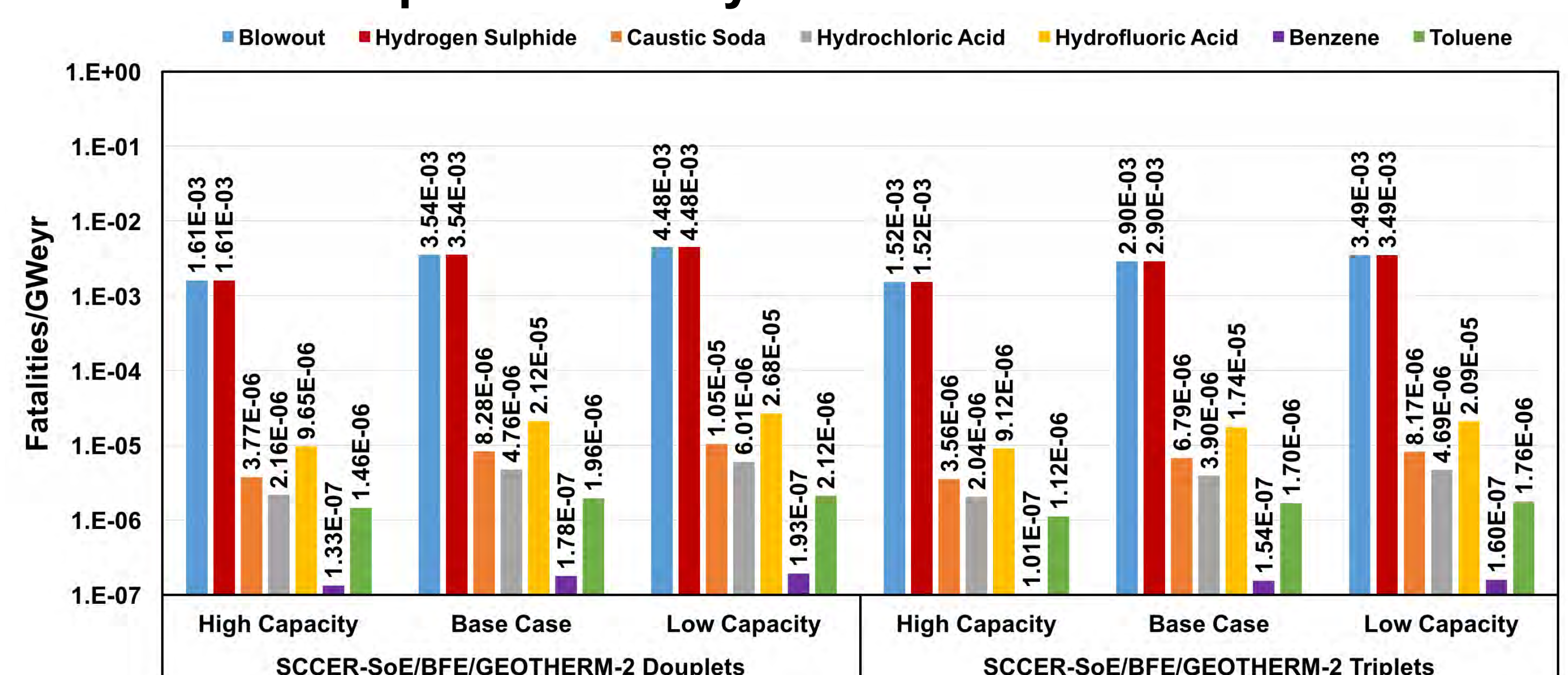
$NF_{Caustic\ Soda}$, $NF_{Stimulation}$, $NF_{Working\ Fluid}$ and $NF_{Drill+Stim}$ are the normalization factors for Caustic soda, HCl and HF, Benzene and Toluene, Blowouts and H2S, respectively. See the following table for the inputs to the equations.

The table below summarizes the key physical parameters of the deep geothermal plant capacity cases considered in this study for normalization purposes.

	SCCER-SoE/BFE/GEOTHERM-2 Doublets			SCCER-SoE/BFE/GEOTHERM-2 Triplets		
	High Capacity	Base Case	Low Capacity	High Capacity	Base Case	Low Capacity
Net plant power	3.28 MW _e	1.45 MW _e	1.18 MW _e	5.21 MW _e	2.73 MW _e	2.27 MW _e
Production in GWeyr (P _{GWeyr})	6.56e-2 GWeyr	2.99e-2 GWeyr	2.36e-2 GWeyr	1.04e-1 GWeyr	5.46e-2 GWeyr	4.54e-2 GWeyr
Well depth (WD)	5 km					
Number of wells (NW)	2			3		
Surface plant life time (LT)	20 years					
Caustic Soda as additive in the drilling mud per Well (CS _{Well})	1 kg/m					
Additives in Hydraulic Stimulation (total average) per Well (HS _{Well})	HCl: 11820 kg HF: 2470 kg					
Working Fluids used at the power plant at year 1 (WF _{Year1})	Benzene: 1208 kg Toluene: 1197 kg	Benzene: 737 kg Toluene: 730 kg	Benzene: 632 kg Toluene: 626 kg	Benzene: 1465 kg Toluene: 1452 kg	Benzene: 1169 kg Toluene: 1158 kg	Benzene: 1007 kg Toluene: 998 kg
Yearly losses of the working fluids (YLWF)	8%					

Key physical parameters of the capacity cases for deep geothermal plants considered in this study.

Results: Example for Fatality Rates



Fatality rate for the drilling, stimulation and operational phases based on accidents data for the period 1990-2015.

- Among hazardous substances, H2S release exhibits the highest risk whatever the type of consequences (fatalities, injuries, evacuees) followed by the use of HF at the geothermal site.
- Blowout risk is similar to H2S release, which is higher than the most accident-prone hazardous substance used, for all three consequences indicators (fatalities, injuries, evacuees).
- Doublets (2 production wells) and triplets (3 production wells) plant types show similar results in terms of risk related to the different phases considered and for all type of consequences.

Conclusions

- Accident risks of blowouts and H2S release are significantly higher than the risk related to the use of hazardous substances.
- Results for the use of hazardous substances in drilling, stimulation and operational phases point towards low risk levels, except for evacuees (particularly HCl and HF).
- Based on these results, the drilling and stimulation phases in deep geothermal systems exhibit higher risks compared to the operational phase.
- Deep geothermal systems compare favorably to, for example, natural gas (7.19E-2 fatalities/GWeyr for OECD countries, according to Burgherr and Hirschberg, 2014)
- Environmental impacts due to accidental releases of hazardous substances should not be neglected: toxicity and exposure levels as well as location-specific factors should also be taken into consideration.

Induced seismicity risk analysis in OpenQuake. Basel 2009 case study, validation and GIS integration.

Marco Broccardo, Laurentiu Danciu, Arnaud Mignan, Stefan Wiemer.
Acknowledgment: Lukas Heiniger OQ assistance, Simona Esposito GIS assistance

Abstract

The objective of this project is to create a standardized environment in OpenQuake (OQ) for hazard and risk assessment of induced seismicity. The developed tools are used as computational components in different projects. Among these, the most important are: Advanced Traffic Light System (ATLAS), RAMSIS AP3, and SCCER Task 4.1 (risk governance framework for induced seismicity). The GIS integration offers an appealing environment for creating risk and losses geo-reference databases for a given geothermal project. The development framework is tested versus the benchmark case study of Basel 2009 (Mignan *et al.* 2015)

Hazard benchmark case study Basel, 2009

- Classical PSHA analysis
- Intensity measure EMS-98 scale (I_{EMS})
- Source: point source. Injection site
- Frequency-magnitude distribution: Truncated Gutenberg Richter
- Epistemic Uncertainties, logic tree (Figure 1): 2 rate models, 3Mmax, 8 Ground Motion Predictive Equations (GMPE), 2 Ground Motion Intensity Conversion Equation (GMICE), 4 Intensity Predictive Equations (IPE). Number of branches 120

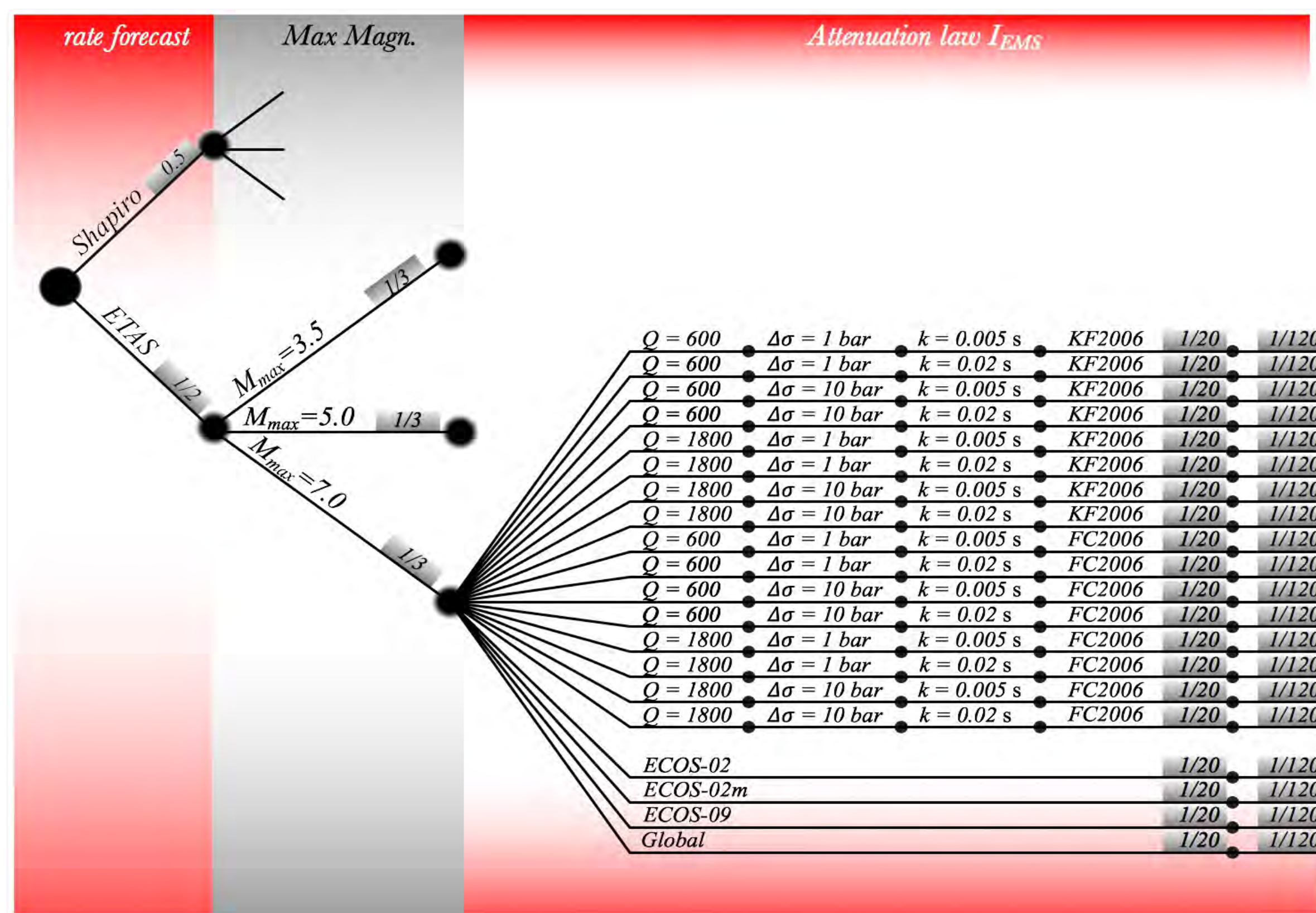


Figure 1: Logic tree

OpenQuake hazard benchmark test

- Definition of a standard procedure for modelling the logic tree in OQ
- GMICE and IPE coded in I-Python
- Test the new implementation versus the benchmark (Mignan *et al.*)
- Results show perfect matching between benchmark and OQ implementation (Figure 2)

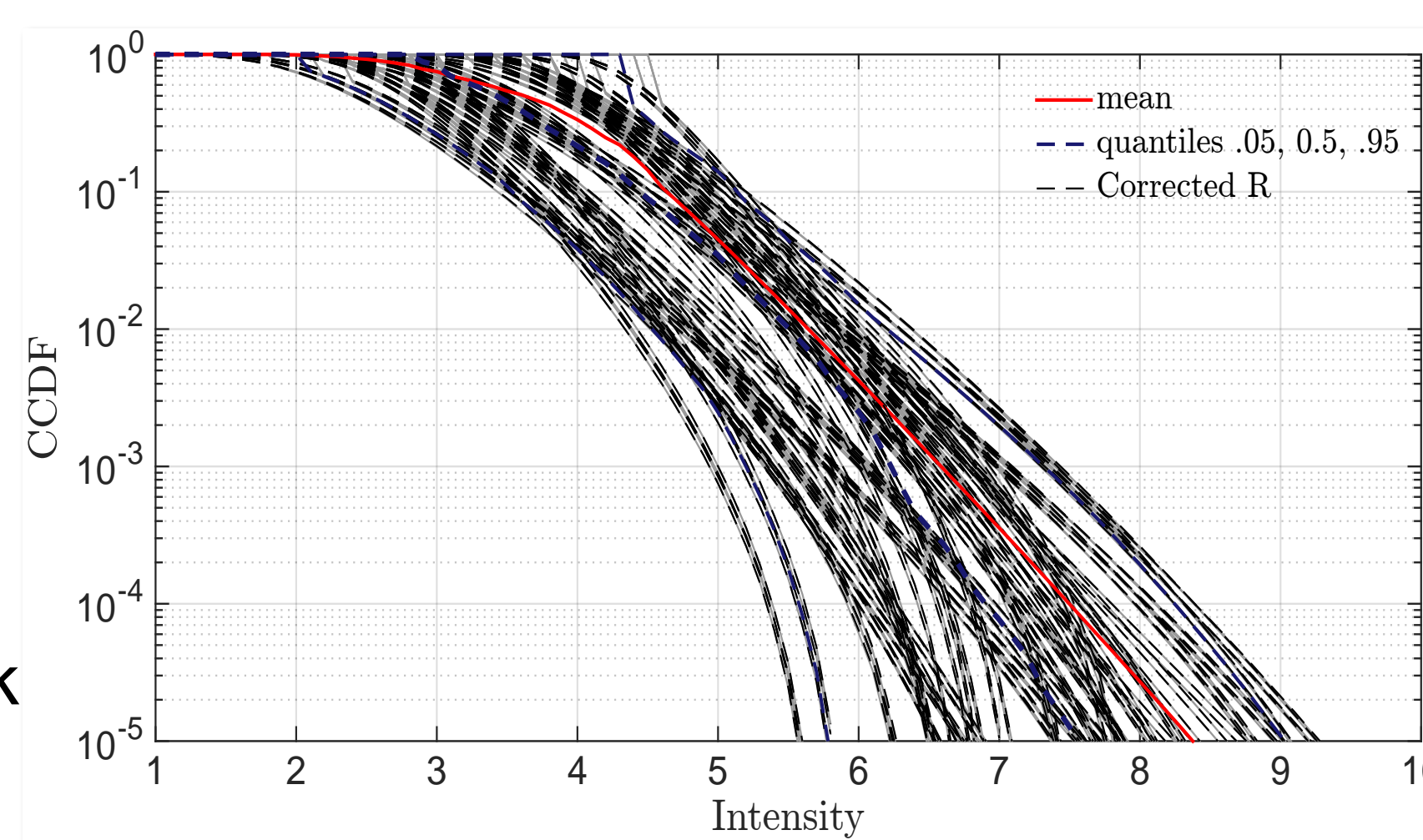


Figure 2: Hazard benchmark

OpenQuake hazard outputs

- 120 Hazard curves computed for 79 locations. Maps created by the median value at $P(I_{EMS} > i_{\Delta\sigma}) = 10^{-3}$ and via Kriging interpolation (Figure 3).

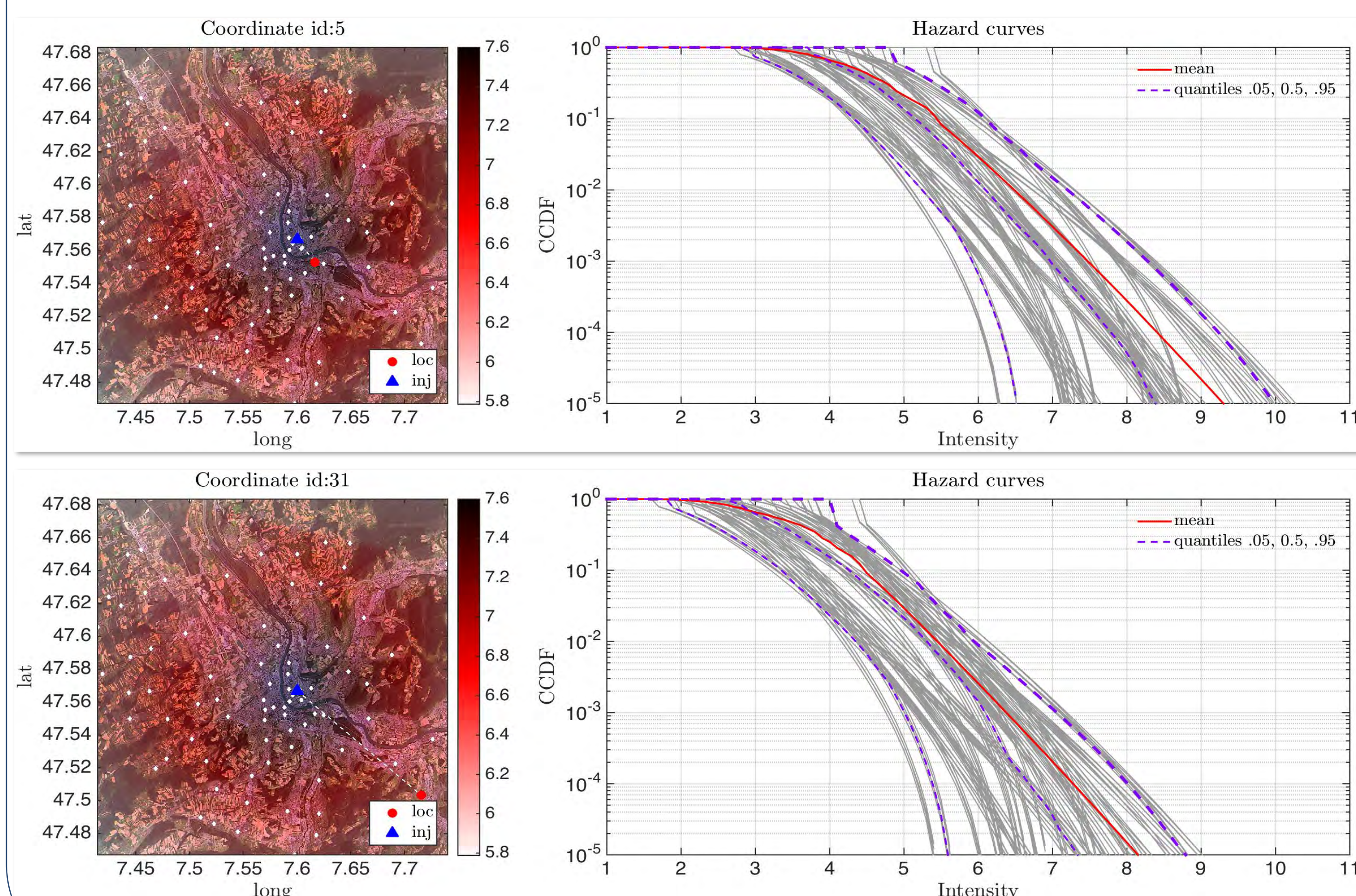


Figure 3: Hazard curves for two different locations

OpenQuake risk assessment

- "PSHA risk analysis". Fully deterministic, the vulnerability functions are used as pure mapping.
- The structural vulnerability model (Mignan *et al.*), is coded in a user friendly I-python environment
- Exposure model (Mignan *et al.*) is coded in a user friendly I-python environment
- Risk maps (Figure 4) obtained for 79 locations and extended via Kriging interpolation. Median value at $P(L > l) = 10^{-3}$ (L =losses [CHF])

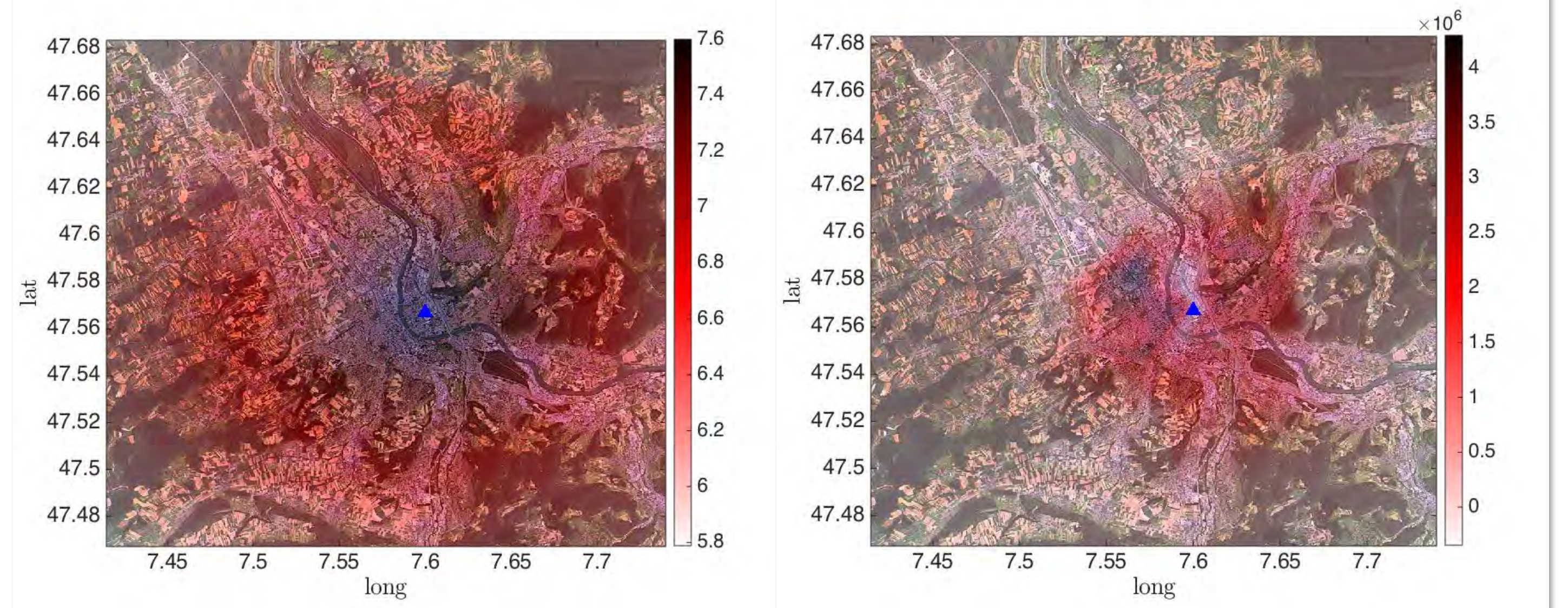


Figure 4: Hazard map (left), Risk map (right)

Risk disaggregation per location and building class

- OQ output: for each location computes risk curves for a given class of building, and the aggregate risk. Figure 5

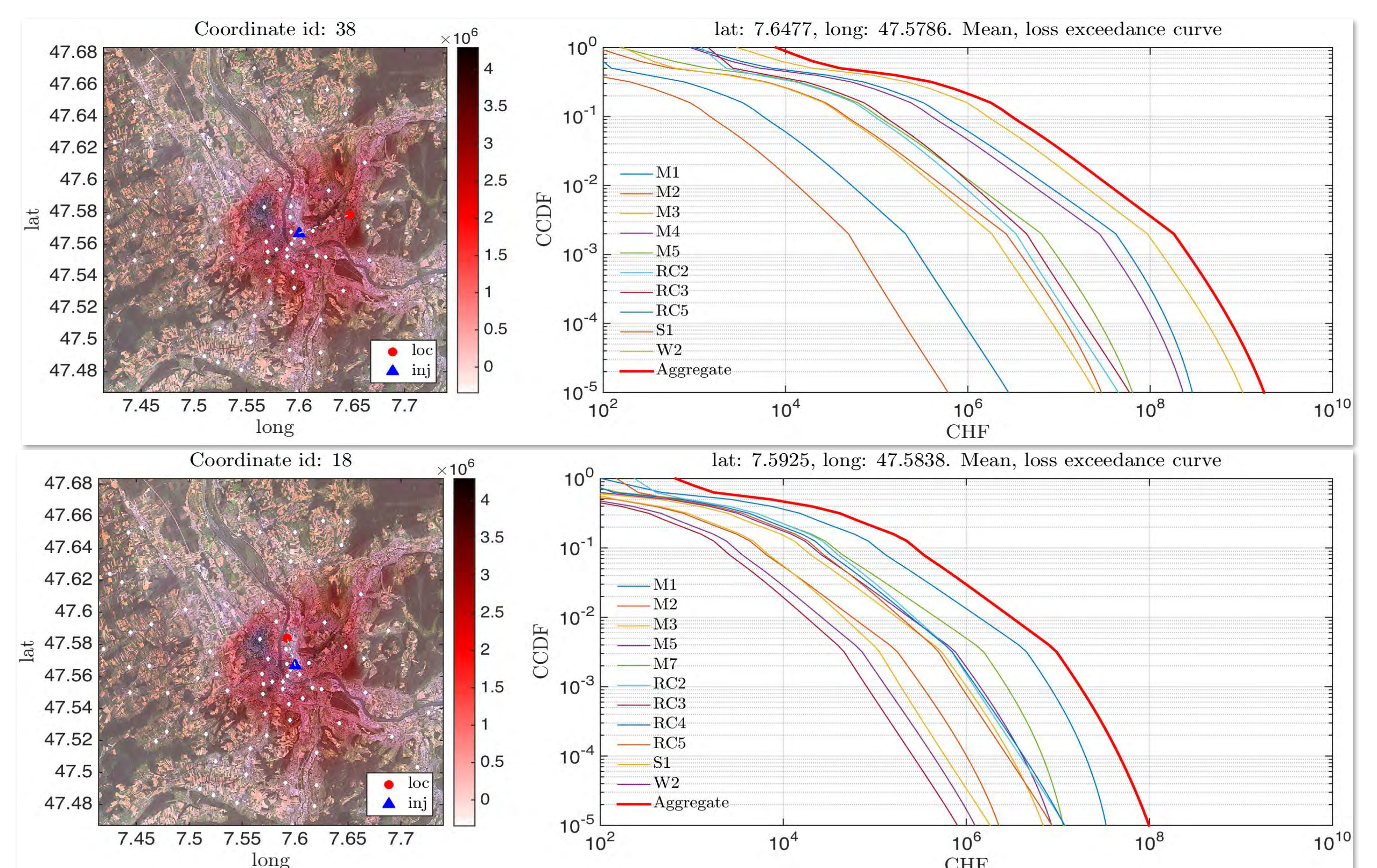


Figure 5: Risk curves for two different locations and different building classes

Aggregate risk curves

- Aggregate curves computed via local aggregate risk and combination of comonotonic random variables. (Broccardo *et al.* 2017)
- Curves represent an upper bound of the true risk

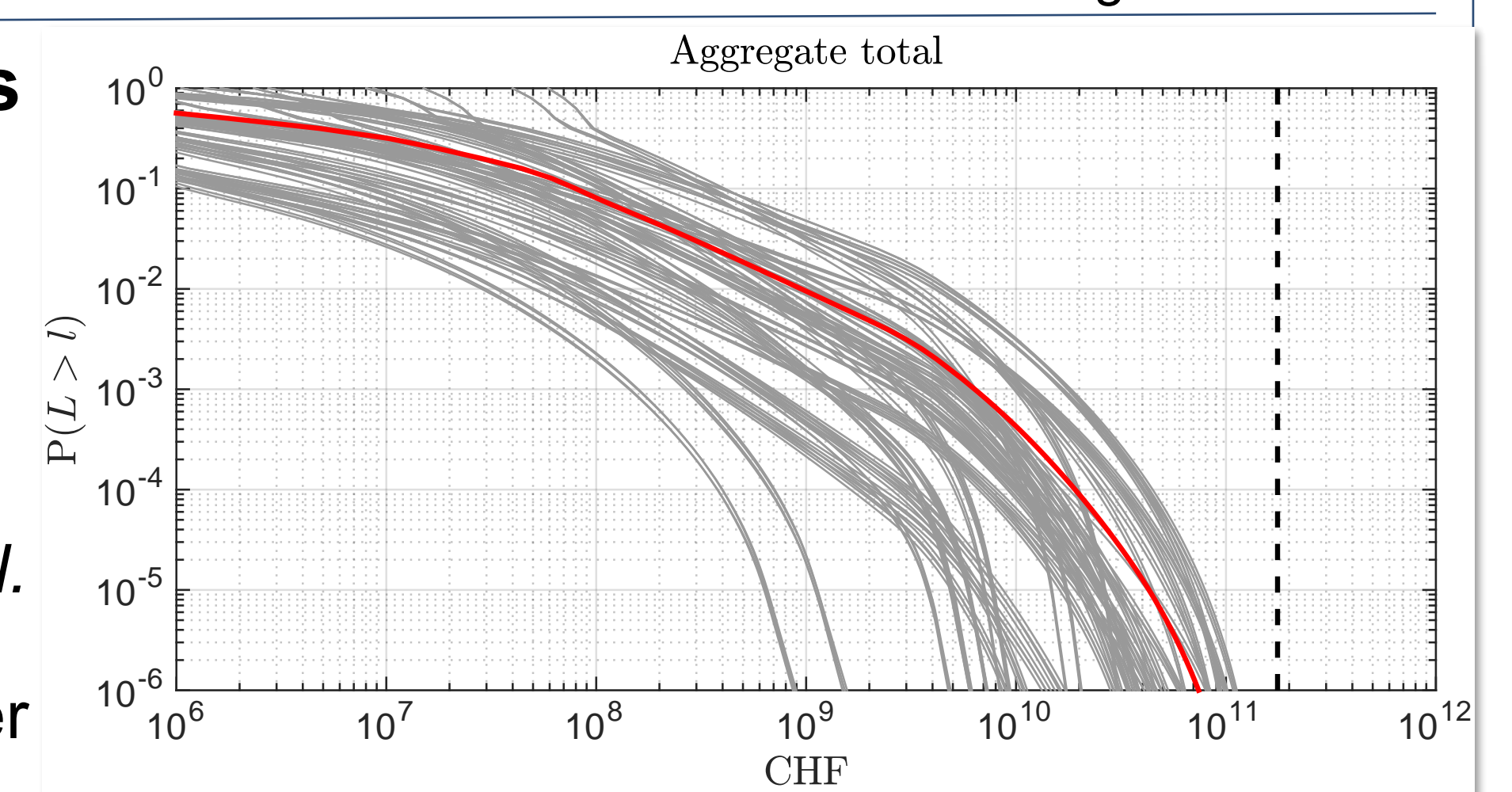


Figure 7: Aggregate risk curves

Aggregate risk curves

- Creation of Geo-Reference Database (ArchGIS) composed of:
 - Building environment layer (source Open Street)
 - Damage layer (source OQ)
 - Loss layer (source OQ) (Figure 8)

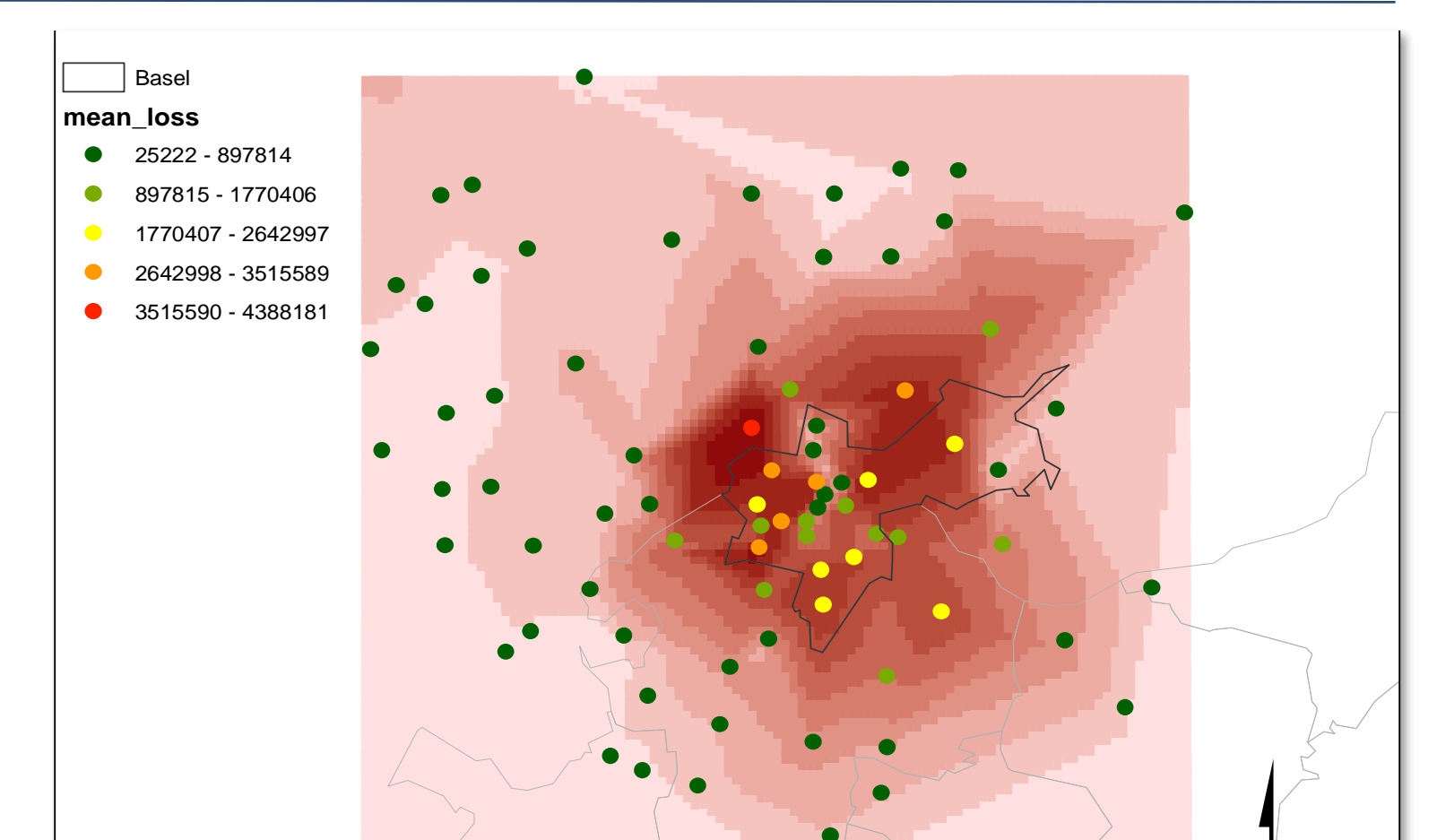


Figure 8: GIS loss layer

References

- Mignan, A., Landtwing, D., Kästli, P., Mena, B., & Wiemer, S. (2015). Induced seismicity risk analysis of the 2006 Basel, Switzerland, enhanced geothermal system project: Influence of uncertainties on risk mitigation. *Geothermics*, 53, 133-146.
- Broccardo M., Danciu L., Stojadinovic B., Wiemer S. (2017) Individual and societal risk metrics as parts of a risk governance framework for induced seismicity, *16th World Conference on Earthquake Engineering, 16WCEE*, Santiago, Chile.

Nonstructural Damage Tests on Masonry Building Walls: First Phase

Max Didier, Marco Broccardo, Giuseppe Abbiati, Laurentiu Danciu, Katrin Beyer, Bozidar Stojadinovic, Domenico Giardini

Objective

This project aims to investigate the likelihood of nonstructural damage, i.e. cosmetic cracks, on typical masonry panels, which are widely used in Swiss buildings, in case of induced seismicity. In the first phase of the test, five 1.20x1.20x0.15m walls with mortar plaster of 12-15mm thickness on one side were tested using three different load sequences. The first load sequence represents induced earthquakes with magnitude below 3.8 (Bin 1), the second load sequence represents induced and natural earthquakes with magnitudes between 3.8 and 5 (Bin 2), and the last load sequence represents European natural earthquakes selecting according to Mergos and Beyer (2014), namely Bin 3. Test outcomes show that: the first load sequence did not cause observable damage; the second load sequence caused observable nonstructural damage; the third load sequence caused significant structural and nonstructural damage. The second phase of the project will consist in testing additional ten walls to extract empirical vulnerability functions for nonstructural damage for modern Swiss masonry panels. The project is part of the NFP70 on Energy Turnaround, and led by the Chair of Structural Dynamics and Earthquake Engineering at ETH.

Input Selection and Binning

The original dataset of induced motions was composed of: PEER East US induced motions dataset, Basel 2009, St. Gallen 2013 and a selection of West US induced motions (Figure 1).

- Bin 1: $M \in [3.0, 3.8]$; $R \in [0, 15]$ km
- Bin 2: $M \in (3.8, 5]$; $R \in [0, 20]$ km
- Bin 3: Natural seismicity (Mergos and Beyer, 2014)

Since the number of records resulted insufficient for deriving a robust load sequence, we increased the number of records for Bin 1 & 2 following these criteria:

- Bin 1: Scaling the given set of ground motions
- Bin 2: Inclusion of natural earthquakes with the same magnitude, distance range, and soil condition.

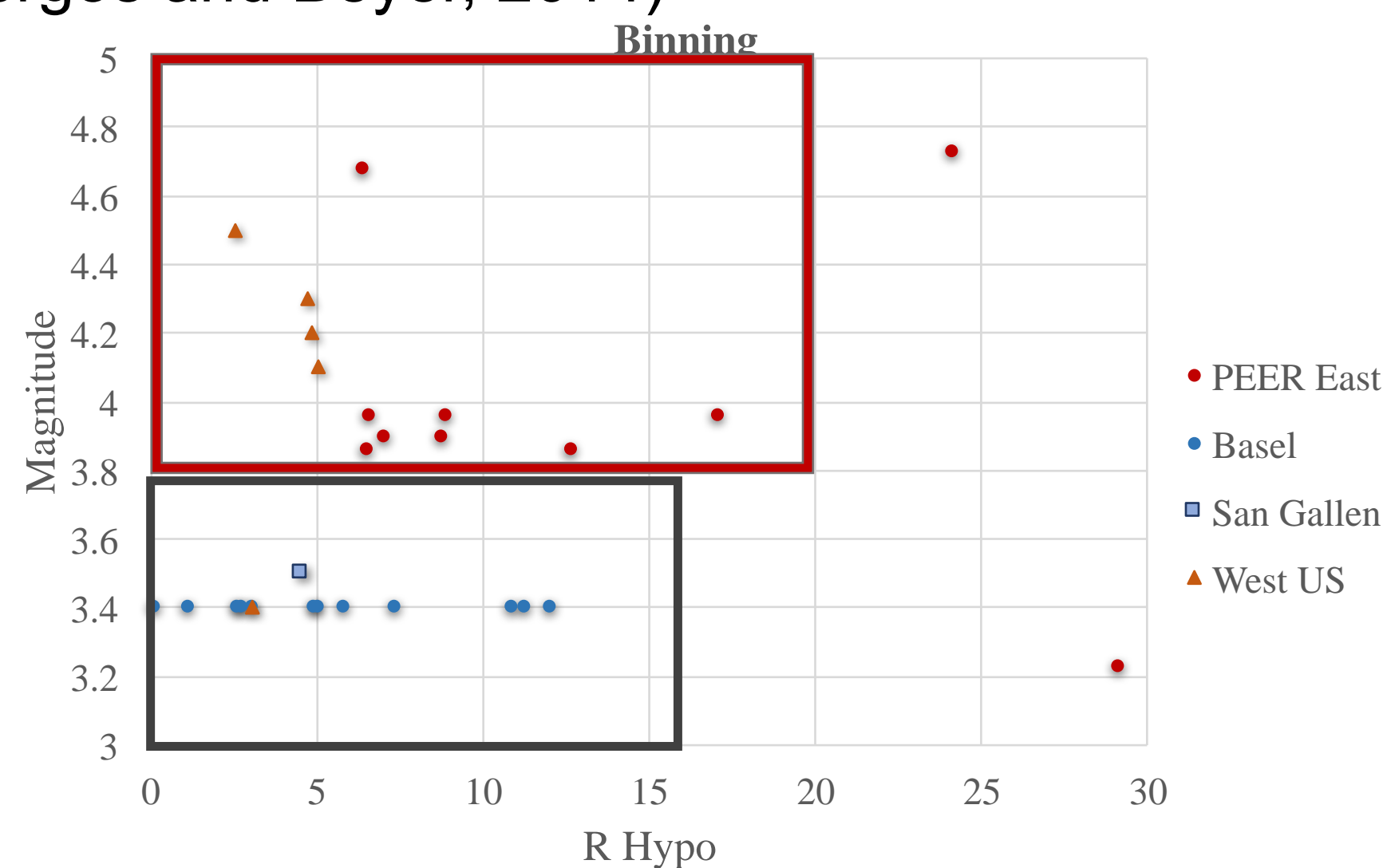


Figure 1 Original dataset

Augmented dataset

Bin 1 The scaling was based on Magnitude and GMPEs and derived as follow:

- Select GMPE (Ground Motion predictive equations) for induced seismicity which closely represents the data. We selected 4 GMPEs based on Atkinson *et al.* (2015) and Douglas *et al.* (2013) (Figure 2-i).
- Compute the reference median for the recorded M_s and the given R_s .
- Scale the median for the new magnitude level.
- Compute the ratio between scaled and reference median for each GMPE.
- Apply the mean of the scaling factor to the recorded time series (Figure 2-ii)
- We defined the following magnitude levels $M = [3.0, 3.2, 3.4, 3.6, 3.8]$. The resulting total number of records is 71.

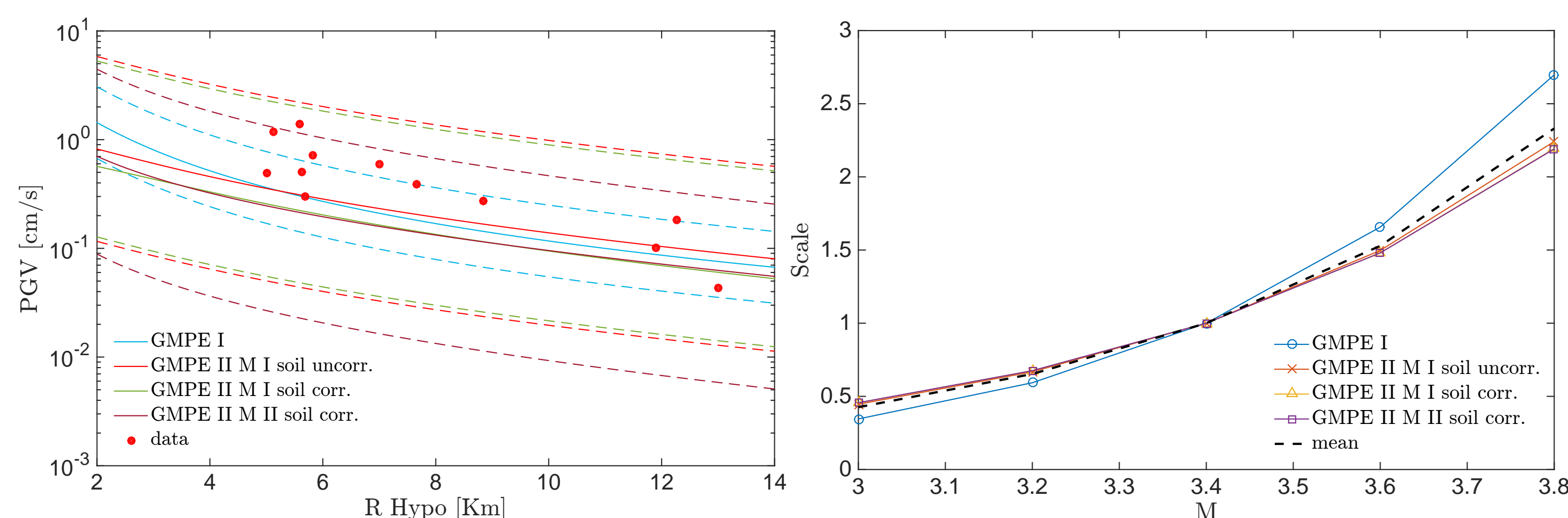


Figure 2 selected GMPEs (left) and scaling factors (right)

Bin 2 is improved with 63 natural records which are the first principal component of the recorded motions. Records belong to classes A, B (according Eurocode 8). Figure 3 shows the selected motions. Total number of motions for the augmented bin 2 is 72.

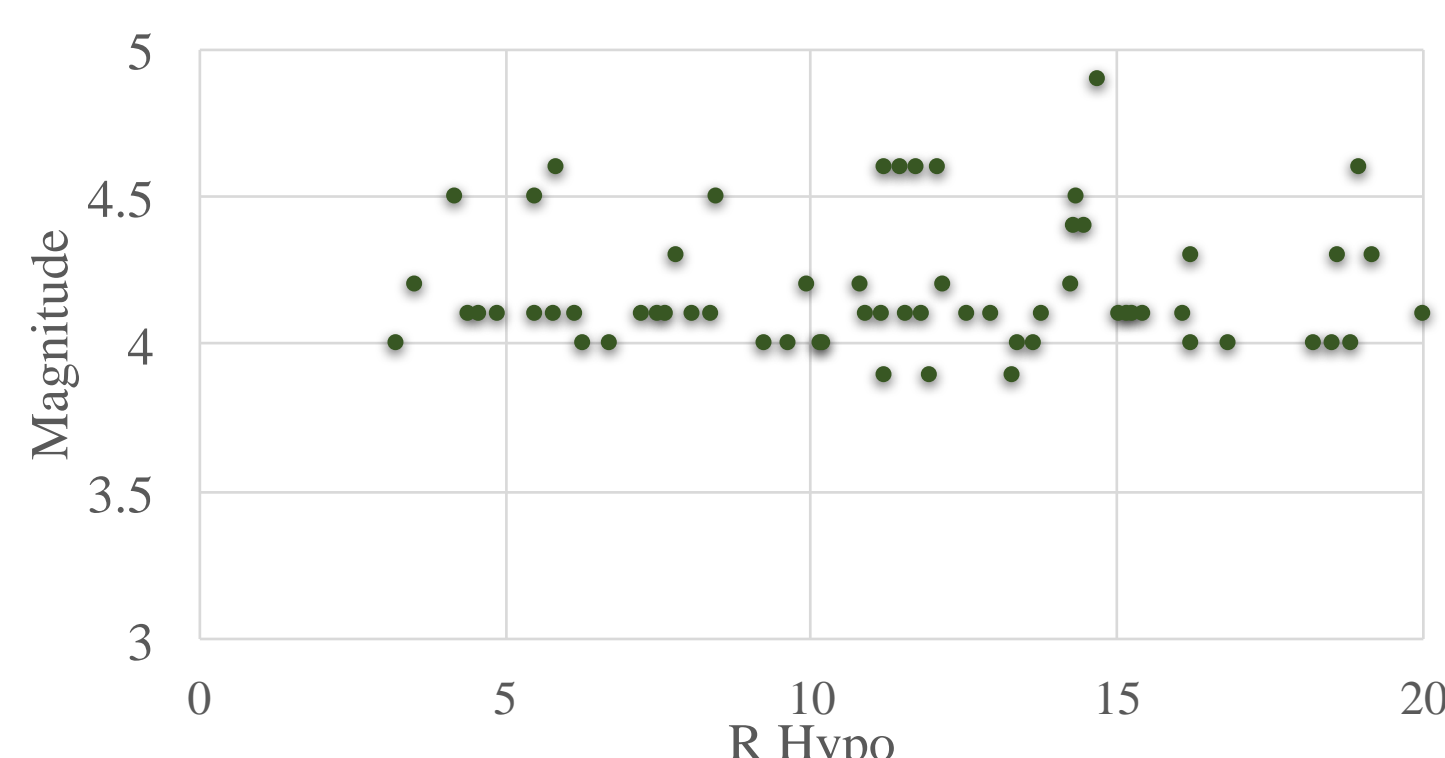


Figure 3 Bin 2 natural motions

Ground Motion Sequence

The response of an elastic single-degree-of-freedom system of 0.3s period and 2% damping, which represents a prototype one-story masonry building, was calculated for each record. Then, the rainflow-counting algorithm was applied to each displacement response history and resulting amplitudes were averaged to produce a quasi-static cyclic load sequence per ground motion bin. Figure 4 reports the test sequences for Bin 1 & 2. The test sequence corresponding to Bin 3 can be found in Mergos and Beyer (2014).

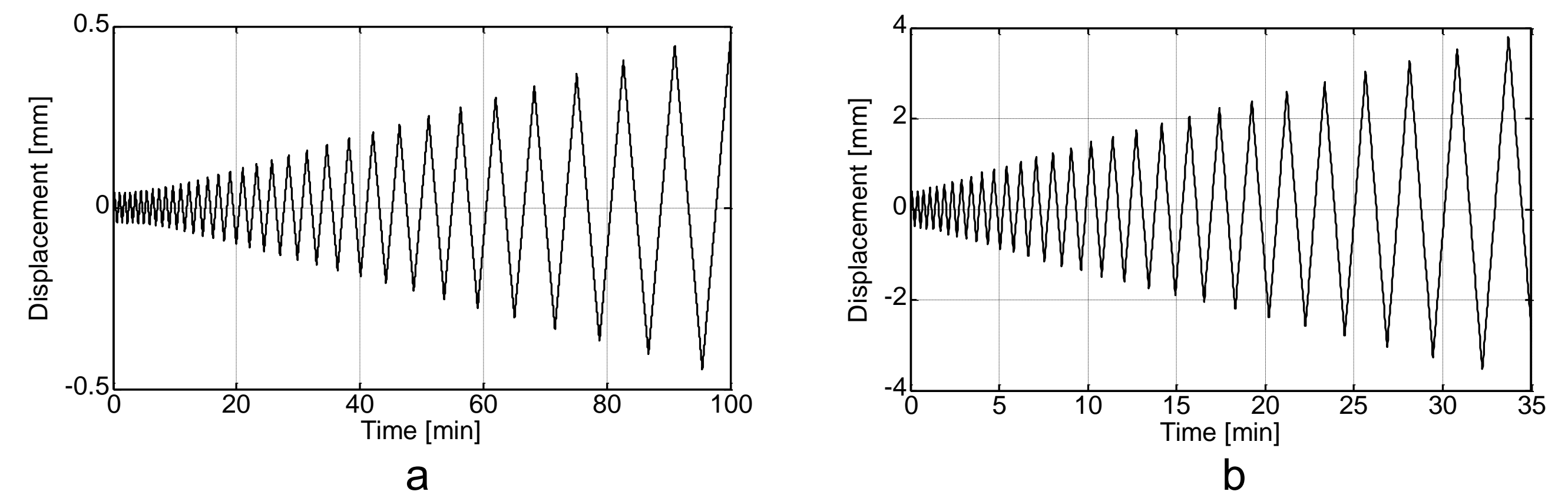


Figure 4 Load sequences corresponding to Bin 1 (left) and Bin 2 (right).

Experimental Setup

Figure 5 shows a schematic of the three-actuator setup that was used to conduct the tests. In detail, the horizontal actuator imposed the displacement sequence to the wall top. A laser displacement sensor provided the feedback for the displacement control loop. A vertical load equal to 10% of the vertical yielding strength of the wall was applied by means of the two vertical actuators, which were used in force control. A cantilever boundary condition was obtained by correcting vertical forces to zero the bending moment at the wall top. Seven Linear Variable Differential Transformers (LVDTs) measured local displacements at the bottom and the top of the wall as well as the foundation slip. A random speckle pattern was painted on the plaster surface to perform Digital Imaging Correlation (DIC) measurements. DIC pictures were shot at predefined values of the transversal displacement. A subsequent plane strain analysis was performed and synchronized with LVDT and actuator measurements.

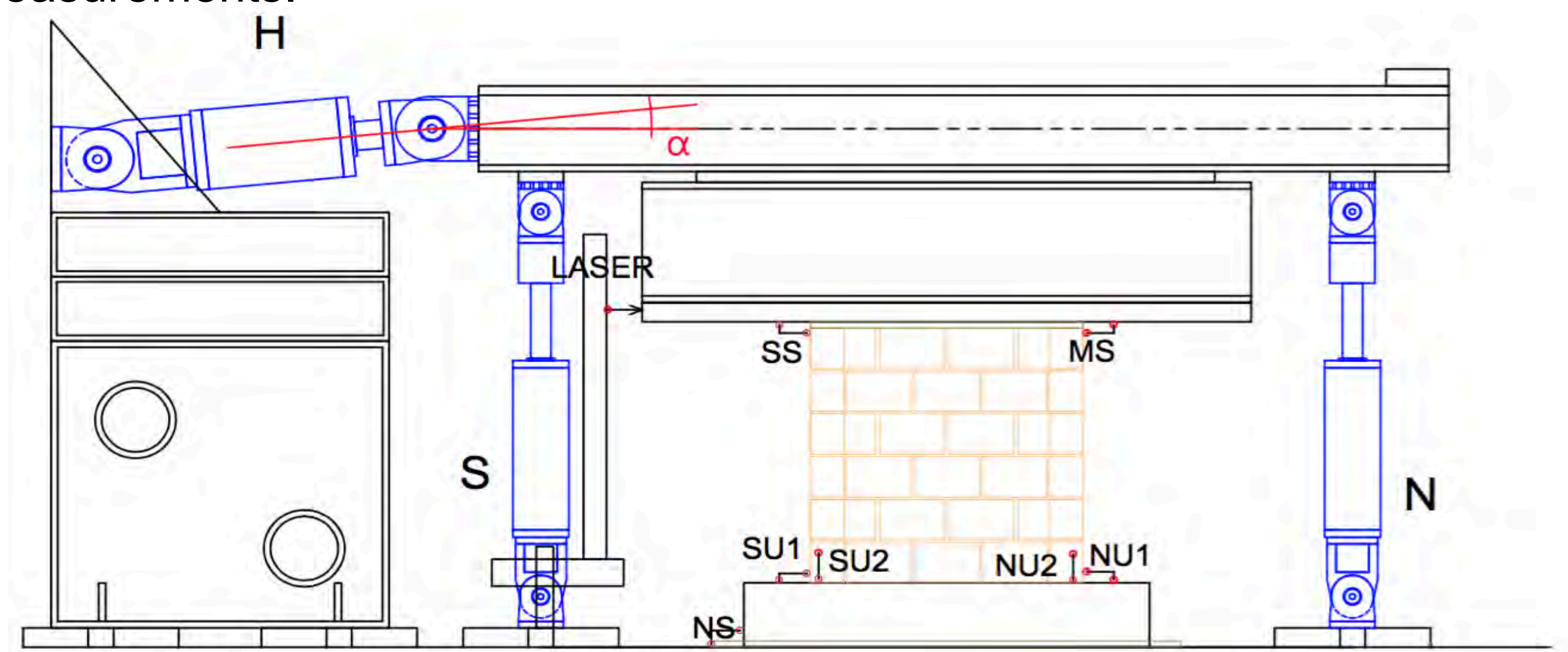


Figure 5 Experimental setup

Preliminary Results

The first wall was used to calibrate the tests setup and related results were excluded from the crack analysis, which was conducted on the remaining 4 walls. Pictures taken during the test sequence were processed with the Vic2D DIC software to estimate plaster displacement and strain fields. The following crack analysis was performed in Matlab. In detail, the location of cracks was picked on the last picture of each test, where crack opening was more visible. Then, crack width growth was monitored over the entire sequence in terms of relative displacement between two points located on either side of the selected crack. First visible cracks were systematically observed on the un-plastered side of the wall and close to mortar joints for transversal displacements of about 1.50 mm. Visible cracks on plaster were triggered for transversal displacements of about 1.80 mm. Figure 6 shows an overview of the crack analysis for Wall 3, Bin 2 sequence.

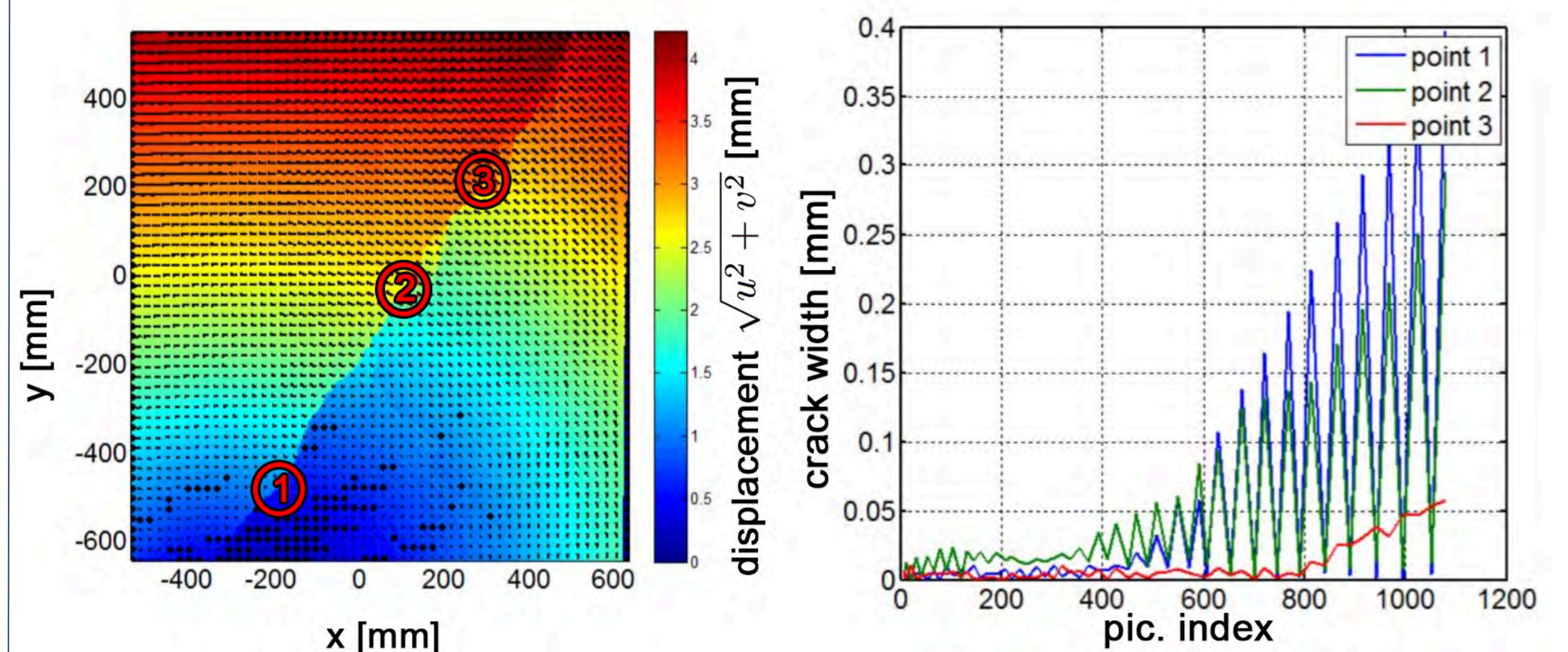


Figure 6 Wall 3 Bin 2: displacement, location of tracked crack widths (left); time history of crack widths (right)

References

- Mergos, P. E., & Beyer, K. (2014). Loading protocols for European regions of low to moderate seismicity. *Bulletin of Earthquake Engineering*, 12(6), 2507-2530.
- Atkinson, G. M. (2015). Ground-motion prediction equation for small-to-moderate events at short hypocentral distances, with application to induced-seismicity hazards. *Bulletin of the Seismological Society of America*.
- Douglas, J., Edwards, B., Convertito, V., Sharma, N., Tramelli, A., Kraaijpoel, D., Troise, C. (2013). Predicting ground motion from induced earthquakes in geothermal areas. *Bulletin of the Seismological Society of America*, 103(3), 1875-1897.

Social discourses on deep geothermal energy

Olivier Ejderyan, Michael Stauffacher – D-USYS TdLab, ETHZ

Research context

Actors active in the development of deep geothermal energy (DGE) have stressed that its large scale deployment does not depend only on technological innovation but also on its social acceptance (Majer et al. 2012;) Social sciences are enrolled to enquire social perceptions in order to anticipate acceptance when planning a geothermal project.



Public information event in Geneva preceding the launch of a seismic exploration campaign. Photo: O. Ejderyan

Social sciences can make valuable contribution to public engagement procedures for siting, planning, and risk management of DGE infrastructures. Here it is important to underline that “there is no “cookbook recipe” applicable to all projects that might imply induced seismicity and there can barely be one” (Trutnevte & Ejderyan, submitted).

The assessment of social acceptance and the development of adequate public engagement procedures must link multiple scales. It is therefore always dependent on bringing together different contexts. Analyzing public discourses on DGE provides crucial information on these contexts.

The goals of this research is to contribute conceptually and empirically to the development of public engagement procedures for DGE that are coherent from a general energy policy point of view, yet address local specificities.

Methods

This research combines media analyses and ethnographic case studies. Through media analysis it is possible to analyse how DGE is framed in the public sphere at various levels. Ethnographic case studies enable to analyse how such frames are mobilised on concrete DGE projects.



Swiss newspaper headings on DGE Collage: O. Ejderyan

Name	Sources	References
Aspects financiers	53	129
Aspects techniques	83	383
Connaissances	77	197
Développement de la géothermie	83	226
Gouvernance	74	347
Questions énergétiques	68	202
Risque	81	283
Comparaison risque autres énergies	2	2
Evaluation des risques	11	14
Evocation de risques	2	2
Impact sur la santé	2	3
Risque de séisme	67	197
Evocation du risque de séisme	20	24
Explications techniques séisme	7	8
Importance du risque de séisme	39	76
Minimisation importance séisme	41	86
N'est pas la raison de l'échec de Saint Gall	2	2
Relativisation	33	48
Doit être accepté-trade off	8	8
Relativisation-faible-normal-insignifiant	12	18
Spécifique à un lieu	5	7
Spécifique à une technologie	13	15
Risque contrôlé	19	31
Question des assurances	1	2
Risque écologique	21	26
Risque forage	25	33
sécurité prise au sérieux	2	5
Spécificité Bâle	51	109

Screenshot of code categorization indicating the number of statements and articles per category.

The media analysis is completed with case studies in St. Gallen (Muratore et al. 2016), Haute-Sorne and Geneva.

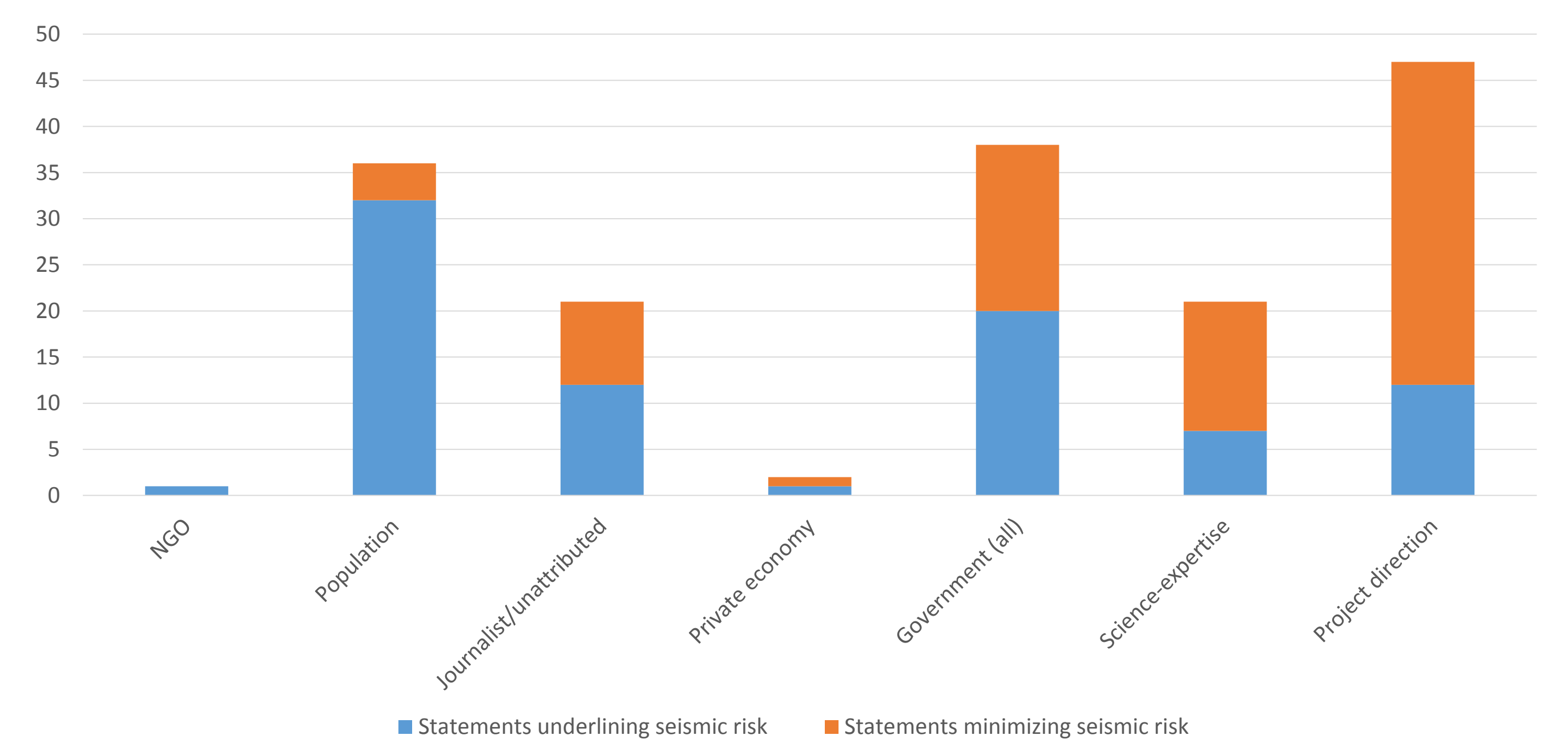
Results

The media analysis reveals that 6 main frames are used in the French speaking press. Media frames do not inform about the distribution of opinions in the population. But they are a suitable indicator to anticipate on the issues that will be raised as well as on the structure of arguments that will be used. These frames are consistent with the 4 frames identified in the

Frame	Statements	Articles
Technical	383	83
Governance	347	74
Risk	284	81
Transition	202	68
Knowledge	194	77
Cost	129	53

Media frames identified in Swiss-French newspapers, with number of statements and articles where occurring.

study on Swiss-German media (Stauffacher et al. 2015), indicating that there is a public discourse at national level. The main difference is the important of the “Governance” frame in Swiss-French speaking media. This frames highlights ongoing debates about the actors and institutions that should be included or not in decision-making about the development of DGE.



Statements on seismic risk associated to DGE by type of actors, in Le Temps, Tribune de Genève and Le Quotidien Jurassien (1997-2015)

The media analysis highlights the diversity of positions held by actors. For instance, detailed examination of statements related to seismic risk indicates that promoters of DGE tend to relativize risk through various rhetorical means while the population stresses its significance.

Conclusion

The media analysis shows that there are structuring elements in reporting on DGE. In order to evaluate in which respect these elements are central to social discourse on DGE, it is necessary to examine how frames are mobilised by concerned publics in actual DGE projects

First results of the case study in Haute-Sorne indicate the relevance of framing analysis to identify the main issues that will be raised. However they also show that media reports tend to homogenize actors categories and reduce the complexity of positions towards DGE. Must be addressed before designing public engagement procedures.

References

Majer, E. et al. 2012. *Protocol for Addressing Induced Seismicity Associated with Enhanced Geothermal Systems*. Washington DC.

Muratore, Stefano et al. 2016. *Tiefengeothermie: Das Projekt St. Gallen. USYS TdLab Transdisciplinäre Fallstudie 2015*. Zürich.

Stauffacher, M., N. Muggli, A. Scolobig, C. Moser 2015. *Framing deep geothermal energy in mass media: the case of Switzerland*. Technological Forecasting and Social Change 98: 60-70.

Trutnevte, Evelina, and Olivier Ejderyan. Submitted. “Managing Geogeneity-Induced Seismicity with Society.” *Journal of Risk Research*.